Title
Cellular Mechanisms Underlying Retinal Wave Generation

Author
Ford, Kevin

Publication Date
2011

Peer reviewed|Thesis/dissertation

Cellular Mechanisms Underlying Retinal Wave Generation

By

Kevin J Ford

A dissertation submitted in partial satisfaction of the requirements for the degree of

Doctor of Philosophy

in

Molecular & Cell Biology

in the

Graduate Division

of the

University of California, Berkeley

Committee in charge:

Professor Marla B. Feller, Chair
Professor Richard H. Kramer
Professor Ehud Y. Isacoff
Professor Michael R. Deweese

Fall 2011

ABSTRACT

Cellular Mechanisms Underlying Retinal Wave Generation

By

Kevin J Ford

Doctor of Philosophy in Molecular & Cell Biology

University of California, Berkeley

Professor Marla B. Feller, Chair

The intricate patterning and complex circuitry of the nervous system beg the question of how such precise and ordered connections are formed during development. Genetically encoded information certainly instructs coarse projections of neuronal processes, and it has long been appreciated that sensory experience can fine tune connections. However, many functional neuronal circuits are present prior to birth and therefore must be organized in the absence of sensory experience. What instructs the formation of these circuits?

Spontaneous activity is prevalent in the developing nervous system and may play a role in organizing functional circuits. Spontaneous activity has been most extensively studied in the developing retina, where bursts of action potentials propagate among neighboring ganglion cells in a wave like fashion. These 'retinal waves' exist for an extended period of time prior to vision during which connections between retinal projection neurons and target regions of the brain are being refined. It is thought that information relevant for the refinement of these connections is provided in the spatial and temporal patterns of retinal waves.

In my thesis work, I set out to determine how the developing retina generates the distinct spatial and temporal patterns of retinal waves. A population of interneurons called starburst amacrine cells generates retinal waves during the first week after birth in mice. These starburst cells release acetylcholine onto neighboring starburst cells and retinal ganglion cells. How does this excitatory network generate precise patterns of activity?

Using a combination of calcium imaging, electrophysiology, and a cell-based sensor of acetylcholine, I characterized the features of the developing starburst cell network that give rise to the initiation, propagation, and termination of retinal waves. I incorporated these features of the starburst network into a computational model to explain how the spatial and temporal features of waves rely upon the properties of the underlying network. Finally, I described the molecular mechanisms of a key feature in starburst cells, a minute long slow afterhyperpolarization, that sets the frequency and spatial coverage of waves. These findings provide a detailed understanding of how spatial and temporal patterns of spontaneous activity are generated in the retina, and

provide a basis for further experiments to determine the relevant information within these patterns that instruct the wiring of visual circuits.

Last, I provide evidence that the slow afterhyperpolarizartions in starburst amacrine cells are mediated by two-pore potassium channels, which are traditionally thought to be leak channels. Our findings suggest that slow variations of second messengers, including cAMP and IP3, are read out by two-pore channels to alter neuronal excitability. These findings would have relevance to similar conductances found throughout the nervous system.

In memory of
Martin, Dennis, and Maxine Ford
and
Shirley Vlcek

TABLE OF CONTENTS

LIST OF FIGURES

Chapter I:

Chapter II:

Chapter III:

ACKNOWLEDGEMENTS

I thank Marla for being the perfect mentor. Her enthusiasm and support helped me gain confidence as a scientist. I have truly transitioned from student to scientist through her advice and training. I will do my best to become a mentor in her image.

I thank my committee for their thoughtful advice. Though many thesis meeting may have gone on longer than expected, I thoroughly enjoyed the enthusiasm of these discussions.

I thank all the members of the Feller and Feldman labs, present and past, for both their scientific and social support. I have been lucky to have such collaborative and fun colleagues throughout my time in the lab. I thank Aude Felix for collaboration on Chapter 2.

I thank my high school biology teacher, Ms. Butler, for planting a seed of curiosity about the workings of life. The opportunities she provided me in high school have directly led to where I am today.

I thank my parents for their unwavering support, constant encouragement, and love. They were always there for me when times are tough, and encouraged me through each step of way. I am as proud to be their son as they are of me.

I thank Heesoo for all the love and support she gives me every day; though we probably talk about science far more than we should….

Chapter 1, in full, is a reprint of the material as it appears in:
Kevin J. Ford and Marla B. Feller. Assembly and disassembly of a retinal cholinergic network, Visual Neuroscience, *Visual Neuroscience*. (2011) 28:1-11.
The dissertation author was the primary author of this paper.

Chapter 2 is original work submitted as:
Kevin J. Ford, Aude L. Felix, Marla B. Feller. Cellular Mechanisms underlying cholinergic retinal waves.
The dissertation author was the primary author of this paper. It is included with permission from all authors.

Chapter 3 is original work in preparation.

VITA

2001-2005 B.S., Department of Biology, *summa cum* laude,
University of California, San Diego

2005-2007 Ph.D. Department of Biology, University of California, San Diego

2007-2011 Ph.D. Department of Molecular & Cell Biology,
University of California, Berkeley

PUBLICATIONS

Aaron G Blankenship, Kevin J Ford, Juliette Johnson, Rebecca P Seal, Robert H Edwards, David R Copenhagen, Marla B Feller. Synaptic and Extrasynaptic Factors Governing Glutamatergic Retinal Waves. *Neuron*. (2009) 62,2: 230 – 241.

William Barkis, Kevin Ford, Marla Feller. Non-cell autonomous factor induces the transition from excitatory to inhibitory GABA signaling in retina independent of activity. *PNAS*. *published ahead of print December 6, 2010, doi:10.1073/pnas.1008775108.*

Kevin J. Ford and Marla B. Feller. Assembly and disassembly of a retinal cholinergic network, Visual Neuroscience, *Visual Neuroscience*. (2011) 28:1-11.

Kevin J. Ford, Aude L. Felix, Marla B. Feller. Cellular Mechanisms underlying cholinergic retinal waves. *Submitted*

AWARDS

2001-2005 Provosts Honors, Revelle College, University of California, San Diego

2003 Amylin Pharmaceuticals Inc. Research Scholarship Recipient

2004-2005 William Stout Scholarship recipient

2008-2011 Ruth L. Kirschstein National Research Service Award

2009 Elizabeth Roboz Einstein Fellowship in Neurosciences and Human Development

I. Assembly and disassembly of a retinal cholinergic network

Abstract

In the few weeks prior to the onset of vision, the retina undergoes a dramatic amount of development. Neurons migrate into position and target appropriate synaptic partners to assemble the circuits that mediate vision. During this period of development, the retina is not silent, but rather exhibits spontaneous correlated activity called retinal waves. The retina assembles and disassembles a series of transient circuits that use distinct mechanisms to generate waves. During the first postnatal week, this transient circuit is comprised of reciprocal cholinergic connections between starburst amacrine cells. A few days before the eyes open, these cholinergic connections are eliminated as glutamatergic circuits involved in processing visual information are formed. Here we discuss the assembly and disassembly of this transient cholinergic network and the role it plays in various aspects of retinal development.

Introduction

The mammalian retina has long been a model system for study of development of neural circuits in the CNS. The development of the retina requires several steps. First, the 7 cell types that comprise the retina need to be generated in the right proportion. Second, postmitotic cells leave the ventricular zone and migrate to one of three cell layers. Third, they start to form synaptic connections with other retinal neurons. Finally, these groups of synaptically coupled cells evolve into the circuits contained in the adult retina.

Acetylcholine (ACh) signaling plays a key role throughout these developmental stages. Prior to synapse formation, paracrine action of ACh is essential for regulating early developmental events, such as regulation of the cell cycle and the growth of neurites. In addition, cholinergic synapses are among the earliest to mature and thereby constitute the earliest functional circuits in the retina. Here we review the maturation of the retinal cholinergic circuit, describing its role in mediating early spontaneous activity and the development of non-cholinergic circuits.

ACh in the retina is produced by a subtype of amacrine cell termed the starburst amacrine cell (SAC). Of the roughly 30 morphologically distinct amacrine cell types (MacNeil *et al.*, 1999), the starburst amacrine cell is perhaps the best characterized (Famiglietti, 1983; Tauchi & Masland, 1984; Vaney, 1984). So named for its radially symmetric processes, SACs are the only neurons to produce ACh in the adult retina (Hayden *et al.*, 1980). The population of SACs is divided into two sub-populations with somas located in the proximal inner nuclear layer (regular) or in the ganglion cell layer (displaced) (Famiglietti, 1983). In addition to releasing ACh, SACs also release GABA (O'Malley & Masland, 1989) and adenosine (Blazynski, 1989). In the mature retina, ACh release acts on both muscarinic and nicotinic receptors to modulate response properties of many different types of ganglion cells (Masland & Ames, 1976; Masland *et al.*, 1984; Schmidt *et al.*, 1987; Baldridge, 1996; Strang *et al.*, 2005). The SAC is of

particular importance in a retinal circuit that detects motion (Fried *et al.*, 2002; reviewed in Taylor & Vaney, 2003), the topic of another review in this series.

In mature retina, ACh released from SACs acts exclusively on other cell types (Baldridge, 1996). However, during development cholinergic signaling occurs between SACs. Long before eye opening, ACh is produced by SACs and functional cholinergic receptors exist on SACs as well as other cells of the developing retina. SACs are spontaneously active and can release ACh onto neighboring SACs and ganglion cells. We refer to this early, transient signaling between SACs as the cholinergic network.

A key developmental function for the cholinergic network is the generation of retinal waves. During an extended period of time prior to visual input, the developing retina exhibits propagating spontaneous activity, termed retinal waves (Meister *et al.*, 1991; Wong *et al.*, 1993; Feller *et al.*, 1996). The cholinergic network appears at birth in mice and mediates the initiation and propagation of waves until the second postnatal week, when waves are mediated by glutamatergic circuits (Bansal *et al.*, 2000; Wong *et al.*, 2000; Zhou & Zhao, 2000).

In this review, we first describe the assembly of the transient cholinergic circuit, which involves early expression of proteins associated with release and action of ACh. Second, we review the process by which SACs orchestrate the wave generating circuit. Third, we describe the transition from cholinergic waves to glutamatergic waves, which requires the disassembly of the cholinergic connections that mediate waves. Last, we review the evidence that SACs and waves play a role in the development of retinal circuits, including dendritic refinement and stratification. (The role of retinal waves in the targeting and refinement of retinofugal synapses has been reviewed elsewhere (Torborg & Feller, 2005; Huberman *et al.*, 2008a; Feldheim & O'Leary, 2010)).

Assembly of the cholinergic network

The proteins associated with cholinergic synapses appear early in development (Figure I-1). SACs first begin to express choline-acetyltransferase (ChAT), the enzyme responsible for synthesis of acetylcholine, at embryonic day 17 (E17) in rats (Kim *et al.*, 2000). SAC cell bodies organize into two layers on opposite sides of the nascent inner plexiform layer (IPL) shortly before birth. By postnatal day 3 (P3) two distinct bands are apparent within the IPL, representing regular and displaced populations of SACs (Bansal *et al.*, 2000; Kim *et al.*, 2000). Expression of the vesicular transporter for ACh (VAChT) follows a similar developmental profile, with punctate expression found at birth (Stacy & Wong, 2003). Evidence for presynaptic release machinery, including synaptic vesicle protein 2C (SV2C, (Wang *et al.*, 2003)), synaptophysin (Dhingra *et al.*, 1997), and SNAP-25 (West Greenlee *et al.*, 1998) are present at birth as well.

The broad distribution of nicotinic and muscarinic receptors at birth indicates that ACh released from SACs is poised to act on several cell types. mRNA expression of nicotinic acetylcholine receptors (nACHRs) subunits alpha 3-4 and beta 2-4 is present in the embryonic and early postnatal retina (Hoover & Goldman, 1992). Dividing cells in the ventricular zone have M1 muscarinic receptor dependent calcium increases in response to carbachol application, whereas differentiated amacrine and ganglion cells have voltage-gated channel dependent calcium increases in respond to nicotine (Wong, 1995). Among the responsive amacrine cells are SACs themselves, which are

depolarized at this early age by ACh acting on nicotinic receptors (Zheng *et al.*, 2004). The presence nAChRs on SACs indicates that they have the potential to form a recurrent excitatory network at this early stage of development.

Despite the abundance of pre- and postsynaptic components for cholinergic signaling, there is little ultrastructural evidence of conventional synapses at this early stage of development. Conventional synapses between amacrine and ganglion cells begin to form after P3 in mice (Fisher, 1979) and ChAT expression precedes synapse formation by at least 2 days in chick retina (Spira *et al.*, 1987). However, despite the lack of structural evidence for synapses, there is physiological evidence for cholinergic synaptic transmission between pairs of SACs at this early age. Paired recordings between SACs from embryonic rabbit showed that SACs can indeed release both ACh and GABA to excite neighboring SACs in a reciprocal fashion (Zheng *et al.*, 2004) (Figure I-2D). Postsynaptic nAChR mediated currents are slow, appearing to reflect an asynchronous and/or diffuse release of ACh from the presynaptic SAC. Paired recordings of SACs in early postnatal mice reveal similar slow currents (Ford *et al.*, 2010).

SACs also form GABAergic synapses with other SACs and with subpopulations of ganglion cells. Unlike most GABAergic neurons in the retina, SACs express the GABA synthesizing enzyme GAD-67 rather than the GAD-65 isoform (Brandon & Criswell, 1995). GAD-67 expression is present early in development (Famiglietti & Sundquist, 2010). SACs can release GABA onto neighboring SACs during the first postnatal week in rabbit (Zheng *et al.*, 2004). Direction selective ganglion cells also form GABAergic synapses with SACs well before eye opening (Lee *et al.*, 2010; Wei *et al.*, 2011).

A distinguishing feature of the SAC network is that the somas of SACs form a mosaic -- a term used to describe the regular arrangement of somas with a minimal spacing between them (reviewed in Vaney, 1990; Cook & Chalupa, 2000; Novelli *et al.*, 2005). SAC mosaics arise very early in development. SAC somas are initially positioned randomly with respect to each other as they migrate from the ventricular zone toward the developing ganglion cell layer. By birth in mice, SAC somas have distributed in a mosaic fashion so that there is a minimum distance observed between somas (Galli-Resta *et al.*, 1997; Galli-Resta *et al.*, 2000). The formation of the soma mosaic correlates with the complete coverage of the IPL by SAC processes.

Homotypic interactions between SAC processes are thought to instruct the initial formation of the mosaic (Reese & Galli-Resta, 2002). The developmental window during which these interactions establish the mosaic is finite, as disruption of microtubules (Galli-Resta *et al.*, 2002) or ablation of subsets of SACs by excitotoxicity (Farajian *et al.*, 2004) a few days after birth fails to disrupt the established mosaic. At this point, the mechanisms by which interactions between SAC processes mediate the development of mosaics are unknown.

The role of starburst amacrine cells in generation of retinal waves

The most well studied function of the early cholinergic network in the retina is the generation of retinal waves (Figure I-2). Retinal waves consist of bursts of action potentials in retinal ganglion cells that propagate in a wave front across the plane of the retina. Retinal waves occur in many species including turtle (Sernagor *et al.*, 2003),

chick (Catsicas *et al.*, 1998; Wong *et al.*, 1998; Sernagor *et al.*, 2000), mice (Mooney *et al.*, 1996; Bansal *et al.*, 2000), rabbit (Zhou, 1998), ferret (Meister *et al.*, 1991; Wong *et al.*, 1993; Feller *et al.*, 1996), and primate (Warland *et al.*, 2006). Across all species, waves share similar characteristic features. Waves initiate at random positions and propagate at speeds ranging from ~100μm/s (mouse, (Singer *et al.*, 2001)) up to 400μm/s (chick, (Sernagor *et al.*, 2000)). Individual waves stop at discrete but shifting borders that reflect recently active regions of retina (Feller *et al.*, 1996). This refractory period following a wave lasts for approximately one minute (Feller *et al.*, 1996; Feller *et al.*, 1997), shortly after which an additional wave can be initiated and spread over the same area (Figure I-2A). In addition, this refractory period dictates the frequency with which a local region of the retina experiences a wave.

The circuitry underlying the generation of retinal waves progresses through three stages that reflect the maturation of retinal circuits (Blankenship & Feller, 2010) (Figure I-3A). Before formation of the IPL (E17 in mice (Kim *et al.*, 2000), E25 in rabbit (Sharma & Ehinger, 1997)), retinal waves propagate through the developing ganglion cell layer. These early stage waves are blocked by gap-junction antagonists (Syed *et al.*, 2004b). With the initial extension of SAC processes to form the IPL, waves transition from propagation via gap-junctions to propagation via activation of nAChRs (Feller *et al.*, 1996). Finally, a third stage of waves develop several days before the eyes open and co-exist with light responses for a short period of time (Demas *et al.*, 2003). These waves are blocked by ionotropic glutamate receptors (Wong *et al.*, 2000; Zhou & Zhao, 2000; Blankenship *et al.*, 2009).

The cholinergic network plays an exclusive role in generating waves during an extended period of development. Neighboring ganglion cells and SACs receive simultaneous slow nAChR and GABA-A mediated currents that give rise to correlated action potential firing (Feller *et al.*, 1996; Zhou, 1998). In perinatal mice, ferrets, and rabbits, waves monitored by calcium imaging are blocked by nAChR antagonists (Feller *et al.*, 1996; Penn *et al.*, 1998; Bansal *et al.*, 2000; Zhou & Zhao, 2000), but not by ionotropic or metabotropic GABA or glutamate receptor antagonists (Zhou & Zhao, 2000). Gap-junction signaling seems to play a role in the generation of these waves in chick (Catsicas *et al.*, 1998), but is involved to a lesser extent in mammalian retina (Bansal *et al.*, 2000; Syed *et al.*, 2004b).

The features of the developing cholinergic network that give rise to waves are now beginning to be understood. The generation of waves requires a source of depolarization for wave initiation, a network of excitatory interactions for propagation and a source of inhibition that limits the spatial extent of waves and dictates the minimum interval between waves. We discuss the properties of the cholinergic network that give rise to these features below.

Initiation

SACs themselves are the likely source of wave initiation. In order for a wave to start, a cell or group of cells must spontaneously excite neighboring cells to initiate the spread of depolarization. Waves initiate at random locations (Feller *et al.*, 1996), suggesting that the cells responsible for the spontaneous excitation that drives wave initiation are present uniformly across the retina. In the presence of neurotransmitter antagonists,

SACs from rabbit retinas exhibit spontaneous depolarizations that could be measured with cell attached, whole cell recordings, and calcium imaging (Zheng *et al.*, 2006) (Figure I-2B). Spontaneous depolarizations occur fairly regularly with a frequency of about once per 20s in cell attached and current clamp recordings, though spontaneous calcium transients were less regular. These spontaneous depolarizations presumably lead to release of ACh onto neighboring SACs, which may trigger the start of a wave. Indeed, we find that injecting current to depolarize a single SAC can robustly initiate a wave in mouse retina (Ford *et al.*, 2010).

The ion channels that underlie spontaneous depolarizations in SACs are unknown. Activation of TTX sensitive sodium channels, which are present in developing SACs (Zhou & Fain, 1996), are unlikely to be the cause of spontaneous depolarization, as TTX does not block retinal waves (Stellwagen *et al.*, 1999). Spontaneous opening of calcium channels may provide a depolarizing drive. Adult SACs have N-, P/Q-, and R-type calcium channels (Cohen, 2001; Kaneda *et al.*, 2007), but these channels are activated at depolarized potentials. Some L-type voltage gated calcium channels are activated at hyperpolarized potentials (Koschak *et al.*, 2001) and have been implicated in pacemaking neurons (Putzier *et al.*, 2009). Retinal waves are blocked by the L-type channel antagonist nifedipine (Singer *et al.*, 2001), suggesting that these channels may play a role in either the spontaneous depolarization or propagation of waves.

Propagation

Waves propagate through a cholinergic circuit that depends on activation of a specific subtype of nAChRs. Studies of adult rabbit retina have demonstrated strong expression of alpha7 homomeric channels (Dmitrieva *et al.*, 2007) as well as alpha3/beta2 containing heteromeric channels (Keyser *et al.*, 2000) throughout the IPL. Expression of alpha3 and alpha8 containing receptors during the period of cholinergic waves has been shown in chick retina (Hamassaki-Britto *et al.*, 1994). Waves are blocked by α-conotoxin-MII, a toxin that is most specific for alpha3/beta2 containing nAChRs, but not α-bungarotoxin (targeted to homomeric alpha7 nAChRs) or α-conotoxin-AU1B (targeted to alpha3/beta4 containing receptors) (Penn *et al.*, 1998; Bansal *et al.*, 2000). Further evidence for a unique set of receptors mediating waves came from studies using knockout mice -- mice lacking either alpha3 or beta2 subunits lacked cholinergic retinal waves (Bansal *et al.*, 2000; Sun *et al.*, 2008; Stafford *et al.*, 2009). Hence, wave propagation depends upon activation of specific heteromeric alpha3/beta2 nAChRs even though other nAChRs exist in the retina.

In addition to ACh, SACs and ganglion cells receive GABAergic input through GABA-A receptors during waves (Feller *et al.*, 1996; Zhou, 1998). At this developmental age GABA-A mediated currents are depolarizing due to the accumulation of intracellular chloride (Zhang *et al.*, 2006b; Barkis *et al.*, 2010). GABA-A receptor activation is not required for the propagation of waves in rabbit or mice (Syed *et al.*, 2004b; Wang *et al.*, 2007), but does influence the structure of the firing patterns (Wang *et al.*, 2007). Not all studies have reached this conclusion – early waves in both turtle (Sernagor *et al.*, 2003) and ferret (Fischer *et al.*, 1998; but see Stellwagen *et al.*, 1999) depend on GABA-A receptor activation.

A possible explanation for the widespread effects of ACh during waves is that ACh is released by volume transmission – the diffuse release of neurotransmitter in the absence of pre- and postsynaptic specializations (for a comparison of direct vs. volume ACh transmission see (Sarter *et al.*, 2009)). Several lines of evidence support this. First, retinal ganglion cells with dendritic arbors at opposite ends of the IPL are synchronized during waves, despite the fine stratification of SAC processes (Wong & Oakley, 1996). Second, slow synaptic currents recorded between pairs of SACs (Zheng *et al.*, 2004) (Figure I-2D) indicate that ACh acts diffusely. Third, cholinergic retinal waves are present prior to the formation of conventional synapses, as identified in electron microscopy studies (Fisher, 1979; Greiner & Weidman, 1981). Finally, in rabbit retina, calcium waves propagate through the ventricular zone that are correlated with waves in the ganglion cells (Syed *et al.*, 2004a). The ventricular zone waves are blocked by muscarinic receptor antagonists as well as nAChR antagonists, implying that ACh released during waves in the ganglion cell layer diffuses tens of microns to the ventricular zone where it activates muscarinic receptors.

Refractory period

The frequency of retinal waves is limited by a refractory period following waves. Over a period of about one minute, waves initiated at random points appear to tile the retina, avoiding regions active recently (Feller *et al.*, 1996)(Figure I-2A). Depolarization by focal application of high potassium solution could also cause a refractory period within the affected region. This refractory period is thought to be imparted by a slow after-hyperpolarization (sAHP) following depolarization in SACs (Zheng *et al.*, 2006) (Figure I-2C). The sAHP is blocked by cadmium, suggesting that it is activated by calcium entry through voltage-gated calcium channels. Interestingly, the channel underlying the sAHP is inhibited by elevating levels of cAMP, similar to the calcium-activated potassium channel which is thought to underlie sAHPs in various other regions of the brain (Alger & Nicoll, 1980; Lancaster & Adams, 1986; Sah & Isaacson, 1995; Vogalis *et al.*, 2001), the molecular identity of which is unknown. Elevating cAMP increases the frequency of retinal waves (Stellwagen *et al.*, 1999; Hanganu *et al.*, 2006), consistent with the notion that the sAHP limits the frequency of waves.

Recent studies have incorporated the measured features of the cholinergic network into computational models. Modeling studies are of use in identifying the relevant features of a circuit that give rise to the physiological output. For instance, two modeling studies have shown that in order to achieve propagating waves that have finite borders, i.e. do not encompass the entire retina, there must be local variability in the refractory state of the retina (Godfrey & Swindale, 2007; Hennig *et al.*, 2009). This variability is generated by random spontaneous depolarizations of SACs followed by sAHPs that occur in between waves. While spontaneous depolarization of SACs between waves has been observed in rabbit (asterisk Figure I-2C) (Zheng *et al.*, 2006), we have not observed these in mouse (Ford *et al.*, 2010). As the details of the SAC network are worked out for different species, there will likely be different, and perhaps disparate, solutions that generate very similar waves.

Role of cholinergic signaling in establishing non-cholinergic retinal circuits

Influence on later progenitor cells:

Cholinergic retinal waves occur during a period of rapid retinal development. Progenitor cells in the ventricular zone are dividing and differentiating into each of the 7 types of retinal cells (Figure I-1). These newly differentiated cells must then migrate to the proper position within the retina and extend processes to form the neuropil layers. The onset of cholinergic waves correlates with the formation of the IPL, where amacrine and ganglion cells processes stratify into 10 discrete layers (in mice) that process visual information in parallel (Masland, 2001; Roska & Werblin, 2001; Wassle, 2004). Once stratified in these layers, bipolar, amacrine, and ganglion cells must form synapses with their proper partners to form functional circuits that process visual information. Before the onset of vision, these discrete synaptic layers are visible (Kim *et al.*, 2000; Drenhaus *et al.*, 2003; Famiglietti & Sundquist, 2010) and some functional circuits are already established (Elstrott *et al.*, 2008; Wei *et al.*, 2011). To what extent does the cholinergic network shape the outcome of these developmental events?

Rhythmic increases in intracellular calcium play an important role in cell proliferation and differentiation (reviewed in Martins & Pearson, 2008) for retinal neurons born during cholinergic waves. ACh drives increases in intracellular calcium of progenitor cells in the ventricular zone through activation of M1 muscarinic receptors (Wong, 1995), which can alter their progression in the cell cycle (Pearson *et al.*, 2002). Blocking muscarinic receptors in chick eyes leads to an increase in the size of the eye (Pearson *et al.*, 2002). A probable source for ACh acting on muscarinic receptors is from cholinergic waves, which drive correlated calcium waves in the ventricular zone (Syed *et al.*, 2004a). In other parts of the nervous system, elevation of intracellular calcium can also influence neuronal migration (reviewed in Komuro & Kumada, 2005) and neurotransmitter selection (reviewed in Spitzer *et al.*, 2004). It remains to be seen whether calcium increases caused by retinal waves have similar effects.

IPL stratification

The retina is a highly laminar structure. Cell bodies reside in three vertically oriented layers composed of the distinct cell classes. The IPL comprises axons from bipolar cells, processes from amacrine cells, and dendrites of ganglion cells. These processes are separated into the On and Off layers corresponding to the functional responses to light of the corresponding cells. Within On and Off layers, processes are further segregated into at least 10 different strata where distinct neural computations are performed. The structural layering and corresponding functional separation has made the retina an ideal model system for studying synapse specificity – i.e. the process by which pre- and postsynaptic neurons wire to their appropriate partners.

The development of lamina in the IPL occurs in several steps. First, amacrine cells extend processes into the IPL. The processes of different amacrine cells identified by cell-specific antibody staining form discrete layers as soon as they first appear (Famiglietti & Sundquist, 2010). Second, the dendrites of ganglion cells extend into the IPL. While some ganglion cells initially stratify within their appropriate mature lamina, a

large portion of ganglion cells stratify diffusely throughout future On and Off layers. Next, On and Off bipolar cell axons extend into the IPL where they stratify into the appropriate layers (Johnson *et al.*, 2003). Finally, ganglion cells restrict their dendrites to their mature lamina (reviewed in (Xu & Tian, 2004)). Below we discuss how SACs could play a role in these developmental steps.

A growing body of literature from zebrafish studies points to a critical role for amacrine cells in patterning the IPL. The processes of amacrine cells have directed growth within their target layers without exuberant growth in other layers (Godinho *et al.*, 2005). While ganglion cells are the first-born cells in the retina, they play a lesser role in formation of layers in the IPL. A genetic model in which ganglion cells are never born have delayed IPL formation, although this is partially corrected and normal lamination of the IPL occurs throughout most of the retina (Kay *et al.*, 2004). Hence, interactions between amacrine cells are sufficient to give rise to the layering within the IPL. Interestingly, bipolar cell axons target correctly to the normal IPL in these mutants, but fail to innervate regions of abnormal IPL (Kay *et al.*, 2004), suggesting that amacrine cells provide the laminar cues for bipolar cell axon targeting. Finally, ganglion cells exhibit directed outgrowth of their processes within established layers of amacrine cell processes (Mumm *et al.*, 2006), implying that amacrine cells can provide lamination cues for ganglion cells. A zebrafish homologue of the SAC has not been conclusively identified (though see (Kay *et al.*, 2004)), so it is unclear what role SACs in particular play in these developmental events.

In mammals, SACs are among the first cells to extend processes within the IPL (Kim *et al.*, 2000) and could potentially serve as a foundation for the layering of subsequent strata within the IPL. Lamination signals, such as members of the immunogblobulin superfamily (Yamagata & Sanes, 2008) or semaphorins (Matsuoka *et al.*, 2011), expressed on SAC processes could instruct the processes of other amacrine, ganglion, and bipolar cells to stratify above, below or between the two cholinergic strata. Despite this early genesis, it is unlikely that SACs provide lamination cues for other amacrine and bipolar cells. Retinal deletion of the transcription factor islet-1 results in a near complete loss of ChAT positive amacrine cells (Elshatory *et al.*, 2007). Despite this loss of differentiated SACs, several markers for other amacrine cell types still form layers within the IPL. Similarly, a genetic model of retinal blastoma lacks several markers of mature SACs but stratification of other amacrine and bipolar cell types are not altered (Chen *et al.*, 2007). Furthermore, SACs ablated by immuno-toxin (Gunhan *et al.*, 2002) or by excitotoxicity with L-glutamate (Reese *et al.*, 2001) at two to three days after birth show no defects in the stratification of bipolar cells, suggesting that SAC processes do not provide an instructive role for stratification of these cell types.

While SACs are unlikely to guide the lamination of other amacrine and bipolar cells, they may instruct the localization of some types of ganglion cell dendrites. Using random dye labeling, a certain class of bi-stratified ganglion cell, mostly likely corresponding to direction selective ganglion cells, was found to co-stratify with the cholinergic processes shortly after birth (Stacy & Wong, 2003), although other mono-stratified ganglion cells never stratified with the cholinergic bands. Recently, genetically labeled mouse lines of functionally identical ganglion cell classes have been developed that allow for consistent characterization across development (Huberman *et al.*, 2008b; Kim *et al.*, 2008; Huberman *et al.*, 2009). The dendrites of genetically identified

direction selective ganglion cells co-stratify with SAC processes shortly after birth (Kim 2010, Wei 2011), supporting the hypothesis that SACs provide an instructive role for lamination of certain ganglion cell types.

The dendrites of most retinal ganglion cells initially arborize diffusely within the IPL before restricting their dendrites to distinct lamina (Bodnarenko *et al.*, 1999; Bansal *et al.*, 2000; Sernagor *et al.*, 2001; Xu & Tian, 2004; Coombs *et al.*, 2007; Kim *et al.*, 2010). Some studies have implicated a role for activity in bipolar cells in the segregation of ganglion cell dendrites. Hyperpolarizing ON bipolar cells during the period of glutamatergic retinal waves using the drug APB prevents the segregation into ON and OFF layers (Bodnarenko & Chalupa, 1993; Bodnarenko *et al.*, 1995). Additionally, mice that lack the MHCI receptor CD3zeta have altered glutamatergic retinal waves. The ganglion cells of these mice have reduced dendritic motility and have more diffuse dendrites within the IPL (Xu *et al.*, 2010). However, not all manipulations of activity during development alter dendritic stratification. Preventing synaptic release of glutamate from ON bipolar cells by expression of tetanus toxin fails to prevent the stratification of ganglion cell dendrites, although synapse formation onto ON bipolar cells is reduced (Kerschensteiner *et al.*, 2009).

Is there a role for cholinergic waves in the stratification process? Blocking nAChRs during the period of cholinergic waves reduces the motility of filipodia on the dendrites of ganglion cells (Wong & Wong, 2001), demonstrating that waves can drive structural changes in dendrites. Studies in turtle have demonstrated that blocking cholinergic waves with nAChR antagonists inhibits dendritic growth (Mehta & Sernagor, 2006) and reduces receptive field sizes (Sernagor & Grzywacz, 1996). Additionally, mice lacking the beta2 subunit of the nAChR had a delay in, though did not prevent, the fine stratification of ganglion cell dendrites (Bansal *et al.*, 2000). These findings indicate that cholinergic waves do influence the outgrowth of ganglion cell dendrites but are not the primary factor dictating their final organization.

One intriguing hypothesis for a role of retinal waves is in the development of direction selective circuits. Retinal waves have directional information both in their propagation and in the observation that there is a propagation bias, with more waves traveling toward the nasal direction than the other cardinal axes (Stafford *et al.*, 2009; Elstrott & Feller, 2010). However, direction selective ganglion cells participate equally in all waves irrespective of propagation direction (Elstrott & Feller, 2010) and complete blockade of retinal activity using intraocular muscimol injections did not prevent the development of direction selectivity (Wei *et al.*, 2011). These findings indicate that waves are not likely to provide the instructive signal for the establishment of asymmetric direction selective circuits. However, whether retinal waves play a role in the refinement of DS circuits remains to be determined.

Is there a role for cholinergic waves in the transitions between wave-generating circuits?

Another role of cholinergic waves in development of the retina circuitry may be to terminate early stage gap-junction mediated waves (Figure I-3). Knock-out animals that lack nAChR receptor subunits still exhibit wave like activity under certain recording conditions, such as elevated temperature (alpha3(-/-): (Bansal *et al.*, 2000), beta2(-/-) (Sun *et al.*, 2008; Stafford *et al.*, 2009)). This activity is likely mediated by gap-junctions

(Sun *et al.*, 2008), as in earlier stage waves. Similarly, a study using a genetic model which eliminates ChAT in a large portion of the retina found normal cholinergic waves in the spared region, but compensatory waves in the region lacking ChAT (Stacy *et al.*, 2005). These studies point to a sequential maturation of the retinal circuitry that relies on checkpoints to make transitions from one stage (gap-junction mediated waves) to the next (cholinergic transmission mediated waves). This sort of checkpoint model of neuronal development (Ben-Ari & Spitzer, 2010) is further evidenced in the disassembly of the cholinergic network to make way for glutamatergic signaling (Blankenship & Feller, 2010).

Disassembly of the cholinergic network

Shortly before eye opening, retinal waves transition from being mediated by ACh to glutamate. Bipolar cell axons invade the IPL and begin to release glutamate at the end of the first week after birth in rodents (Johnson *et al.*, 2003). Shortly thereafter, waves change their pharmacological profile and spatiotemporal properties. Waves are no longer blocked by nAChR antagonists but rather are sensitive to a combination of AMPA and NMDA antagonists (Wong *et al.*, 1998; Zhou & Zhao, 2000; Blankenship *et al.*, 2009). These glutamatergic waves occur as periodic clusters of activity followed by periods of silence (Kerschensteiner & Wong, 2008; Blankenship *et al.*, 2009). Waves exist simultaneously with light responses and disappear a few days after eye opening in a manner that is independent of visual experience (Demas *et al.*, 2003).

With the onset of glutamatergic waves, the SAC network loses the features necessary for propagation of cholinergic waves. First, mature SACs are no longer depolarized by application of nicotine (Baldridge, 1996). This is the result of a rapid decline in nAChR activation that coincides with the start of glutamatergic waves (Zheng *et al.*, 2004). Second, acetylcholinesterase, the enzyme that degrades ACh, is increased during this time window (Hutchins *et al.*, 1995), which would decrease the spread of ACh. Third, the action of GABA becomes hyperpolarizing a few days before the onset of glutamatergic waves (Zhang *et al.*, 2006b; Barkis *et al.*, 2010). Intracellular chloride is reduced as the expression of the potassium-chloride transporter KCC2 is increased in ganglion cells (Zhang *et al.*, 2006a). Mature SAC processes have a graded expression of KCC2 that increases along the length of the process (Gavrikov *et al.*, 2006). When this graded distribution of KCC2 occurs is unknown. Fourth, SACs become less excitable because maturation of processes increases the electronic space constant. The long and skinny processes of SACs likely prevent the spread of depolarization between processes, which would serve to electrically isolate the soma from the processes. A further decrease in the excitability of SACs is imparted by the loss of voltage gated sodium channels (Zhou & Fain, 1996) and an increase in expression of the voltage gated potassium channel Kv3.1 (Ozaita *et al.*, 2004; Zheng *et al.*, 2006).

At this same time, other circuits involving SACs are rapidly maturing. GABAergic connections between SACs are maintained during this period (Zheng *et al.*, 2004) and cholinergic and GABAergic synapses onto direction-selective ganglion cells develop (Lee *et al.*, 2010; Wei *et al.*, 2011). SACs greatly extend their processes as much as 7

fold and develop varicosities at the distal portions that are presumed to be the sites of GABA release (Wong & Collin, 1989).

The nature of cholinergic transmission in the adult retina is not well understood. Many ganglion cells with dendrites distal to the cholinergic strata within the IPL still respond to ACh released from SACs (Schmidt *et al.*, 1987). Paired recordings between SACs and direction selective ganglion cells reveal symmetrical sites of ACh release (Lee *et al.*, 2010), however ultrastructural reconstruction of synaptic contacts onto direction selective ganglion cells failed to find evidence for these cholinergic synapses (Briggman *et al.*, 2011). Furthermore, expression of SNAP-25, a SNARE protein involved in evoked release of neurotransmitter, is transiently highly expressed in SAC processes during the period of cholinergic waves (West Greenlee *et al.*, 1998), suggesting that the presynaptic machinery for neurotransmitter release might change during development.

The onset of glutamatergic waves may play an active role in the disassembly of cholinergic circuits, similar to the transition from gap-junction to cholinergic waves (Blankenship & Feller, 2010) (Figure I-3). Mice lacking the vesicular glutamate transporter VGLUT1 lack glutamate release from bipolar cells. These mice still have retinal waves at the period of time when littermate control animals have glutamatergic waves. Interestingly, these later waves in the VGLUT1 knockout mice are unaffected by glutamate receptor antagonists but are blocked by nAChR antagonists (Blankenship *et al.*, 2009). Glutamate signaling from bipolar cells is therefore required to dismantle the cholinergic network.

The mechanisms underlying this transition are not understood. SACs have functional kainate, AMPA, and NMDA receptors shortly after birth (Acosta *et al.*, 2007) suggesting that they can respond to glutamate when it is first released by bipolar cells. In addition to ionotropic receptors, SACs also express the metabotropic glutamate receptor 2 starting shortly after birth in rodents (Koulen *et al.*, 1996). Action of glutamate on either ionotropic or metabotropic receptors on SACs could result in down-regulation of functional nAChRs and perhaps the regulation of other proteins that are necessary for cholinergic waves. The mechanisms involved in this transition will likely be of general importance, as several other developing neural circuits such as the spinal cord, hind brain, cochlea, and hippocampus transition through different stages of spontaneous activity before reaching their mature state (Blankenship & Feller, 2010).

Conclusions

Here we have reviewed the assembly, disassembly and function of cholinergic circuits in retinal development. Starburst amacrine cells release acetylcholine and nicotinic and muscarinic acetylcholine receptors appear early in development to provide signaling that influences events prior to synapse formation. The processes of starburst amacrine cells define the early strata of the developing inner plexiform layer and therefore may play a role in organizing processes of other cells. For a brief period of development, starburst amacrine cells can mutually excite each other. These recurrent excitatory connections provide the substrate for the initiation and propagation of retinal waves. Future work will continue to elucidate how other transient features of developing

starburst cells and the nature of their synaptic connections influences the propagation properties of retinal waves.

One outstanding question that remains is how early signaling in the retina influences the formation of retinal circuits. The assembly of this cholinergic circuit is critical for driving the transition from an earlier, gap junction-mediated wave generating circuit. Similarly, maturation of the glutamatergic wave generating circuit drives the disassembly of the cholinergic network. Hence, each circuit is critical for eliminating the circuit before it. In addition, retinal waves drive correlated depolarizations of many synaptic partners (e.g. starburst amacrine cells and direction selective ganglion cells). Whether these early signaling events are critical for the maturation of these functional circuits remains an open question. Answers to these questions require a deeper understanding of the interplay between activity and other cellular mechanisms that underlie the wiring up of functional circuits.

References

Acosta, M.L., Chua, J. & Kalloniatis, M. (2007) Functional activation of glutamate ionotropic receptors in the developing mouse retina. *The Journal of Comparative Neurology*, **500**, 923-941.

Alger, B.E. & Nicoll, R.A. (1980) Epileptiform burst afterhyperolarization: calcium-dependent potassium potential in hippocampal CA1 pyramidal cells. *Science*, **210**, 1122-1124.

Baldridge, W.H. (1996) Optical recordings of the effects of cholinergic ligands on neurons in the ganglion cell layer of mammalian retina. *The Journal of Neuroscience: The Official Journal of the Society for Neuroscience*, **16**, 5060-5072.

Bansal, A., Singer, J.H., Hwang, B.J., Xu, W., Beaudet, A. & Feller, M.B. (2000) Mice lacking specific nicotinic acetylcholine receptor subunits exhibit dramatically altered spontaneous activity patterns and reveal a limited role for retinal waves in forming ON and OFF circuits in the inner retina. *The Journal of Neuroscience: The Official Journal of the Society for Neuroscience*, **20**, 7672-7681.

Barkis, W.B., Ford, K.J. & Feller, M.B. (2010) Non-cell-autonomous factor induces the transition from excitatory to inhibitory GABA signaling in retina independent of activity. *Proc Natl Acad Sci U S A*, **107**, 22302-22307.

Ben-Ari, Y. & Spitzer, N.C. (2010) Phenotypic checkpoints regulate neuronal development. *Trends in Neurosciences*, **33**, 485-492.

Blankenship, A.G. & Feller, M.B. (2010) Mechanisms underlying spontaneous patterned activity in developing neural circuits. *Nature Reviews. Neuroscience*, **11**, 18-29.

Blankenship, A.G., Ford, K.J., Johnson, J., Seal, R.P., Edwards, R.H., Copenhagen, D.R. & Feller, M.B. (2009) Synaptic and extrasynaptic factors governing glutamatergic retinal waves. *Neuron*, **62**, 230-241.

Blazynski, C. (1989) Displaced cholinergic, GABAergic amacrine cells in the rabbit retina also contain adenosine. *Visual Neuroscience*, **3**, 425-431.

Bodnarenko, S.R. & Chalupa, L.M. (1993) Stratification of ON and OFF ganglion cell dendrites depends on glutamate-mediated afferent activity in the developing retina. *Nature*, **364**, 144-146.

Bodnarenko, S.R., Jeyarasasingam, G. & Chalupa, L.M. (1995) Development and regulation of dendritic stratification in retinal ganglion cells by glutamate-mediated afferent activity. *J Neurosci*, **15**, 7037-7045.

Bodnarenko, S.R., Yeung, G., Thomas, L. & McCarthy, M. (1999) The development of retinal ganglion cell dendritic stratification in ferrets. *Neuroreport*, **10**, 2955-2959.

Brandon, C. & Criswell, M.H. (1995) Displaced starburst amacrine cells of the rabbit retina contain the 67-kDa isoform, but not the 65-kDa isoform, of glutamate decarboxylase. *Visual Neuroscience*, **12**, 1053-1061.

Briggman, K.L., Helmstaedter, M. & Denk, W. (2011) Wiring specificity in the direction-selectivity circuit of the retina. *Nature*, **471**, 183-188.

Catsicas, M., Bonness, V., Becker, D. & Mobbs, P. (1998) Spontaneous Ca2+ transients and their transmission in the developing chick retina. *Curr Biol*, **8**, 283-286.

Chen, D., Opavsky, R., Pacal, M., Tanimoto, N., Wenzel, P., Seeliger, M.W., Leone, G. & Bremner, R. (2007) Rb-mediated neuronal differentiation through cell-cycle-independent regulation of E2f3a. *PLoS Biology*, **5**, e179-e179.

Cohen, E.D. (2001) Voltage-gated calcium and sodium currents of starburst amacrine cells in the rabbit retina. *Visual Neuroscience*, **18**, 799-809.

Cook, J.E. & Chalupa, L.M. (2000) Retinal mosaics: new insights into an old concept. *Trends Neurosci*, **23**, 26-34.

Coombs, J.L., Van Der List, D. & Chalupa, L.M. (2007) Morphological properties of mouse retinal ganglion cells during postnatal development. *The Journal of Comparative Neurology*, **503**, 803-814.

Demas, J., Eglen, S.J. & Wong, R.O.L. (2003) Developmental Loss of Synchronous Spontaneous Activity in the Mouse Retina Is Independent of Visual Experience. *The Journal of Neuroscience*, **23**, 2851-2860.

Dhingra, N.K., Ramamohan, Y. & Raju, T.R. (1997) Developmental expression of synaptophysin, synapsin I and syntaxin in the rat retina. *Brain Research. Developmental Brain Research*, **102**, 267-273.

Dmitrieva, N.A., Strang, C.E. & Keyser, K.T. (2007) Expression of alpha 7 nicotinic acetylcholine receptors by bipolar, amacrine, and ganglion cells of the rabbit retina. *The Journal of Histochemistry and Cytochemistry: Official Journal of the Histochemistry Society*, **55**, 461-476.

Drenhaus, U., Morino, P. & Veh, R.W. (2003) On the development of the stratification of the inner plexiform layer in the chick retina. *The Journal of Comparative Neurology*, **460**, 1-12.

Elshatory, Y., Everhart, D., Deng, M., Xie, X., Barlow, R.B. & Gan, L. (2007) Islet-1 controls the differentiation of retinal bipolar and cholinergic amacrine cells. *The Journal of Neuroscience: The Official Journal of the Society for Neuroscience*, **27**, 12707-12720.

Elstrott, J., Anishchenko, A., Greschner, M., Sher, A., Litke, A.M., Chichilnisky, E.J. & Feller, M.B. (2008) Direction selectivity in the retina is established independent of visual experience and cholinergic retinal waves. *Neuron*, **58**, 499-506.

Elstrott, J. & Feller, M.B. (2010) Direction-selective ganglion cells show symmetric participation in retinal waves during development. *J Neurosci*, **30**, 11197-11201.

Famiglietti, Jr. (1983) [`]Starburst' amacrine cells and cholinergic neurons: mirror-symmetric ON and OFF amacrine cells of rabbit retina. *Brain Research*, **261**, 138-144.

Famiglietti, E.V. & Sundquist, S.J. (2010) Development of excitatory and inhibitory neurotransmitters in transitory cholinergic neurons, starburst amacrine cells, and GABAergic amacrine cells of rabbit retina, with implications for previsual and visual development of retinal ganglion cells. *Visual Neuroscience*, **27**, 19-42.

Farajian, R., Raven, M.A., Cusato, K. & Reese, B.E. (2004) Cellular positioning and dendritic field size of cholinergic amacrine cells are impervious to early ablation of neighboring cells in the mouse retina. *Visual Neuroscience*, **21**, 13-22.

Feldheim, D.A. & O'Leary, D.D. (2010) Visual map development: bidirectional signaling, bifunctional guidance molecules, and competition. *Cold Spring Harb Perspect Biol*, **2**, a001768.

Feller, M.B., Butts, D.A., Aaron, H.L., Rokhsar, D.S. & Shatz, C.J. (1997) Dynamic processes shape spatiotemporal properties of retinal waves. *Neuron*, **19**, 293-306.

Feller, M.B., Wellis, D.P., Stellwagen, D., Werblin, F.S. & Shatz, C.J. (1996) Requirement for cholinergic synaptic transmission in the propagation of spontaneous retinal waves. *Science (New York, N.Y.)*, **272**, 1182-1187.

Fischer, K.F., Lukasiewicz, P.D. & Wong, R.O. (1998) Age-dependent and cell class-specific modulation of retinal ganglion cell bursting activity by GABA. *J Neurosci*, **18**, 3767-3778.

Fisher, L.J. (1979) Development of synaptic arrays in the inner plexiform layer of neonatal mouse retina. *J Comp Neurol*, **187**, 359-372.

Ford, K.J., Felix, A.L. & Feller, M.B. (Year) The role of starburst amacrine cells in initiating retinal waves. Vol. Program No. 335.6, Neuroscience 2010 Abstracts. Society for Neuroscience, City.

Fried, S.I., Münch, T.A. & Werblin, F.S. (2002) Mechanisms and circuitry underlying directional selectivity in the retina. *Nature*, **420**, 411-414.

Galli-Resta, L., Novelli, E. & Viegi, A. (2002) Dynamic microtubule-dependent interactions position homotypic neurones in regular monolayered arrays during retinal development. *Development*, **129**, 3803-3814.

Galli-Resta, L., Novelli, E., Volpini, M. & Strettoi, E. (2000) The spatial organization of cholinergic mosaics in the adult mouse retina. *The European Journal of Neuroscience*, **12**, 3819-3822.

Galli-Resta, L., Resta, G., Tan, S.S. & Reese, B.E. (1997) Mosaics of islet-1-expressing amacrine cells assembled by short-range cellular interactions. *J Neurosci*, **17**, 7831-7838.

Gavrikov, K.E., Nilson, J.E., Dmitriev, A.V., Zucker, C.L. & Mangel, S.C. (2006) Dendritic compartmentalization of chloride cotransporters underlies directional responses of starburst amacrine cells in retina. *Proceedings of the National Academy of Sciences of the United States of America*, **103**, 18793-18798.

Godfrey, K.B. & Swindale, N.V. (2007) Retinal Wave Behavior through Activity-Dependent Refractory Periods. *PLoS Computational Biology*, **3**, e245-e245.

Godinho, L., Mumm, J.S., Williams, P.R., Schroeter, E.H., Koerber, A., Park, S.W., Leach, S.D. & Wong, R.O. (2005) Targeting of amacrine cell neurites to appropriate synaptic laminae in the developing zebrafish retina. *Development*, **132**, 5069-5079.

Greiner, J.V. & Weidman, T.A. (1981) Histogenesis of the ferret retina. *Experimental Eye Research*, **33**, 315-332.

Gunhan, E., Choudary, P.V., Landerholm, T.E. & Chalupa, L.M. (2002) Depletion of cholinergic amacrine cells by a novel immunotoxin does not perturb the formation of segregated on and off cone bipolar cell projections. *The Journal of Neuroscience: The Official Journal of the Society for Neuroscience*, **22**, 2265-2273.

Hamassaki-Britto, D.E., Gardino, P.F., Hokoc, J.N., Keyser, K.T., Karten, H.J., Lindstrom, J.M. & Britto, L.R. (1994) Differential development of alpha-bungarotoxin-sensitive and alpha-bungarotoxin-insensitive nicotinic acetylcholine receptors in the chick retina. *J Comp Neurol*, **347**, 161-170.

Hanganu, I.L., Ben-Ari, Y. & Khazipov, R. (2006) Retinal waves trigger spindle bursts in the neonatal rat visual cortex. *J Neurosci*, **26**, 6728-6736.

Hayden, S.A., Mills, J.W. & Masland, R.M. (1980) Acetylcholine synthesis by displaced amacrine cells. *Science (New York, N.Y.)*, **210**, 435-437.

Hennig, M.H., Adams, C., Willshaw, D. & Sernagor, E. (2009) Early-Stage Waves in the Retinal Network Emerge Close to a Critical State Transition between Local and Global Functional Connectivity. *J. Neurosci.*, **29**, 1077-1086.

Hinds, J.W. & Hinds, P.L. (1983) Development of retinal amacrine cells in the mouse embryo: evidence for two modes of formation. *J Comp Neurol*, **213**, 1-23.

Hoover, F. & Goldman, D. (1992) Temporally correlated expression of nAChR genes during development of the mammalian retina. *Experimental Eye Research*, **54**, 561-571.

Huberman, A.D., Feller, M.B. & Chapman, B. (2008a) Mechanisms underlying development of visual maps and receptive fields. *Annu Rev Neurosci*, **31**, 479-509.

Huberman, A.D., Manu, M., Koch, S.M., Susman, M.W., Lutz, A.B., Ullian, E.M., Baccus, S.A. & Barres, B.A. (2008b) Architecture and activity-mediated refinement of axonal projections from a mosaic of genetically identified retinal ganglion cells. *Neuron*, **59**, 425-438.

Huberman, A.D., Wei, W., Elstrott, J., Stafford, B.K., Feller, M.B. & Barres, B.A. (2009) Genetic identification of an On-Off direction-selective retinal ganglion cell subtype reveals a layer-specific subcortical map of posterior motion. *Neuron*, **62**, 327-334.

Hutchins, J.B., Bernanke, J.M. & Jefferson, V.E. (1995) Acetylcholinesterase in the developing ferret retina. *Experimental Eye Research*, **60**, 113-125.

Johnson, J., Tian, N., Caywood, M.S., Reimer, R.J., Edwards, R.H. & Copenhagen, D.R. (2003) Vesicular Neurotransmitter Transporter Expression in Developing Postnatal Rodent Retina: GABA and Glycine Precede Glutamate. *The Journal of Neuroscience*, **23**, 518-529.

Kaneda, M., Ito, K., Morishima, Y., Shigematsu, Y. & Shimoda, Y. (2007) Characterization of voltage-gated ionic channels in cholinergic amacrine cells in the mouse retina. *Journal of Neurophysiology*, **97**, 4225-4234.

Kay, J.N., Roeser, T., Mumm, J.S., Godinho, L., Mrejeru, A., Wong, R.O. & Baier, H. (2004) Transient requirement for ganglion cells during assembly of retinal synaptic layers. *Development*, **131**, 1331-1342.

Kerschensteiner, D., Morgan, J.L., Parker, E.D., Lewis, R.M. & Wong, R.O. (2009) Neurotransmission selectively regulates synapse formation in parallel circuits in vivo. *Nature*, **460**, 1016-1020.

Kerschensteiner, D. & Wong, R.O.L. (2008) A precisely timed asynchronous pattern of ON and OFF retinal ganglion cell activity during propagation of retinal waves. *Neuron*, **58**, 851-858.

Keyser, K.T., MacNeil, M.A., Dmitrieva, N., Wang, F., Masland, R.H. & Lindstrom, J.M. (2000) Amacrine, ganglion, and displaced amacrine cells in the rabbit retina express nicotinic acetylcholine receptors. *Visual Neuroscience*, **17**, 743-752.

Kim, I.-J., Zhang, Y., Meister, M. & Sanes, J.R. (2010) Laminar restriction of retinal ganglion cell dendrites and axons: subtype-specific developmental patterns revealed with transgenic markers. *The Journal of Neuroscience: The Official Journal of the Society for Neuroscience*, **30**, 1452-1462.

Kim, I.B., Lee, E.J., Kim, M.K., Park, D.K. & Chun, M.H. (2000) Choline acetyltransferase-immunoreactive neurons in the developing rat retina. *The Journal of Comparative Neurology*, **427**, 604-616.

Kim, I.J., Zhang, Y., Yamagata, M., Meister, M. & Sanes, J.R. (2008) Molecular identification of a retinal cell type that responds to upward motion. *Nature*, **452**, 478-482.

Komuro, H. & Kumada, T. (2005) Ca2+ transients control CNS neuronal migration. *Cell Calcium*, **37**, 387-393.

Koschak, A., Reimer, D., Huber, I., Grabner, M., Glossmann, H., Engel, J. & Striessnig, J. (2001) alpha 1D (Cav1.3) subunits can form l-type Ca2+ channels activating at negative voltages. *The Journal of Biological Chemistry*, **276**, 22100-22106.

Koulen, P., Malitschek, B., Kuhn, R., Wässle, H. & Brandstätter, J.H. (1996) Group II and group III metabotropic glutamate receptors in the rat retina: distributions and developmental expression patterns. *The European Journal of Neuroscience*, **8**, 2177-2187.

Lancaster, B. & Adams, P.R. (1986) Calcium-dependent current generating the afterhyperpolarization of hippocampal neurons. *J Neurophysiol*, **55**, 1268-1282.

Lee, S., Kim, K. & Zhou, Z.J. (2010) Role of ACh-GABA cotransmission in detecting image motion and motion direction. *Neuron*, **68**, 1159-1172.

MacNeil, M.A., Heussy, J.K., Dacheux, R.F., Raviola, E. & Masland, R.H. (1999) The shapes and numbers of amacrine cells: matching of photofilled with Golgi-stained cells in the rabbit retina and comparison with other mammalian species. *The Journal of Comparative Neurology*, **413**, 305-326.

Martins, R.A.P. & Pearson, R.A. (2008) Control of cell proliferation by neurotransmitters in the developing vertebrate retina. *Brain Research*, **1192**, 37-60.

Masland, R.H. (2001) The fundamental plan of the retina. *Nat Neurosci*, **4**, 877-886.

Masland, R.H. & Ames, A., 3rd (1976) Responses to acetylcholine of ganglion cells in an isolated mammalian retina. *J Neurophysiol*, **39**, 1220-1235.

Masland, R.H., Mills, J.W. & Cassidy, C. (1984) The functions of acetylcholine in the rabbit retina. *Proceedings of the Royal Society of London. Series B, Containing Papers of a Biological Character. Royal Society (Great Britain)*, **223**, 121-139.

Matsuoka, R.L., Nguyen-Ba-Charvet, K.T., Parray, A., Badea, T.C., Chédotal, A. & Kolodkin, A.L. (2011) Transmembrane semaphorin signalling controls laminar stratification in the mammalian retina. *Nature*, **470**, 259-263.

Mehta, V. & Sernagor, E. (2006) Early neural activity and dendritic growth in turtle retinal ganglion cells. *The European Journal of Neuroscience*, **24**, 773-786.

Meister, M., Wong, R.O., Baylor, D.A. & Shatz, C.J. (1991) Synchronous bursts of action potentials in ganglion cells of the developing mammalian retina. *Science*, **252**, 939-943.

Mooney, R., Penn, A.A., Gallego, R. & Shatz, C.J. (1996) Thalamic relay of spontaneous retinal activity prior to vision. *Neuron*, **17**, 863-874.

Mumm, J.S., Williams, P.R., Godinho, L., Koerber, A., Pittman, A.J., Roeser, T., Chien, C.B., Baier, H. & Wong, R.O. (2006) In vivo imaging reveals dendritic targeting of laminated afferents by zebrafish retinal ganglion cells. *Neuron*, **52**, 609-621.

Novelli, E., Resta, V. & Galli-Resta, L. (2005) Mechanisms controlling the formation of retinal mosaics. *Prog Brain Res*, **147**, 141-153.

O'Malley, D.M. & Masland, R.H. (1989) Co-release of acetylcholine and gamma-aminobutyric acid by a retinal neuron. *Proceedings of the National Academy of Sciences of the United States of America*, **86**, 3414-3418.

Ozaita, A., Petit-Jacques, J., Völgyi, B., Ho, C.S., Joho, R.H., Bloomfield, S.A. & Rudy, B. (2004) A unique role for Kv3 voltage-gated potassium channels in starburst amacrine cell signaling in mouse retina. *The Journal of Neuroscience: The Official Journal of the Society for Neuroscience*, **24**, 7335-7343.

Pearson, R., Catsicas, M., Becker, D. & Mobbs, P. (2002) Purinergic and muscarinic modulation of the cell cycle and calcium signaling in the chick retinal ventricular zone. *The Journal of Neuroscience: The Official Journal of the Society for Neuroscience*, **22**, 7569-7579.

Penn, A.A., Riquelme, P.A., Feller, M.B. & Shatz, C.J. (1998) Competition in retinogeniculate patterning driven by spontaneous activity. *Science (New York, N.Y.)*, **279**, 2108-2112.

Putzier, I., Kullmann, P.H.M., Horn, J.P. & Levitan, E.S. (2009) Cav1.3 channel voltage dependence, not Ca2+ selectivity, drives pacemaker activity and amplifies bursts in nigral dopamine neurons. *The Journal of Neuroscience: The Official Journal of the Society for Neuroscience*, **29**, 15414-15419.

Reese, B.E. & Galli-Resta, L. (2002) The role of tangential dispersion in retinal mosaic formation. *Prog Retin Eye Res*, **21**, 153-168.

Reese, B.E., Raven, M.A., Giannotti, K.A. & Johnson, P.T. (2001) Development of cholinergic amacrine cell stratification in the ferret retina and the effects of early excitotoxic ablation. *Visual Neuroscience*, **18**, 559-570.

Roska, B. & Werblin, F. (2001) Vertical interactions across ten parallel, stacked representations in the mammalian retina. *Nature*, **410**, 583-587.

Sah, P. & Isaacson, J.S. (1995) Channels underlying the slow afterhyperpolarization in hippocampal pyramidal neurons: neurotransmitters modulate the open probability. *Neuron*, **15**, 435-435.

Sarter, M., Parikh, V. & Howe, W.M. (2009) Phasic acetylcholine release and the volume transmission hypothesis: time to move on. *Nature Reviews. Neuroscience*, **10**, 383-390.

Schmidt, M., Humphrey, M.F. & Wässle, H. (1987) Action and localization of acetylcholine in the cat retina. *Journal of Neurophysiology*, **58**, 997-1015.

Sernagor, E., Eglen, S.J. & O'Donovan, M.J. (2000) Differential effects of acetylcholine and glutamate blockade on the spatiotemporal dynamics of retinal waves. *The Journal of Neuroscience: The Official Journal of the Society for Neuroscience*, **20**, RC56-RC56.

Sernagor, E., Eglen, S.J. & Wong, R.O. (2001) Development of retinal ganglion cell structure and function. *Progress in Retinal and Eye Research*, **20**, 139-174.

Sernagor, E. & Grzywacz, N.M. (1996) Influence of spontaneous activity and visual experience on developing retinal receptive fields. *Current Biology: CB*, **6**, 1503-1508.

Sernagor, E., Young, C. & Eglen, S.J. (2003) Developmental modulation of retinal wave dynamics: shedding light on the GABA saga. *The Journal of Neuroscience: The Official Journal of the Society for Neuroscience*, **23**, 7621-7629.

Sharma, R.K. & Ehinger, B. (1997) Mitosis in developing rabbit retina: an immunohistochemical study. *Experimental Eye Research*, **64**, 97-106.

Singer, J.H., Mirotznik, R.R. & Feller, M.B. (2001) Potentiation of L-type calcium channels reveals nonsynaptic mechanisms that correlate spontaneous activity in the developing mammalian retina. *J Neurosci*, **21**, 8514-8522.

Spira, A.W., Millar, T.J., Ishimoto, I., Epstein, M.L., Johnson, C.D., Dahl, J.L. & Morgan, I.G. (1987) Localization of choline acetyltransferase-like immunoreactivity in the embryonic chick retina. *J Comp Neurol*, **260**, 526-538.

Spitzer, N.C., Root, C.M. & Borodinsky, L.N. (2004) Orchestrating neuronal differentiation: patterns of Ca2+ spikes specify transmitter choice. *Trends Neurosci*, **27**, 415-421.

Stacy, R.C., Demas, J., Burgess, R.W., Sanes, J.R. & Wong, R.O.L. (2005) Disruption and Recovery of Patterned Retinal Activity in the Absence of Acetylcholine. *J. Neurosci.*, **25**, 9347-9357.

Stacy, R.C. & Wong, R.O.L. (2003) Developmental relationship between cholinergic amacrine cell processes and ganglion cell dendrites of the mouse retina. *The Journal of Comparative Neurology*, **456**, 154-166.

Stafford, B.K., Sher, A., Litke, A.M. & Feldheim, D.A. (2009) Spatial-Temporal Patterns of Retinal Waves Underlying Activity-Dependent Refinement of Retinofugal Projections. *Neuron*, **64**, 200-212.

Stellwagen, D., Shatz, C.J. & Feller, M.B. (1999) Dynamics of Retinal Waves Are Controlled by Cyclic AMP. *Neuron*, **24**, 673-685.

Strang, C.E., Andison, M.E., Amthor, F.R. & Keyser, K.T. (2005) Rabbit retinal ganglion cells express functional alpha7 nicotinic acetylcholine receptors. *American Journal of Physiology. Cell Physiology*, **289**, C644-655-C644-655.

Sun, C., Warland, D.K., Ballesteros, J.M., van der List, D. & Chalupa, L.M. (2008) Retinal waves in mice lacking the β2 subunit of the nicotinic acetylcholine receptor. *Proceedings of the National Academy of Sciences*, **105**, 13638-13643.

Syed, M.M., Lee, S., He, S. & Zhou, Z.J. (2004a) Spontaneous waves in the ventricular zone of developing mammalian retina. *Journal of Neurophysiology*, **91**, 1999-2009.

Syed, M.M., Lee, S., Zheng, J. & Zhou, Z.J. (2004b) Stage-dependent dynamics and modulation of spontaneous waves in the developing rabbit retina. *J Physiol*, **560**, 533-549.

Tauchi, M. & Masland, R.H. (1984) The shape and arrangement of the cholinergic neurons in the rabbit retina. *Proc R Soc Lond B Biol Sci*, **223**, 101-119.

Taylor, W.R. & Vaney, D.I. (2003) New directions in retinal research. *Trends in Neurosciences*, **26**, 379-385.

Torborg, C.L. & Feller, M.B. (2005) Spontaneous patterned retinal activity and the refinement of retinal projections. *Prog Neurobiol*, **76**, 213-235.

Vaney, D.I. (1984) 'Coronate' amacrine cells in the rabbit retina have the 'starburst' dendritic morphology. *Proceedings of the Royal Society of London. Series B, Containing Papers of a Biological Character. Royal Society (Great Britain)*, **220**, 501-508.

Vaney, D.I. (1990) *The mosaic of amacrine cells in the mammalian retina*. Pergamon Press, Oxford, ROYAUME-UNI.

Vogalis, F., Furness, J.B. & Kunze, W.A. (2001) Afterhyperpolarization current in myenteric neurons of the guinea pig duodenum. *Journal of Neurophysiology*, **85**, 1941-1951.

Voinescu, P.E., Emanuela, P., Kay, J.N. & Sanes, J.R. (2009) Birthdays of retinal amacrine cell subtypes are systematically related to their molecular identity and soma position. *The Journal of Comparative Neurology*, **517**, 737-750.

Wang, C.-T., Blankenship, A.G., Anishchenko, A., Elstrott, J., Fikhman, M., Nakanishi, S. & Feller, M.B. (2007) GABA(A) receptor-mediated signaling alters the structure of spontaneous activity in the developing retina. *The Journal of*

Neuroscience: The Official Journal of the Society for Neuroscience, **27**, 9130-9140.

Wang, M.M., Janz, R., Belizaire, R., Frishman, L.J. & Sherry, D.M. (2003) Differential distribution and developmental expression of synaptic vesicle protein 2 isoforms in the mouse retina. *The Journal of Comparative Neurology*, **460**, 106-122.

Warland, D.K., Huberman, A.D. & Chalupa, L.M. (2006) Dynamics of spontaneous activity in the fetal macaque retina during development of retinogeniculate pathways. *J Neurosci*, **26**, 5190-5197.

Wassle, H. (2004) Parallel processing in the mammalian retina. *Nat Rev Neurosci*, **5**, 747-757.

Wei, W., Hamby, A.M., Zhou, K. & Feller, M.B. (2011) Development of asymmetric inhibition underlying direction selectivity in the retina. *Nature*, **469**, 402-406.

West Greenlee, M.H., Finley, S.K., Wilson, M.C., Jacobson, C.D. & Sakaguchi, D.S. (1998) Transient, high levels of SNAP-25 expression in cholinergic amacrine cells during postnatal development of the mammalian retina. *The Journal of Comparative Neurology*, **394**, 374-385.

Wong, R.O. (1995) Cholinergic regulation of [Ca2+]i during cell division and differentiation in the mammalian retina. *The Journal of Neuroscience: The Official Journal of the Society for Neuroscience*, **15**, 2696-2706.

Wong, R.O. & Collin, S.P. (1989) Dendritic maturation of displaced putative cholinergic amacrine cells in the rabbit retina. *The Journal of Comparative Neurology*, **287**, 164-178.

Wong, R.O., Meister, M. & Shatz, C.J. (1993) Transient period of correlated bursting activity during development of the mammalian retina. *Neuron*, **11**, 923-938.

Wong, R.O. & Oakley, D.M. (1996) Changing patterns of spontaneous bursting activity of on and off retinal ganglion cells during development. *Neuron*, **16**, 1087-1095.

Wong, W.T., Myhr, K.L., Miller, E.D. & Wong, R.O. (2000) Developmental changes in the neurotransmitter regulation of correlated spontaneous retinal activity. *The Journal of Neuroscience: The Official Journal of the Society for Neuroscience*, **20**, 351-360.

Wong, W.T., Sanes, J.R. & Wong, R.O. (1998) Developmentally regulated spontaneous activity in the embryonic chick retina. *The Journal of Neuroscience: The Official Journal of the Society for Neuroscience*, **18**, 8839-8852.

Wong, W.T. & Wong, R.O. (2001) Changing specificity of neurotransmitter regulation of rapid dendritic remodeling during synaptogenesis. *Nature Neuroscience*, **4**, 351-352.

Xu, H. & Tian, N. (2004) Pathway-specific maturation, visual deprivation, and development of retinal pathway. *The Neuroscientist: A Review Journal Bringing Neurobiology, Neurology and Psychiatry*, **10**, 337-346.

Xu, H.P., Chen, H., Ding, Q., Xie, Z.H., Chen, L., Diao, L., Wang, P., Gan, L., Crair, M.C. & Tian, N. (2010) The immune protein CD3zeta is required for normal development of neural circuits in the retina. *Neuron*, **65**, 503-515.

Yamagata, M. & Sanes, J.R. (2008) Dscam and Sidekick proteins direct lamina-specific synaptic connections in vertebrate retina. *Nature*, **451**, 465-469.

Zhang, L.L., Fina, M.E. & Vardi, N. (2006a) Regulation of KCC2 and NKCC during development: membrane insertion and differences between cell types. *J Comp Neurol*, **499**, 132-143.

Zhang, L.L., Pathak, H.R., Coulter, D.A., Freed, M.A. & Vardi, N. (2006b) Shift of intracellular chloride concentration in ganglion and amacrine cells of developing mouse retina. *J Neurophysiol*, **95**, 2404-2416.

Zheng, J., Lee, S. & Zhou, Z.J. (2006) A transient network of intrinsically bursting starburst cells underlies the generation of retinal waves. *Nature Neuroscience*, **9**, 363-371.

Zheng, J.J., Lee, S. & Zhou, Z.J. (2004) A developmental switch in the excitability and function of the starburst network in the mammalian retina. *Neuron*, **44**, 851-864.

Zhou, Z.J. (1998) Direct Participation of Starburst Amacrine Cells in Spontaneous Rhythmic Activities in the Developing Mammalian Retina. *The Journal of Neuroscience*, **18**, 4155-4165.

Zhou, Z.J. & Fain, G.L. (1996) Starburst amacrine cells change from spiking to nonspiking neurons during retinal development. *Proceedings of the National Academy of Sciences of the United States of America*, **93**, 8057-8062.

Zhou, Z.J. & Zhao, D. (2000) Coordinated transitions in neurotransmitter systems for the initiation and propagation of spontaneous retinal waves. *The Journal of Neuroscience: The Official Journal of the Society for Neuroscience*, **20**, 6570-6577.

Figure I-1: Timeline showing major developmental events in mouse retina. Starburst cells become postmitotic between E11 and E17. ChAT expression is first seen at E17 and increases during the first week after birth. The IPL first appears at E17 and SAC processes form two discrete bands by P3. Conventional synapses first appear between amacrine and ganglion cells in the IPL at P3. Retinal waves transition through three stages during development: gap-junction, cholinergic, and glutamatergic. Bipolar cells first innervate the IPL at P7. Eyes open around P12. Ganglion cell dendrites stratify into lamina for an extended time beginning around P9 and continuing through the first month. The action of GABA switches from depolarizing to hyperpolarizing around P8. SACs are initially responsive to ACh action on nAChRs, but lose this responsiveness with the corresponding transition to glutamatergic waves. References:(1) (Voinescu *et al.*, 2009) (2) (Kim *et al.*, 2000) (3) (Hinds & Hinds, 1983) (4) (Fisher, 1979) (5) (Bansal *et al.*, 2000) (6) (Johnson *et al.*, 2003) (7) (Xu & Tian, 2004) (8) (Barkis *et al.*, 2010) (9) (Zheng *et al.*, 2004) (approximate age from rabbit data)

Developmental Timeline

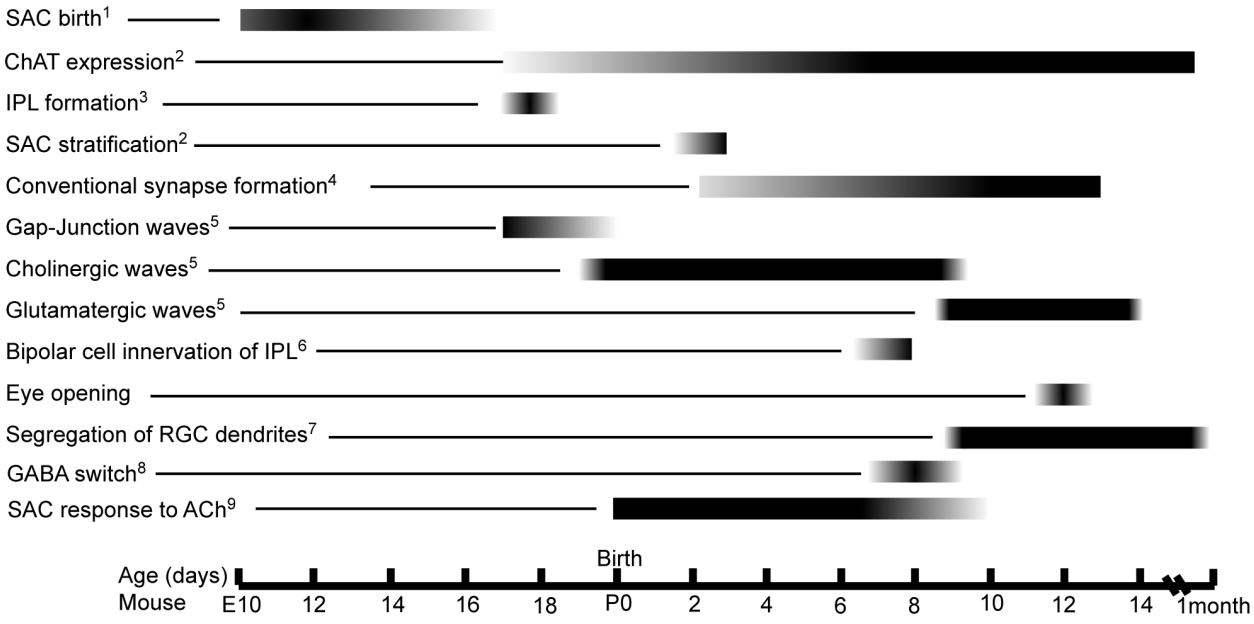

Figure I-2: Properties of cholinergic waves are generated by the SAC network.
A. Spatial and temporal properties of waves assessed with calcium imaging.
TOP: Low power calcium imaging of Fura-2AM labeled neonatal ferret retinas show decreases in fluorescence following calcium increases associated with waves.
BOTTOM: Spatial propagation of 30 waves during four consecutive minutes. Each panel shows the propagation of waves that occurred during a one-minute period. Cholinergic retinal waves initiate at random locations and propagate over finite regions. Waves occur at intervals between waves of around one minute for a given region (for example see asterisk). Adapted from (Feller *et al.*, 1996).
B. Cell-autonomous spontaneous depolarization of SACs may initiate retinal waves.
SACs (red regions and traces) from perinatal rabbit retinas loaded with Fura-2AM show spontaneous depolarizations in the presence of antagonists to ionotropic and metabotropic glutamate, GABA, glycine, and ACh receptors, whereas retinal ganglion cells do not (blue regions and traces). Adapted from (Zheng *et al.*, 2006).
C. The inter-wave refractory period may be due to a slow after-hyperpolarization in SACs.
Current clamp recording from a SAC in rabbit retina showing wave evoked and spontaneous (asterisk) depolarizations followed by slow after-hyperpolarizations. Adapted from (Zheng *et al.*, 2006).
D. Waves may propagate via reciprocal connections between SACs.
Voltage clamp recordings from pairs of neighboring SACs show both fast GABAergic postsynaptic currents and slow cholinergic postsynaptic currents. Top: Schematic of voltage command of presynaptic SAC (-70mV to 0mV). Bottom: Evoked PSCs at positive and negative holding potentials to isolate cholinergic and GABAergic currents, respectively. Adapted from (Zheng *et al.*, 2004).

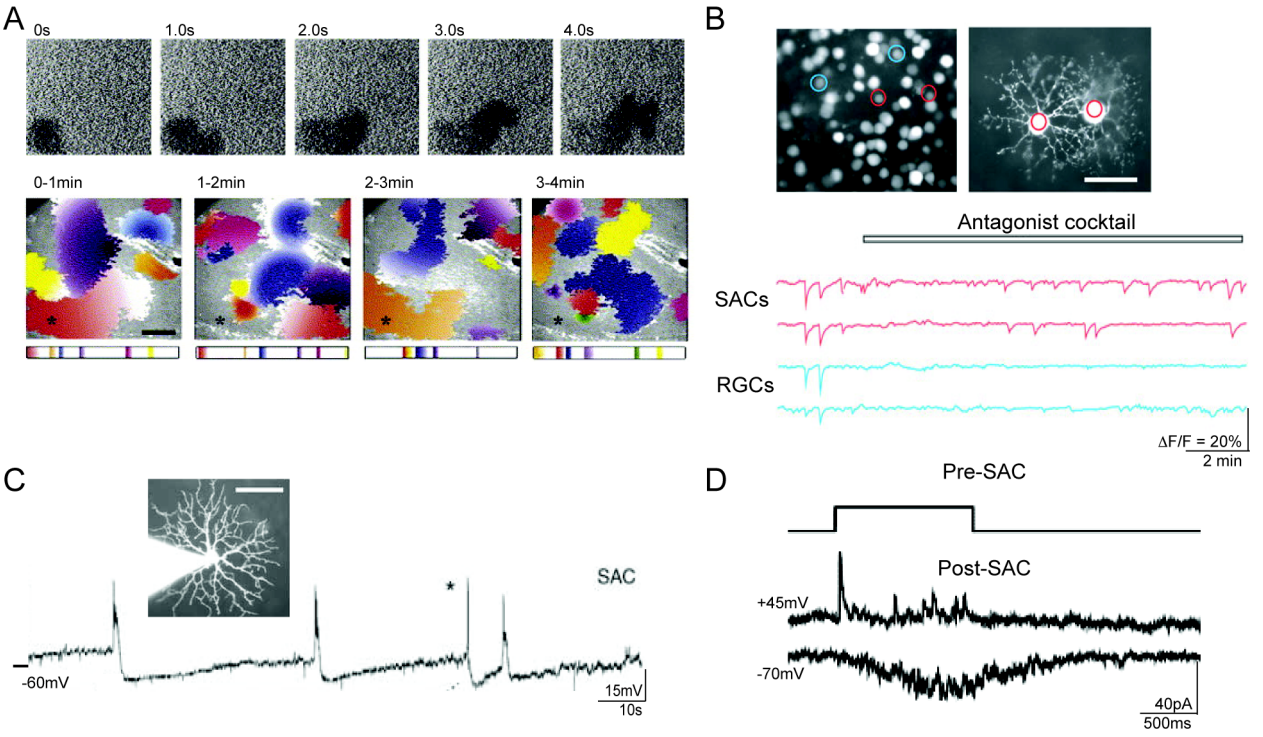
A
0s
1.0s
2.0s
3.0s
4.0s
0-1min
1-2min
2-3min
3-4min
B
Antagonist cocktail
SACs
RGCs
ΔF/F = 20%
2 min
C
SAC
-60mV
15mV
10s
D
Pre-SAC
Post-SAC
+45mV
-70mV
40pA
500ms

Figure I-3: Wave circuits transition through check-points.
A. Schematics of changing circuits that mediate waves. Left: Prior to birth waves are thought to propagate via gap-junctions between ganglion cells. Middle: Postnatal day 1-10, waves are propagated via SAC release of acetylcholine onto other SACs (black box). Acetylcholine also depolarizes ganglion cells. During this period of development, the gap-junction signaling between ganglion cells is reduced (red box).
Right: P10-P15 bipolar cells release glutamate to propagate waves in a mechanism that is thought to involve spillover of glutamate to excite neighboring bipolar cells (black box). Cholinergic signaling between SACs is reduced (red box). Adapted from (Blankenship & Feller, 2010).
B. Summary timeline of how genetic disruption of cholinergic or glutamatergic waves result in an extended action of the previous wave generating circuit
In wild type mice gap-junction mediated waves (gray) are followed by cholinergic waves (blue) starting at P0, then glutamatergic waves (green) at P10. In mice lacking the Beta2 subunit of the nicotinic acetylcholine receptor, gap-junction mediated waves persist until ~P8. In mice lacking vesicular glutamate transporter VGLUT1, cholinergic waves persist through the second postnatal week.

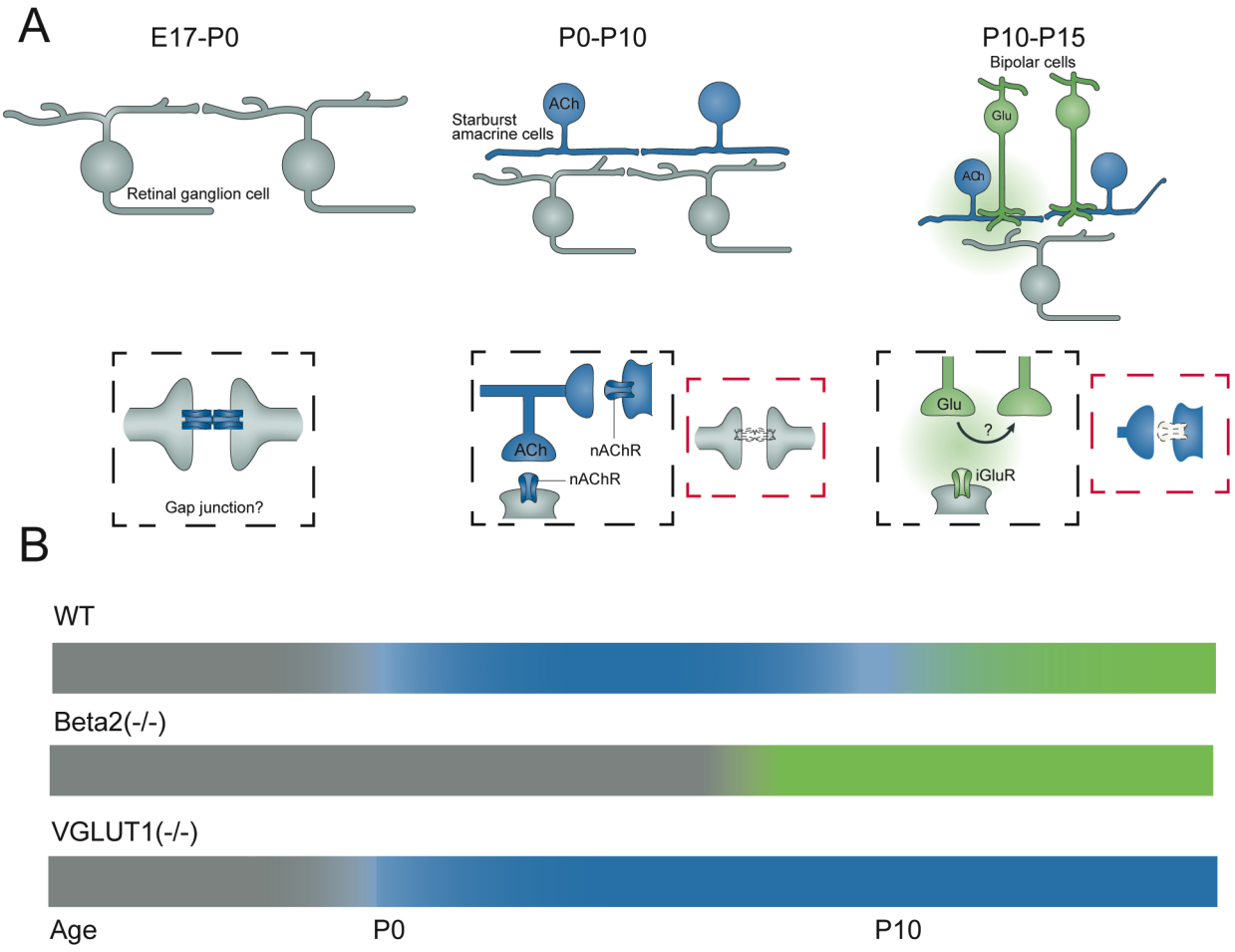
A
E17-P0
P0-P10
P10-P15
Retinal ganglion cell
Starburst amacrine cells
ACh
Bipolar cells
Glu
ACh
Gap junction?
ACh
nAChR
nAChR
Glu
?
iGluR
B
WT
Beta2(-/-)
VGLUT1(-/-)
Age
P0
P10

II. Cellular mechanisms underlying cholinergic retinal waves

Abstract

Prior to vision, a transient network of recurrently connected cholinergic interneurons, called starburst amacrine cells (SACs), generates spontaneous retinal waves. Retinal waves occur with a periodicity of minutes and propagate within distinct but shifting boundaries. These spatial and temporal patterns of retinal waves provide instructive cues for the refinement of retinal projections to the brain. Here we combine electrophysiological recording, two-photon calcium imaging, a cell-based ACh optical sensor and computational modeling to elucidate the mechanisms of wave initiation and propagation in developing mouse retina. Waves initiate via rare spontaneous depolarizations of SACs and propagate through recurrent cholinergic connections between SACs and volume release of ACh. Individual SACs have slow afterhyperpolarizations that induce SACs to have variable depolarizations during sequential waves. Using a computational model in which the properties of SACs are based on these physiological measurements, we reproduce the frequency, speed, and size of recorded waves. This study represents a complete description of the circuit that mediates cholinergic retinal waves and indicates that variability of the interneurons that generate this network activity may be critical for the robustness of waves across different species and stages of development.

Introduction

As neural circuits emerge during development, they exhibit transient features that give rise to periodic correlated activity. For example, in the developing retina, prior to the development of light responses, a transient circuit gives rise to propagating waves of activity, termed retinal waves (Galli & Maffei, 1988; Meister *et al.*, 1991; reviewed in Blankenship & Feller, 2010; Ford & Feller, 2011) . Retinal waves initiate at random points in the retina, propagate with a speed of approximately 100 microns/second, and their spatial extent is defined by a set of finite but shifting boundaries that are dependent upon a local refractory period (Feller *et al.*, 1996; Feller *et al.*, 1997).

The precise initiation, propagation and termination properties are proposed to be critical for driving refinement of retinal projections to the brain (Huberman *et al.*, 2008; Xu *et al.*, 2011). For example, the periodic initiation of waves induces depolarizations and calcium transients that may be tuned to drive axon guidance (Pfeiffenberger *et al.*, 2006; Nicol *et al.*, 2007) and plasticity mechanisms (Butts *et al.*, 2007; Shah & Crair, 2008). Propagation speed sets the time scale over which neighboring cells are correlated, which may be critical for retinotopic map refinement (Chandrasekaran *et al.*, 2007). Finally, the spatial extent of wave propagation is important for establishing eye-specific segregation of retinal inputs within the thalamus (Xu *et al.*, 2011).

Retinal waves persist for an extended period of development and as retinal circuits change with age, so does the wave generation mechanism. The most well understood wave-generating circuit is based upon cholinergic signaling. Cholinergic retinal waves are mediated by a network of cholinergic amacrine cells called starburst amacrine cells (SACs) (Feller *et al.*, 1996; Zhou, 1998). SACs release both

acetylcholine (ACh) and GABA onto neighboring SACs and retinal ganglion cells, allowing depolarization to propagate across the retina (Zheng *et al.*, 2004). How does this network comprised of recurrent excitatory connections generate waves with finite but shifting boundaries and periodicity of once-per-minute?

Several computational models have been proposed to explain how wave generation can emerge from a network of comprised of SACs (reviewed in Godfrey & Eglen, 2009). One recent study (Hennig *et al.*, 2009) concluded that propagation boundaries of waves and wave periodicity relied upon slow afterhyperpolarizations (sAHPs) in SACs generated by robust spontaneous depolarization of SACs between waves, as recently demonstrated in rabbit retina (Zheng *et al.*, 2006). Here, we use targeted recordings and calcium imaging to characterize intrinsic properties of SACs in mice, including their ability to initiate waves, spontaneous rate of depolarization, and slow afterhyperpolarization. In addition, we use paired recordings and a cell-based optical assay for release of ACh to gain insights into the connectivity that underlies wave propagation. We incorporate these properties into a computational model and compare the results of simulated waves to waves detected with calcium imaging. This combination of methods allows us to test specific hypotheses regarding the relative importance of intrinsic properties, network connectivity, and noise in the generation of spatial and temporal features of retinal waves.

Results

SACs have very low spontaneous depolarization rates

First, we asked how retinal waves are initiated. We performed calcium imaging at single cell resolution in retinas from mice expressing GFP-tagged IL-2 receptor under control of the mGluR2 promoter (Watanabe *et al.*, 1998; Wang *et al.*, 2007) or ChAT-Cre/TdTom (Ivanova *et al.*, 2010), which selectively label SACs. Retinas from mGluR2-GFP or ChAT-Cre/TdTom mice were bolus-loaded with the calcium indicator Oregon Green BAPTA-1 AM (Stosiek *et al.*, 2003; Blankenship *et al.*, 2009) to compare the frequency of spontaneous depolarization of SACs in the presence and absence of synaptic coupling to other SACs (Figure II-1A). We observed waves as large changes in fluorescence that propagated among nearby neurons. In control solution, correlated spontaneous increases in intracellular calcium concentration ($[Ca^{2+}]_i$) were observed in all SACs (Figure II-1B-D, n=386 cells in 15 retinas), with very few uncorrelated increases in $[Ca^{2+}]_i$ between waves (11 of 2995 calcium transients were not associated with waves). Therefore, SACs rarely exhibit activity during the intervals between waves.

To determine the intrinsic rate of depolarization of SACs, we performed similar experiments while blocking waves. When coupling between SACs was blocked using a combination of nAChR and $GABA_A$-R antagonists (n=7) or nAChR antagonists alone (n=8), SACs rarely exhibited spontaneous calcium transients during a 15-20 minute recording period (Figure II-1B-D), in sharp contrast to the observations in rabbit (Zheng *et al.*, 2006). Spontaneous calcium transients were modulated with age: the rate decreased while the amplitude increased (Figure II-1D). The low rate of intrinsic spontaneous depolarization is consistent with the low level of activity between waves. Hence, in mouse retina, SACs spontaneously depolarize at a rate significantly lower

than the frequency of waves. These findings indicate that in contrast to rabbit, developing mouse retina SACs do not function as strong pacemakers that dictate the dynamics of circuit activation.

Depolarization of a single SAC can initiate waves

We found that SACs have infrequent spontaneous depolarizations in the absence of synaptic input and rarely depolarize independent of waves. Can these sparse depolarizations initiate waves?

To determine whether depolarization of a single SAC is sufficient to initiate a wave, we performed targeted recordings from GFP+ neurons in mGluR2-GFP retinas that were bolus-loaded with OGB-1 AM (Figure II-2). In the design of this experiment it was critical to take into account the existence of a refractory period following depolarization of a cluster of cells during which they cannot participate in subsequent waves. In mice, this refractory period lasts approximately 30-50 seconds (Bansal *et al.*, 2000). Hence, depolarizing current was injected for 1.5s at 60s intervals. The amplitude of the current injections induced a fractional change in fluorescence similar to spontaneous calcium transients (Figure II-1D), indicating that they induced depolarizations that were within normal physiological range. The frequency of current injections occurred at a range of intervals following the preceding wave.

Calcium increases were simultaneously monitored in the region surrounding the target cell to detect the initiation of propagating waves. Waves could be evoked by current injection in 8 of 17 of recorded SACs (Figure II-2B). In the SACs where a single depolarization resulted in the initiation of a wave, successful wave initiations occurred only if the interval between the depolarization and the preceding wave was greater than 40 seconds (Figure II-2C, see Methods). Though these findings do not prove that waves are initiated by depolarization of single SACs, they do indicate that depolarization of single SACs is sufficient to initiate waves when the local region of the retina is in a non-refractory state.

SACs form excitatory connections with other SACs

The substrate for retinal wave propagation is proposed to be a network of recurrently connected SACs (Zheng *et al.*, 2004). To determine whether SACs form excitatory connections in mouse retina during the period of cholinergic retinal waves, we performed targeted paired whole cell voltage clamp recordings (Figure II-3A). To isolate cholinergic synapses between recorded cells, paired recordings were carried out in the presence of GABA-R blockers (50 μM TPMPA, 2 μM CPG 55845, and 5 μM gabazine to block $GABA_C$, $GABA_B$ and $GABA_A$ respectively, n=6 pairs) or GABA-R blockers with ionotropic glutamate receptor blockers (20 μM DNQX and 50 μM AP5 to block AMPA and NMDA receptors, n=4 pairs). Depolarization of one SAC consistently evoked a PSC in the second SAC (n=13/13). SACs were reciprocally connected in the subset we tested (n=3/3 bidirectional pairs, Figure II-3D), indicating there is a strong connection between SACs (Note, presynaptic calcium currents washed out within 5 min following break-in, therefore we were only able to test for reciprocal connections in a limited number of pairs.) Postsynaptic responses were recorded as a sustained inward current peaking several hundred milliseconds after termination of the presynaptic voltage step (peak amplitude: 25.3±12.7pA, mean±SD), similar to responses recorded in rabbit retina

(Zheng *et al.*, 2004). Evoked EPSCs reversed near 0mV (n=5, Figure II-3C), consistent with them being mediated by nAChRs (Sargent, 1993; Feller *et al.*, 1996). During waves, nearby SACs received periodic simultaneous compound postsynaptic currents (cPSC, V_{hold}= -70mV, n=6 pairs, Figure II-3E). cPSCs had slow kinetics, consistent with evoked PSCs measured between SAC-SAC pairs. These data demonstrate that in mouse retina, SACs form reciprocal excitatory connections, which can provide a substrate for wave propagation.

ACh is released diffusely during waves

Slow postsynaptic currents during waves suggest that ACh released during waves might act in a non-synaptic fashion. One hypothesis is that ACh is released in volume (reviewed in Sarter *et al.*, 2009) and diffuses away from release sites to activate nAChRs on SACs and RGCs throughout the depth of the IPL. To test for diffuse action of ACh, we used cell-based neurotransmitter fluorescent engineered reporters (CNiFERs (Nguyen *et al.*, 2010)) which can detect extracellular ACh within a range of 1-100nM. CNiFERs are HEK-293 cells that express M1 ACh receptors and the FRET based calcium indicator TN-XXL (Figure II-4A). Increases in extracellular ACh are reported as increases in FRET ratios resulting from activation of M1 receptors and subsequent release of intracellular calcium stores. To determine if ACh is released diffusely during waves, we imaged M1-CNiFERs placed on top of the inner limiting membrane (ILM, Figure II-4A-B) to prevent disruption of cholinergic synapses within the IPL. Large spontaneous increases in FRET were observed in all CNiFERs imaged from retinas aged P0-P6 (n=310 transients from 20 retinas, Figure II-4B). In contrast, no FRET increases were detected in control CNiFERs expressing the fluorescent protein mCherry instead of M1 receptors (n=11), indicating that the FRET responses were due to ACh activation of M1 receptors and not activation of endogenous receptors on HEK-293 cells. FRET transients were observed with the ILM intact (n=10/10 retinas), ruling out damage to the IPL as a cause for diffuse release of ACh. Simultaneous voltage clamp recording from nearby RGCs revealed that FRET transients were preceded by large EPSCs associated with waves (n=10, Figure II-4B-C). We conclude that ACh released by SACs during waves diffuses far from the site of release.

SACs spontaneously depolarize at an infrequent rate when nAChRs, and therefore waves, are blocked (see Figure II-1). We hypothesize that these spontaneous depolarizations initiate waves due to the release of ACh onto neighboring SACs. To test if spontaneous depolarizations in the absence of waves cause diffuse release of ACh, we imaged CNiFERs on P0-P6 retinas in the presence of nAChR antagonist. We observed small FRET transients in CNiFERs in several experiments when waves were blocked (n=8/11 retinas, Figure II-4B,D). Spontaneous FRET transients in wave blockers occurred with an irregular frequency (Figure II-4E) and were not associated with any EPSCs recorded in nearby ganglion cells (n=5 simultaneous recordings, Figure II-4B). Hence, we conclude that the spontaneous depolarization of SACs results in diffuse release of ACh..

Slow afterhyperpolarization in SACs is highly variable

SACs form a dense mosaic over the entire retina, yet waves have distinct boundaries. These boundaries are determined at least in part by a refractory period, in

that waves fail to propagate into regions that have recently participated in a wave. It has been proposed that the source of this refractory period is a slow afterhyperpolarization (sAHP) in SACs (Zheng *et al.*, 2006). In rabbit retina, after a SAC is depolarized by a wave, it undergoes a hyperpolarization lasting over 15 seconds, which prevents that SAC from participating in subsequent waves. Since nearby SACs are depolarized simultaneously during a wave, there are local regions of the retina in which a large percentage of SACs are hyperpolarized following a wave, which in turn makes that region refractory to subsequent waves. Both experiments (Feller *et al.*, 1997; Stellwagen *et al.*, 1999) and computational models (Butts *et al.*, 1999; Godfrey & Swindale, 2007; Hennig *et al.*, 2009) have demonstrated that manipulating the duration of the refractory period has profound effects on the spatial and temporal properties of waves.

To identify and characterize the conductance underlying the sAHP in mouse SACs, we performed targeted perforated patch recordings from SACs in retinas acutely isolated from mGluR2-GFP mice (Figure II-5). During waves, SACs exhibit large depolarizations, which consist of calcium spikes that ride on top of a slow graded depolarization, followed by a sAHP that persists for tens of seconds (Figure II-5B, n=48 waves in 4 cells), similar to rabbit retina (Zheng *et al.*, 2006). A sAHP was also evoked in response to a current injection in SACs that were synaptically isolated by the presence of nAChR and $GABA_A$-R antagonists (DHβE 4μM and gabazine 5μM, respectively, Figure II-5C, amplitude: 6.0±3.0mV, rise time: 11.2±2.1s, time to half max decay: 22.3±4.3s, n=3 cells), indicating it was generated cell-autonomously and not due to network interactions.

To characterize the conductance underlying the sAHP, we performed voltage clamp recordings using perforated patch. A step depolarization evoked an outward current (I_{sAHP}) that peaked several seconds after the membrane potential returned to baseline (amplitude: 4.9±1.9pA, rise time: 13.5±3.7s, mean± SD). The I_{sAHP} peak was followed by a slow decay (time to half max decay: 16.2 ± 7.5s, n=32, Figure II-5D), a kinetic profile that closely matched the time course of the sAHP (Figure II-5C). The large variability in peak amplitude and decay was not correlated with differences in access resistance (r^2 <0.02), implying that there is considerable cell-to-cell variability in the current underlying the slow afterhyperpolarization.

Variable participation of SACs during waves

Waves drive diffuse release of ACh, suggesting that neighboring cells receive similar amounts of depolarizing input during waves. However, we have measured remarkably variable sAHP currents in SACs. We asked whether intrinsic variability in the SAC network is reflected in the extent of the depolarization of SACs during waves, as assayed with two-photon calcium imaging. Two-photon imaging has the advantage of strong z-sectioning which assures that the fluorescence signal comes only from the imaged cells and not from out-of-plane fluorescent cells and processes, thereby giving an accurate representation of depolarization in individual cells during waves (Kerr *et al.*, 2005; Bonifazi *et al.*, 2009).

To record calcium transients in SACs, we loaded retinas of mGlur2-GFP or ChAT-Cre/TdTom mice with OGB-1 AM. An XYZ scan was first performed with the laser tuned to 920 nm to preferentially excite GFP/TdTom and identify displaced SACs

(Figure II-6A). Subsequently, with the laser tuned to 790 nm to preferentially excite OGB-1 AM, a single focal plane in the ganglion cell layer was imaged as a function of time with a frame rate of 1 Hz.

Recordings show that the fractional change in fluorescence in RGCs is uniform from wave to wave, consistent with uniform depolarization by diffuse ACh release. In contrast, the amplitude of the $\Delta F/F$ in SACs was significantly variable within the same cell. This variability indicates that a given SAC depolarizes by a different extent for each wave (Figure II-6). We hypothesized that this variability is inversely correlated with the amplitude of previous waves because large depolarizations will evoke a large sAHP that results in a smaller depolarization during the next wave. To test this hypothesis, we plotted the amplitude of each calcium transient as a function of the amplitude of the preceding calcium transient. We found an inverse relationship for calcium transient amplitudes from SACs but not RGCs (Figure II-6E, r^2_{SAC} =0.19; r^2_{GCL} =0.001). Hence, the extent of depolarization of SACs during a wave is influenced by the strength of the previous wave on the time scale of the sAHP.

Computational model of SACs recapitulates spatial and temporal properties of waves

Thus far, we have characterized the spontaneous initiation rate, synaptic connectivity and sAHP of SACs. To determine whether these properties are sufficient to describe the propagation properties of retinal waves, we turn to computational modeling. Simulated waves generated by computational models have distributions of interwave intervals, propagation speed, and wave size that are similar to those measured physiologically using calcium imaging (Feller *et al.*, 1997; Godfrey & Swindale, 2007) or multielectrode array recording (Hennig *et al.*, 2009). Most models are based on the premise that waves are initiated by spontaneous depolarizations in SACs, propagate through an interconnected network of SACs, which in turn become refractory to subsequent waves. A key prediction of all of these models is that there is a substantial level of spontaneous activity of SACs between waves that is important in determining the periodicity and finite propagation of retinal waves. Can we compose a model based on our observation that individual SACs have infrequent spontaneous depolarizations that still robustly generates waves?

To devise a computational model that is consistent with our physiological measurements, we start with a recent model that incorporates spontaneous initiation, synaptic connectivity and a sAHP of SACs (Hennig *et al.*, 2009), which we will refer to as the Hennig model. The Hennig model consists of a homogeneous network of SACs that are more strongly connected to nearby SACs than distant ones (Figure II-7A). In this model, once the SAC has recovered from a sAHP, there is a stochastic depolarization mediated by activation of voltage-gated calcium channels that triggers release of neurotransmitter (Figure II-7B, asterisk). The depolarization of SACs as a function of time is determined by 3 parameters: 1) the spontaneous opening of voltage-gated calcium channels, which is determined by a Poisson process defined by the noise rate constant (K_0); 2) the synaptic inputs from nearby SACs, which are weighted by a set of fixed synaptic strengths ($G_{synaptic}$); and 3) the magnitude of a sAHP (β; Figure II-7B), which is determined by the amount of time that has passed since the last depolarization relative to the decay constant of the conductance (τ_{sAHP}). Motivated by

our experimental observation that there is considerable variability in the current underlying the slow AHP (Figure II-5D) and in depolarization of individual SACs in subsequent waves (Figure II-6), we implemented this variability in the model by varying the decay time of the sAHP. Specifically, we randomly assigned each model SAC a slow decay time constant (τ_{sAHP}) from a Gaussian distribution with a mean of 50s and standard deviation of 25s.

In its original formulation, the Hennig model assumed that the spontaneous depolarization of an isolated starburst amacrine cell was roughly once every 2 minutes, as determined by recordings from rabbit SACs. To accommodate the significantly lower spontaneous depolarization rate we recorded in mice (Figure II-1), we reduced the value of the noise rate constant K_0 from 1400Hz to 1050Hz. Using this fixed value of K_0 we then varied the value of two parameters, the strength of synaptic input, $G_{synaptic}$ and the magnitude of the sAHP, β, to determine how altering them affects the spatial and temporal properties of simulated retinal waves. We tested the success of the model by comparing the interwave interval, the wavefront propagation speed, and the wave size of simulated waves to those recorded with calcium imaging (Figure II-7C-D).

Using this modified Hennig model, we found a large range of $G_{synaptic}$ and β parameters that produced waves of the same size, speed and periodicity as measured experimentally (Figure II-7C-D, Figure II-8A) as well as reproduced other experimental observations, such as the ability to initiate waves with depolarization of a single SAC (Figure II-8E) and large variability in the local participation of SACs in sequential waves (Figure II-8C-D). Hence, a model constrained by the experimentally measured slow rate of spontaneous depolarization and variability in the sAHP in SACs can recapitulate the spatial and temporal features of waves.

Waves require variability in starburst amacrine cell population

How can waves with finite size exist when the rate of initiation is so low? A low initiation rate implies that during the interval between waves, most SACs recover from the sAHP and are non-refractory. Therefore, once a wave is initiated, it should propagate across the entire retina. We hypothesize that to produce waves of finite size there must be variability in the SAC population. Specifically, there must be variability in the proportion of cells that are available for a subsequent wave. With a high rate of spontaneous depolarization, as in rabbit retina and previous models, this variability is introduced by spontaneous depolarizations and subsequent hyperpolarizations between waves. Here, we have introduced an intrinsic source of variability in the sAHP.

We tested whether variability in the sAHP is necessary to generate waves with finite spatial boundaries and once-per-minute periodicity. We assigned each model SAC a fixed τ_{sAHP} of 50s and varied $G_{synaptic}$ and β parameters. With a fixed τ_{sAHP}, we were unable to find values for $G_{synaptic}$ and β that recapitulated physiological waves for the experimentally determined K_0 value (Figure II-8B,D). Increasing $G_{synaptic}$ or decreasing β increased wave frequency to match experimental data, but the waves remained large, with each one covering the entire simulated retina. Decreasing $G_{synaptic}$ or increasing β elicited the opposite behavior: simulated waves were confined in size to those observed experimentally, but they occurred much less frequently. Hence, for the value of K_0 that produces a physiologically realistic rate of spontaneous depolarizations in SACs, there are no values of $G_{synaptic}$ and β that recapitulate physiological waves in a

network comprising SACs with identical sAHPs. These results indicate that variability within the SAC network is necessary to generate waves with the slow periodicity of once-per-minute with finite boundaries.

Discussion

We have presented both novel physiological and modeling data to identify the features of the developing retinal circuit that are critical for generating the observed spatial and temporal properties of retinal waves. Cholinergic retinal waves in mice are initiated by spontaneous depolarizations in SACs that occur at a rate one-tenth the frequency of waves. Spontaneous depolarization of a single SACs causes volume release of ACh, which is sufficient to initiate a wave. The local excitability of SACs, which affects the likelihood of wave initiation or propagation in that region, is governed by the activation of a slow afterhyperpolarization (sAHP). We modified an existing computational model of retinal waves by introducing variability into the duration of sAHPs across the population of SACs, and this crucial modification allowed us to accurately reproduce both the spontaneous activity of isolated SACs and the spatial and temporal features of waves. These results point to the critical role that variability plays in the robust generation of network activity in developing neural circuits.

Below we discuss the validity of our model assumptions and the implications of its predictions.

Wave initiation dictated by interplay between spontaneous depolarizations and network interactions.

How does the intrinsic excitability of individual SACs give rise to the spatial and temporal features of waves? In many oscillatory networks, the intrinsic periodicity of pacemaker neurons embedded in a network strongly sets the frequency of network activation (Bucher *et al.*, 2006; Tohidi & Nadim, 2009). However, this resonance frequency is also influenced by network interactions (Marder & Calabrese, 1996). In addition, there are examples of oscillatory networks in which no pacemakers have been identified, and the oscillations are an emergent property of spontaneous depolarizations, recurrent excitatory connections, and some form of synaptic depression (Tabak *et al.*, 2000; Leznik & Llinas, 2005; Rubin *et al.*, 2009).

Our model assumes that cholinergic waves are initiated by spontaneous activity in single SACs, a claim supported by our observation that depolarization of an individual SAC can initiate a wave (Figure II-2). This assumption is in contrast to previously proposed models for retinal waves in which multiple nearby SACs must be simultaneously active until a “network threshold” is reached (Butts *et al.*, 1999; Godfrey & Swindale, 2007; Hennig *et al.*, 2009). Indeed, a similar model based on a build up of activity in a cluster of nearby cells has been proposed to describe the initiation of rhythmic activity in the pre-Bötzinger complex, which controls respiratory rhythms (Rubin *et al.*, 2009), as well as in the developing spinal cord (Tabak *et al.*, 2000). Our finding that population activity can be initiated by a single neuron is consistent with recent findings in the hippocampus and cortex (Bonifazi *et al.*, 2009; Li *et al.*, 2009).

Though our model assumes that depolarizations in single SACs initiate waves, we found that, in contrast to observations in rabbit retina, a given SAC in mouse retina

has a very low probability of spontaneously depolarizing (Figure II-1). The frequency of wave initiation is limited, but not determined, by the intrinsic pacemaker properties of SACs. In a simple model in which each spontaneous depolarization of a SAC initiates a wave irrespective of previous activity, one can compute the minimum frequency of waves given the experimentally measured data (Figure II-1). The observed low rate of spontaneous depolarization would still produce waves that occur much more frequently than observed (~4 to 150 waves/min in ~1mm^2 retina containing ~1500 SACs). Hence, a balance among three factors determines the frequency of wave initiation: 1) the excitatory effects of spontaneous depolarizations; 2) the excitatory inputs from nearby SACs; and 3) the inhibitory effects of the slow afterhyperpolarizations exhibited by the SACs. The effect of the sAHP on wave initiation is discussed below.

The conductance underlying the spontaneous depolarization of SACs is not yet identified. Spontaneous calcium transients are observed in the presence of fast neurotransmitter receptors blockers (Zheng *et al.*, 2006), suggesting that these depolarizations are intrinsic to SACs. Consistent with this, spontaneous depolarizations have been observed in several types of cultured amacrine cells (Firth & Feller, 2006). Waves are not blocked by voltage gated sodium channel antagonist (Stellwagen *et al.*, 1999) but are blocked by L-type voltage gated channel antagonists (Singer *et al.*, 2001). Indeed, L-type calcium channels have been implicated in spontaneous initiation of early network activity in both hippocampus and neocortex (Crepel *et al.*, 2007; Allene *et al.*, 2008).

Wave propagation via diffuse action of ACh

Our model assumes that waves propagate via excitatory connections between SACs. This substrate for propagation was proposed by a computational model (Feller *et al.*, 1997) and evidence for direct synaptic connections between SACs was provided for rabbit retina (Zheng *et al.*, 2004). Here we confirmed the existence of a recurrent network of SACs in mouse (Figure II-3). In addition, we find that ACh released during waves can be detected several microns above the surface of the retina using a cell-based ACh sensor, indicating volume release of ACh during waves.

We postulate volume release of ACh is responsible for wave propagation. First, using paired recordings of SACs we found that EPSCs last several seconds past the end of the depolarization, indicating they are not mediated by a conventional monosynaptic connection. Second, waves drive correlated calcium transients in ON and OFF ganglion cells (Wong & Oakley, 1996) as well as cells in the inner nuclear layer (Wong *et al.*, 1995). At this age, the processes of SACs in the INL and GCL form two discrete bands (Stacy & Wong, 2003) and therefore do not have direct synaptic connections. Hence, the correlation between ON and OFF ganglion cells, which have processes in distinct layers within the IPL, is evidence of diffuse action of ACh. Indeed, in rabbit retina, there is evidence that ACh released in the inner retina is able to activate muscarinic receptors on cells in the ventricular zone (Syed *et al.*, 2004). Given that later in development, when waves are mediated by a glutamatergic circuit, there is direct evidence that waves are accompanied by volume release of glutamate (Blankenship *et al.*, 2009), these data are consistent with the diffuse action of neurotransmitter as a characteristic feature of developing circuits that exhibit spreading depolarization (Allene *et al.*, 2008).

Wave boundaries are determined by variability in sAHP refractory period

We recorded a slow afterhyperpolarization in SACs following either spontaneous or evoked depolarizations (Figure II-5). Our model predicts that this sAHP influences the network in two ways. First, the sAHP in nearby SACs creates refractory regions of the retina that limit the spatial extent over which waves propagate. Second, these local refractory regions determine whether the spontaneous depolarization of a single SAC can initiate a wave.

The interval between waves is approximately one minute, similar to the time course of the refractory period. Hence, one might expect that this low initiation rate would provide enough time for all SACs to recover from their refractory period before they participate in a subsequent wave. Why is it that each wave fails to propagate over the entire retina? In previous models (Godfrey & Swindale, 2007; Hennig *et al.*, 2009), the refractory period was determined by a high rate of spontaneous activity in SACs that was not correlated with waves. Since this assumption is not consistent with our observation that SACs rarely depolarize independent of waves (Figure II-1), we introduced variability in the form of different duration sAHPs for different SACs. Hence in our model, individual SACs within a local region will participate in a wave depending upon the extent to which the sAHP has recovered from the previous wave. The variability of the sAHP makes this refractoriness a dynamic variable, such that every wave activates a different population of SACs, altering the shapes of the refractory regions and thereby altering the boundaries for waves.

Variability within neuronal circuits is thought to be important for neuronal computations. In olfactory bulb, sister mitral cells innervating the same glomerulus express different levels of voltage-gated ion channels that impart different firing characteristics during stimulus presentation (Padmanabhan & Urban, 2010). This variability reduces redundancy and can provide extra information about stimulus features. Here, variability within the SAC network prevents waves from encompassing the entire retina. Our data points to variability in the conductance underlying the sAHP as a source of variable participation during waves. Single cell genomics studies in developing retina point to diversity of gene expression within SACs (Cherry *et al.*, 2009). How this variability in gene expression maps to functional variability remains an intriguing question.

Experimental Procedures

Animals. All experiments were performed on acutely isolated mouse retinas. Male and female C57Bl/6 mice obtained from Harlan were used for all WT recordings. mGluR2-GFP mice contain a transgene insertion of interleukin-2 receptor fused GFP under control of the mGluR2 promoter (Watanabe *et al.*, 1998). ChAT-Cre/TdTom mice were generated by crossing a mouse in which an IRES-Cre recombinase is knocked in downstream of the endogenous choline acetyl transferase gene (Ivanova *et al.*, 2010) with a separate tdTomato driver line (B6.129S6-ChAT$^{tm1(cre)lowl}$/J x B6.129S6-Gt(ROSA)26Sor$^{tm9(CAG-tdTomato)Hze}$/J, Jackson Labs). All animal procedures were approved by the University of California, Berkeley and conformed to the National Institutes of Health *Guide for the Care and Use of Laboratory Animals*, the Public Health

Service Policy, and the Society for Neuroscience Policy on the Use of Animals in Neuroscience Research.

Whole-Mount Retinal Preparation. P2-P6 mice were anesthetized with isoflurane and decapitated. Retinas were isolated in cold artificial cerebrospinal fluid (ACSF) (in mM: 119 NaCl, 26.2 $NaHCO_3$, 11 glucose, 2.5 KCl, 1 K_2HPO_4, 2.5 $CaCl_2$, 1.3 $MgCl_2$) and mounted RGC side-up on filter paper. Retinas were incubated at room temperature in oxygenated ACSF until transfer to the recording chamber, where they were continually superfused with oxygenated ACSF at 30-34C.

Electrophysiology. Perforated patch and whole cell recordings were made from whole-mount retinas from mice aged P4-P6. Perforated patch recording were necessary because whole cell recordings resulted in rundown of the sAHP (Zheng *et al.*, 2006) (data not shown) and ability to initiate waves. The inner limiting membrane was removed using a glass recording pipette and SACs were identified using fluorescence and targeted using a Sutter micromanipulator. Voltage clamp recordings were sampled at 2.5kHz and filtered at 1kHz. Current clamp recordings were sampled at 5kHz and filtered at 2kHz. Analysis was performed using custom MATLAB (Mathworks) scripts. All reported voltages are corrected for liquid junction potential.

To stimulate SACs (Figure II-2), perforated patch current clamp recordings were used. Recording pipettes were front-filled with a potassium chloride internal solution (in mM: 122 KCl, 20 HEPES, 0.5 EGTA, 2 NaCl, pH 7.2, liquid junction potential: 0mV) and then back-filled with internal solution containing 750µg/ml Amphotericin B made fresh hourly. Seals were formed and then access resistance was monitored continuously. Recordings were performed when access resistance was stable and less than 5% of the input resistance of the cell (typically, R_a 30-80 MOhm, R_{in} 1-2GOhm). 100pA of current was injected for 1.5s every 60s for 10minutes. Cells were excluded if no calcium transient was observed within the recorded cell or if spontaneous break-in occurred.

Whole cell recordings from ganglion cells (Figure II-4) and paired recordings of SACs were performed (Figure II-3) using whole-cell voltage clamp recordings. A cesium based internal (in mM: 110 $CsMeSO_4$, 2.8 NaCl, 4 EGTA, 5 TEA-Cl, 4 adenosine 5′-triphosphate disodium salt, 0.3 guanosine 5′-triphosphate trisodium salt, 20 HEPES and 10 phosphocreatine disodium salt, 0.025 Alexa 568, pH 7.2, liquid junction potential: 10mV) was used to isolate synaptic conductances. Synaptic blockers used to isolate cholinergic currents are described in the Results.

To characterize the sAHP in SACs (Figure II-5), perforated patch voltage and current clamp recordings were used. Current clamp recordings of waves were performed as described in methods above for stimulating SACs. To isolate the sAHP and I_{sAHP}, experiments were performed in the presence of DHβE (4µM) and gabazine (5µM), which block nAChR and GABA-A receptor mediated synaptic conductances, and tolbutamide (100µM), to block an ATP sensitive potassium conductance that develops during prolonged recordings (data not shown). A gluconate-based perforated patch internal was used for voltage clamp experiments by replacing 116mM KCl with equimolar KGluconate (liquid junction potential: 14mV). To ensure stable recording of I_{sAHP}, access resistance was monitored and recordings were performed when access resistance was stable. Maximum amplitude and kinetics of the slow AHP were not

correlated with access resistance.

Calcium Imaging. Retinas from mice aged P2- P6 were bulk loaded with the calcium indicator Oregon Green Bapta-1 AM (OGB-1 AM) using the multicell bolous loading technique (Stosiek *et al.*, 2003; Blankenship *et al.*, 2009). Epifluorscence imaging and analysis as described earlier (Blankenship *et al.*, 2009). Two-photon (Figure II-6) calcium imaging of mGluR2-GFP retinas was performed using a custom-modified two-photon microscope (Fluoview 300, Olympus America Inc.). Focal planes consisting of cell bodies in the ganglion cell layer were used. Time series images were acquired at 1Hz using a 60x objective (Olympus LUMPlanFI/IR 60x/0.90W) with the excitation laser tuned to 790nm. Following acquisition of the calcium signal, the laser was retuned to 920nm to preferentially excite GFP or TdTomato to allow for identification of SACs in the ganglion cell layer. Images were corrected for motion artifacts and filtered to remove line-scan artifacts. Regions of interest were manually drawn around all cells in the field of view. Fluorescence signals were plotted and peaks were manually identified for all cells. To quantify within-cell variability of peak amplitudes, peak amplitudes from each cell were normalized to the mean peak amplitude for all waves in that cell.

For simultaneous perforated patch recording and calcium imaging from P4-P6 mGluR2-GFP retinas (Figure II-2), waves in the region surrounding the recorded cell were detected by thresholding the derivative of the fluorescence signal of a 200x200μm box region around the cell. Fluorescence changes evoked by current injection were assayed by observing the change in fluorescence in the 2s following current injection. Waves triggered by the current injection were identified by an increasing spread of calcium signal originating from the site of recording and confirmed by inspecting the original imaging data. 1 of 12 current injections that evoked a wave occurred on the first current injection (30s after the start of imaging) and preceded any spontaneous waves in the imaged region, hence, the interval of the preceding wave was unknown but was greater than 30s. We found that prolonged recordings, despite perforated patch configuration, resulted in an inability to evoke waves from cells that previously could robustly initiate waves. Therefore, we limited our analysis to the time period before the last evoked wave during the stimulation protocol. Current injections that occurred simultaneously with spontaneous waves were excluded. A total of 24 of 70 current injections met these criteria. 8 of 17 SACs were found to initiate at least one wave. The actual fraction of SACs that can initiate a wave is likely to be higher as our experimental paradigm is subject to rundown.

Analysis of wave front properties (Figures II-7 and 8) was performed using custom scripts in MATLAB, as describe previously (Blankenship *et al.*, 2009).

CNiFERs imaging. M1 and mCherry CNiFERs were acquired (Nguyen *et al.*, 2010). CNiFERs were maintained in a humidified incubator at 37C in growth media containing Dulbecco's Minimum Essentials Medium (Invitrogen) supplemented with 10% FBS (Invitrogen). Prior to experiments, CNiFERs were removed from dishes without trypsin and concentrated in growth media. CNiFERs were loaded into a glass capillary with a tip size ~20μm. M1 and mCherry CNiFERs were pressure ejected onto the inner limiting membrane (ILM) of retinas and allowed to settle onto the surface. Clusters of several dozen cells were imaged at a focal plane ~5-10μm above the ILM. In imaging

with simultaneous voltage clamp recordings, a hole in the ILM was torn usually 50-200μm from the imaged CNiFERs.

FRET images were acquired at 1Hz using a 60x objective. The excitation wavelength was 435nm. Individual FRET channel detection was accomplished by using a Dual-View image splitter (Optical Insights) with appropriate yellow and cyan channel filters. Images were digitized as during calcium imaging experiments above. Background fluorescence was subtracted from both channels. FRET ratios were computed as background corrected YFP/CFP fluorescence averaged over a box region of interest around M1 or mCherry CNiFERs. Peaks were detected manually for analysis. For wave triggered FRET changes, peak wave associated inward currents were detected manually from voltage clamp recordings and FRET measurements were aligned to the times of each peak current.

Modeling. C/C++ code for the wave model was acquired as described in (Hennig *et al.*, 2009). In this model, the membrane potential of each cell is influenced by a set of conductances. A voltage-gated calcium channel conductance was modeled using a Morris-Lecar model. Calcium influx was proportional to the low pass filtered calcium current. The current that gives rise to the sAHP was modeled as a calcium-dependent potassium conductance. The state of this conductance depends on the calcium concentration and a second slower process with a slow time constant (τ_{sAHP}) and fourth order dependence on calcium. The influence of the slow process on the current was weighted with the parameter β. A noise conductance was implemented as filtered shot noise with a voltage-dependent rate that was dependent upon K_0 and the voltage-gated calcium channel activation function. Synaptic conductances were summed from all neighboring cells within a three cell radius (Figure II-7). Published parameters were used for the model except as presented in the Results section. The Hennig model code was modified to output the position and time of active cells (defined by threshold for calcium spike computed from parameter values). Simulations were run for 20 minutes following a 90s warmup period on a 56x56 hexagonal lattice of SACs, using the central 50x50 for analysis. Spacing between cells was set at 25μm.

MATLAB/C code was developed to analyze the spatial and temporal aspects of the data generated from the models (Figures II-7 and 8). The set of active cells during 750ms time steps was recorded and each cell was either assigned a new wave number or inherited a wave number of neighboring cells. Simulated waves that merged were excluded from analysis for comparison with calcium imaging data. Wave speed was calculated in a manner similar to the calcium imaging analysis, using the last active cell of a wave as the end point of the wave path. All simulations and analysis were performed on an Intel Core i7 desktop running Linux. Simulations of the Hennig model took ~45 real-time minutes, limiting extensive parameter searching.

References

Allene, C., Cattani, A., Ackman, J.B., Bonifazi, P., Aniksztejn, L., Ben-Ari, Y. & Cossart, R. (2008) Sequential generation of two distinct synapse-driven network patterns in developing neocortex. *J Neurosci*, **28**, 12851-12863.

Bansal, A., Singer, J.H., Hwang, B.J., Xu, W., Beaudet, A. & Feller, M.B. (2000) Mice lacking specific nicotinic acetylcholine receptor subunits exhibit dramatically altered spontaneous activity patterns and reveal a limited role for retinal waves in forming ON and OFF circuits in the inner retina. *J Neurosci*, **20**, 7672.

Blankenship, A.G. & Feller, M.B. (2010) Mechanisms underlying spontaneous patterned activity in developing neural circuits. *Nat Rev Neurosci*, **11**, 18-29.

Blankenship, A.G., Ford, K.J., Johnson, J., Seal, R.P., Edwards, R.H., Copenhagen, D.R. & Feller, M.B. (2009) Synaptic and Extrasynaptic Factors Governing Glutamatergic Retinal Waves. *Neuron*, **62**, 230.

Bonifazi, P., Goldin, M., Picardo, M.A., Jorquera, I., Cattani, A., Bianconi, G., Represa, A., Ben-Ari, Y. & Cossart, R. (2009) GABAergic Hub Neurons Orchestrate Synchrony in Developing Hippocampal Networks. *Science*, **326**, 1419.

Bucher, D., Taylor, A.L. & Marder, E. (2006) Central Pattern Generating Neurons Simultaneously Express Fast and Slow Rhythmic Activities in the Stomatogastric Ganglion. *J Neurophysiol*, **95**, 3617-3632.

Butts, D.A., Feller, M.B., Shatz, C.J. & Rokhsar, D.S. (1999) Retinal Waves Are Governed by Collective Network Properties. *J. Neurosci.*, **19**, 3580-3593.

Butts, D.A., Kanold, P.O. & Shatz, C.J. (2007) A Burst-Based "Hebbian" Learning Rule at Retinogeniculate Synapses Links Retinal Waves to Activity-Dependent Refinement. *PLoS Biol*, **5**, e61.

Chandrasekaran, A.R., Shah, R.D. & Crair, M.C. (2007) Developmental Homeostasis of Mouse Retinocollicular Synapses. *J. Neurosci.*, **27**, 1746.

Cherry, T.J., Trimarchi, J.M., Stadler, M.B. & Cepko, C.L. (2009) Development and diversification of retinal amacrine interneurons at single cell resolution. *Proc Natl Acad Sci U S A*, **106**, 9495-9500.

Crepel, V., Aronov, D., Jorquera, I., Represa, A., Ben-Ari, Y. & Cossart, R. (2007) A parturition-associated nonsynaptic coherent activity pattern in the developing hippocampus. *Neuron*, **54**, 105-120.

Feller, M.B., Butts, D.A., Aaron, H.L., Rokhsar, D.S. & Shatz, C.J. (1997) Dynamic Processes Shape Spatiotemporal Properties of Retinal Waves. *Neuron*, **19**, 293.

Feller, M.B., Wellis, D.P., Stellwagen, D., Werblin, F.S. & Shatz, C.J. (1996) Requirement for cholinergic synaptic transmission in the propagation of spontaneous retinal waves. *Science*, **272**, 1182.

Firth, S.I. & Feller, M.B. (2006) Dissociated GABAergic retinal interneurons exhibit spontaneous increases in intracellular calcium. *Vis Neurosci*, **23**, 807.

Ford, K.J. & Feller, M.B. (2011) Assembly and disassembly of a retinal cholinergic network. *Visual Neuroscience*, **28**, 1-11.

Galli, L. & Maffei, L. (1988) Spontaneous impulse activity of rat retinal ganglion cells in prenatal life. *Science*, **242**, 90-91.

Godfrey, K.B. & Eglen, S.J. (2009) Theoretical models of spontaneous activity generation and propagation in the developing retina. *Molecular BioSystems*, **5**, 1527-1535.

Godfrey, K.B. & Swindale, N.V. (2007) Retinal Wave Behavior through Activity-Dependent Refractory Periods. *PLoS Computational Biology*, **3**, e245.

Hennig, M.H., Adams, C., Willshaw, D. & Sernagor, E. (2009) Early-Stage Waves in the Retinal Network Emerge Close to a Critical State Transition between Local and Global Functional Connectivity. *J. Neurosci.*, **29**, 1077.

Huberman, A.D., Feller, M.B. & Chapman, B. (2008) Mechanisms Underlying Development of Visual Maps and Receptive Fields. *Annual Review of Neuroscience*, **31**, 479-509.

Ivanova, E., Hwang, G.S. & Pan, Z.H. (2010) Characterization of transgenic mouse

lines expressing Cre recombinase in the retina. *Neuroscience*, **165**, 233-243.

Kerr, J.N., Greenberg, D. & Helmchen, F. (2005) Imaging input and output of neocortical networks in vivo. *Proc Natl Acad Sci U S A*, **102**, 14063-14068.

Leznik, E. & Llinas, R. (2005) Role of Gap Junctions in Synchronized Neuronal Oscillations in the Inferior Olive. *J Neurophysiol*, **94**, 2447-2456.

Li, C.Y., Poo, M.M. & Dan, Y. (2009) Burst spiking of a single cortical neuron modifies global brain state. *Science*, **324**, 643-646.

Marder, E. & Calabrese, R.L. (1996) Principles of rhythmic motor pattern generation. *Physiol. Rev.*, **76**, 687-717.

Meister, M., Wong, R.O., Baylor, D.A. & Shatz, C.J. (1991) Synchronous bursts of action potentials in ganglion cells of the developing mammalian retina. *Science*, **252**, 939-943.

Nguyen, Q.T., Schroeder, L.F., Mank, M., Muller, A., Taylor, P., Griesbeck, O. & Kleinfeld, D. (2010) An in vivo biosensor for neurotransmitter release and in situ receptor activity. *Nat Neurosci*, **13**, 127-132.

Nicol, X., Voyatzis, S., Muzerelle, A., Narboux-Neme, N., Sudhof, T.C., Miles, R. & Gaspar, P. (2007) cAMP oscillations and retinal activity are permissive for ephrin signaling during the establishment of the retinotopic map. *Nat Neurosci*, **10**, 340-347.

Padmanabhan, K. & Urban, N.N. (2010) Intrinsic biophysical diversity decorrelates neuronal firing while increasing information content. *Nat Neurosci*, **13**, 1276-1282.

Pfeiffenberger, C., Yamada, J. & Feldheim, D.A. (2006) Ephrin-As and Patterned Retinal Activity Act Together in the Development of Topographic Maps in the Primary Visual System. *J. Neurosci.*, **26**, 12873-12884.

Rubin, J.E., Hayes, J.A., Mendenhall, J.L. & Del Negro, C.A. (2009) Calcium-activated nonspecific cation current and synaptic depression promote network-dependent burst oscillations. *Proceedings of the National Academy of Sciences*, **106**, 2939-

2944.

Sargent, P.B. (1993) The Diversity of Neuronal Nicotinic Acetylcholine Receptors. *Annual Review of Neuroscience*, **16**, 403-443.

Sarter, M., Parikh, V. & Howe, W.M. (2009) Phasic acetylcholine release and the volume transmission hypothesis: time to move on. *Nat Rev Neurosci*, **10**, 383-390.

Shah, R.D. & Crair, M.C. (2008) Retinocollicular Synapse Maturation and Plasticity Are Regulated by Correlated Retinal Waves. *J. Neurosci.*, **28**, 292.

Singer, J.H., Mirotznik, R.R. & Feller, M.B. (2001) Potentiation of L-type calcium channels reveals nonsynaptic mechanisms that correlate spontaneous activity in the developing mammalian retina. *J Neurosci*, **21**, 8514.

Stacy, R.C. & Wong, R.O. (2003) Developmental relationship between cholinergic amacrine cell processes and ganglion cell dendrites of the mouse retina. *The Journal of Comparative Neurology*, **456**, 154.

Stellwagen, D., Shatz, C.J. & Feller, M.B. (1999) Dynamics of Retinal Waves Are Controlled by Cyclic AMP. *Neuron*, **24**, 673.

Stosiek, C., Garaschuk, O., Holthoff, K. & Konnerth, A. (2003) In vivo two-photon calcium imaging of neuronal networks. *Proceedings of the National Academy of Sciences of the United States of America*, **100**, 7319-7324.

Syed, M.M., Lee, S., He, S. & Zhou, Z.J. (2004) Spontaneous waves in the ventricular zone of developing mammalian retina. *J Neurophysiol*, **91**, 1999-2009.

Tabak, J., Senn, W., O'Donovan, M.J. & Rinzel, J. (2000) Modeling of Spontaneous Activity in Developing Spinal Cord Using Activity-Dependent Depression in an Excitatory Network. *J. Neurosci.*, **20**, 3041-3056.

Tohidi, V. & Nadim, F. (2009) Membrane Resonance in Bursting Pacemaker Neurons of an Oscillatory Network Is Correlated with Network Frequency. *J. Neurosci.*, **29**, 6427-6435.

Wang, C.-T., Blankenship, A.G., Anishchenko, A., Elstrott, J., Fikhman, M., Nakanishi, S. & Feller, M.B. (2007) GABAA Receptor-Mediated Signaling Alters the Structure of Spontaneous Activity in the Developing Retina. *J. Neurosci.*, **27**, 9130.

Watanabe, D., Inokawa, H., Hashimoto, K., Suzuki, N., Kano, M., Shigemoto, R., Hirano, T., Toyama, K., Kaneko, S., Yokoi, M., Moriyoshi, K., Suzuki, M., Kobayashi, K., Nagatsu, T., Kreitman, R.J., Pastan, I. & Nakanishi, S. (1998) Ablation of Cerebellar Golgi Cells Disrupts Synaptic Integration Involving GABA Inhibition and NMDA Receptor Activation in Motor Coordination. *Cell*, **95**, 17.

Wong, R.O., Chernjavsky, A., Smith, S.J. & Shatz, C.J. (1995) Early functional neural networks in the developing retina. *Nature*, **374**, 716-718.

Wong, R.O.L. & Oakley, D.M. (1996) Changing Patterns of Spontaneous Bursting Activity of On and Off Retinal Ganglion Cells during Development. *Neuron*, **16**, 1087.

Xu, H.P., Furman, M., Mineur, Y.S., Chen, H., King, S.L., Zenisek, D., Zhou, Z.J., Butts, D.A., Tian, N., Picciotto, M.R. & Crair, M.C. (2011) An instructive role for patterned spontaneous retinal activity in mouse visual map development. *Neuron*, **70**, 1115-1127.

Zheng, J., Lee, S. & Zhou, Z.J. (2006) A transient network of intrinsically bursting starburst cells underlies the generation of retinal waves. *Nat Neurosci*, **9**, 363.

Zheng, J.J., Lee, S. & Zhou, Z.J. (2004) A developmental switch in the excitability and function of the starburst network in the mammalian retina. *Neuron*, **44**, 851.

Zhou, Z.J. (1998) Direct participation of starburst amacrine cells in spontaneous rhythmic activities in the developing mammalian retina. *J Neurosci*, **18**, 4155.

Figure II-1. Starburst amacrine cells (SACs) rarely exhibit spontaneous depolarizations.
(A) Left: Fluorescence image of an mGluR2-GFP retina loaded with OGB using a filter set that allowed for visualization of both OGB and GFP fluorescence. Right: Fluorescence image of GFP+ cells generated by acquiring an image of the same field using a filter set that allowed for visualization of OGB (not shown) and subtracting it from image shown in A. Regions of interest are shown around each SAC. Scale bar: 20μm.
(B) Time course of ΔF/F averaged over the somas of 3 cells (labeled in A) in the absence (CTR, top) and in the presence of nAChR antagonist DHβE (4μM) and GABA-A receptor antagonist gabazine (5μM) (bottom).
(C) Raster plots of calcium transients generated from the thresholded derivatives of the ΔF/F traces. Numbered cells from B are highlighted in red. All 34 cells from A are shown in CTR (left) and DHβE (4μM) + gabazine (5μM) (right).
(D) Mean number of calcium transients per minute in SACs vs postnatal age for each retina (18-34 SACs per retina) during 10 or 20 minutes of imaging in control (left) and during blockade of waves using either DHβE (2-8μM) + gabazine (5μM) or DHβE (2-8μM) alone (middle). Right: Mean peak ΔF/F vs postnatal age during blockade of waves. Mean±SD of peak ΔF/F evoked by current injection protocol used in Figure II-2 shown in red (n=4 cells).

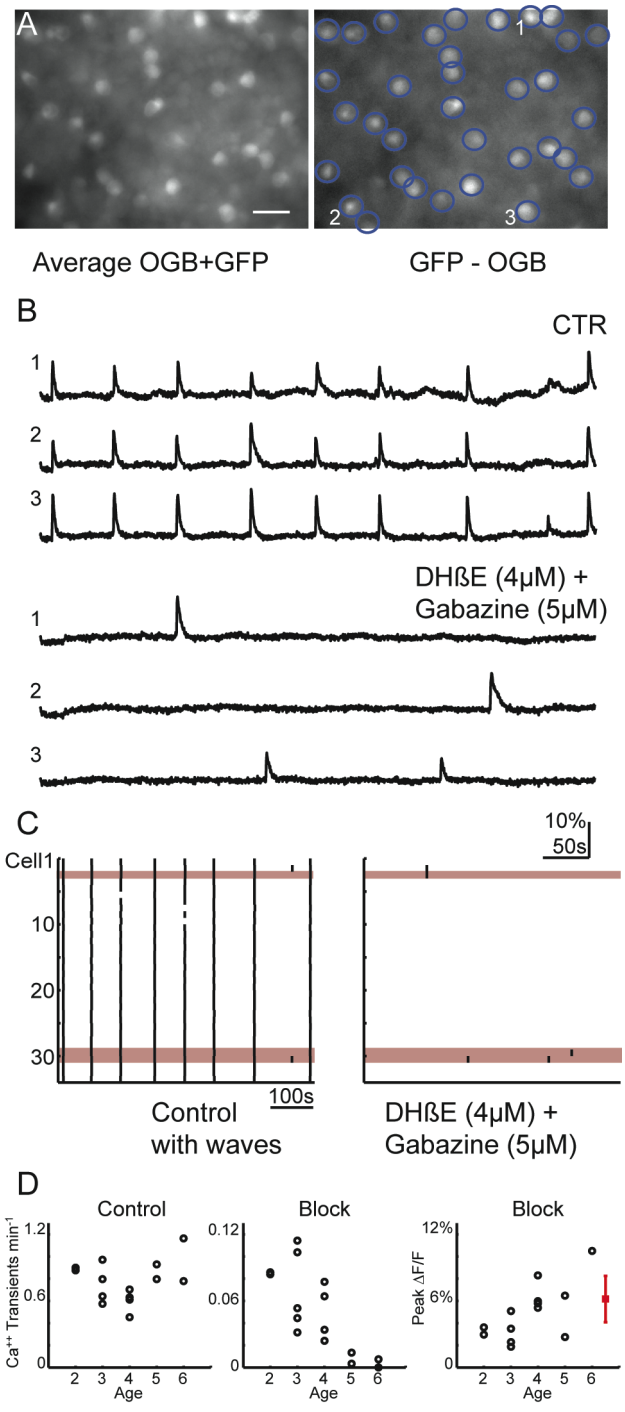
A
1
2
3
Average OGB+GFP
GFP - OGB
B
CTR
1
2
3
DHßE (4µM) +
Gabazine (5µM)
1
2
3
C
10%
50s
Cell1
10
20
30
100s
Control
with waves
DHßE (4µM) +
Gabazine (5µM)
D
Control
Block
Block
Ca++ Transients min-1
1.2
0.6
0
0.12
0.06
0
12%
6%
0
Peak ΔF/F
2 3 4 5 6
Age
2 3 4 5 6
Age
2 3 4 5 6
Age

Figure II-2. Single SACs can initiate retinal waves.
(A) Fluorescence image of an mGlur2-GFP retina loaded with calcium indicator OGB-1AM. Position of recording electrode indicated in red. Scale bar: 50μm.
(B) Two examples of current injection experiments in configuration shown in A. Sequence of images are pseudocolored to represent the fractional change in fluorescence (ΔF/F) at each pixel following current injection. Interval between panels is 0.5s. Int = the interval between current injection and the time of the previous wave. Top: Current injection did evoke a wave; Bottom: current injection did not evoke a wave.
(C) Histogram distribution of the intervals between current injection and the time of the previous wave. Black bars are the distribution of all intervals between current injections and the preceding wave. Red bars indicate the subset of current injections that evoked a wave.

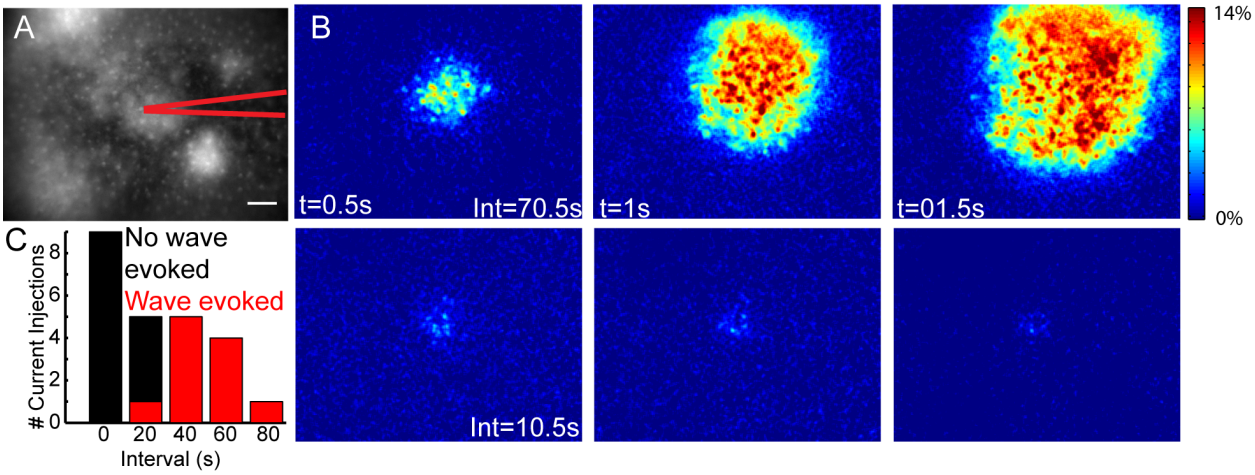
A
B
t=0.5s
Int=70.5s
t=1s
t=01.5s
14%
0%
C
No wave evoked
Wave evoked
Current Injections
0
2
4
6
8
0
20
40
60
80
Interval (s)
Int=10.5s

Figure II-3. SACs make cholinergic connections with neighboring SACs.
(A) Live fluorescence image of a SAC-SAC pair filled with Alexa-568.
(B) Paired recording from two neighboring SACs. Top: voltage clamp recording from presynaptic SAC. Bottom: Postsynaptic currents recorded from postsynaptic SAC at 5 different holding potentials. Voltage command protocols for pre- and post-synaptic cells are shown below current traces.
(C) Current voltage relationship of the peak current measured in the postsynaptic SAC following step depolarization of the presynaptic SAC. Currents are normalized to the maximum inward current for each cell. Line represents the average ± SEM for 5 cell pairs.
(D) Paired recording showing reciprocal connections. Averaged pre- and post-synaptic currents from 4 repetitions are shown for cells in response to a 50ms depolarization from -70mV to -10mV. Holding potential is -70mV.
(E) Simultaneous voltage clamp recordings of compound postsynaptic current from two neighboring SACs (V_h= -70mV). Recording was performed in the presence of GABA receptor antagonists (gabazine 5μM, TPMPA 50μM, CGP 55845 2μM).

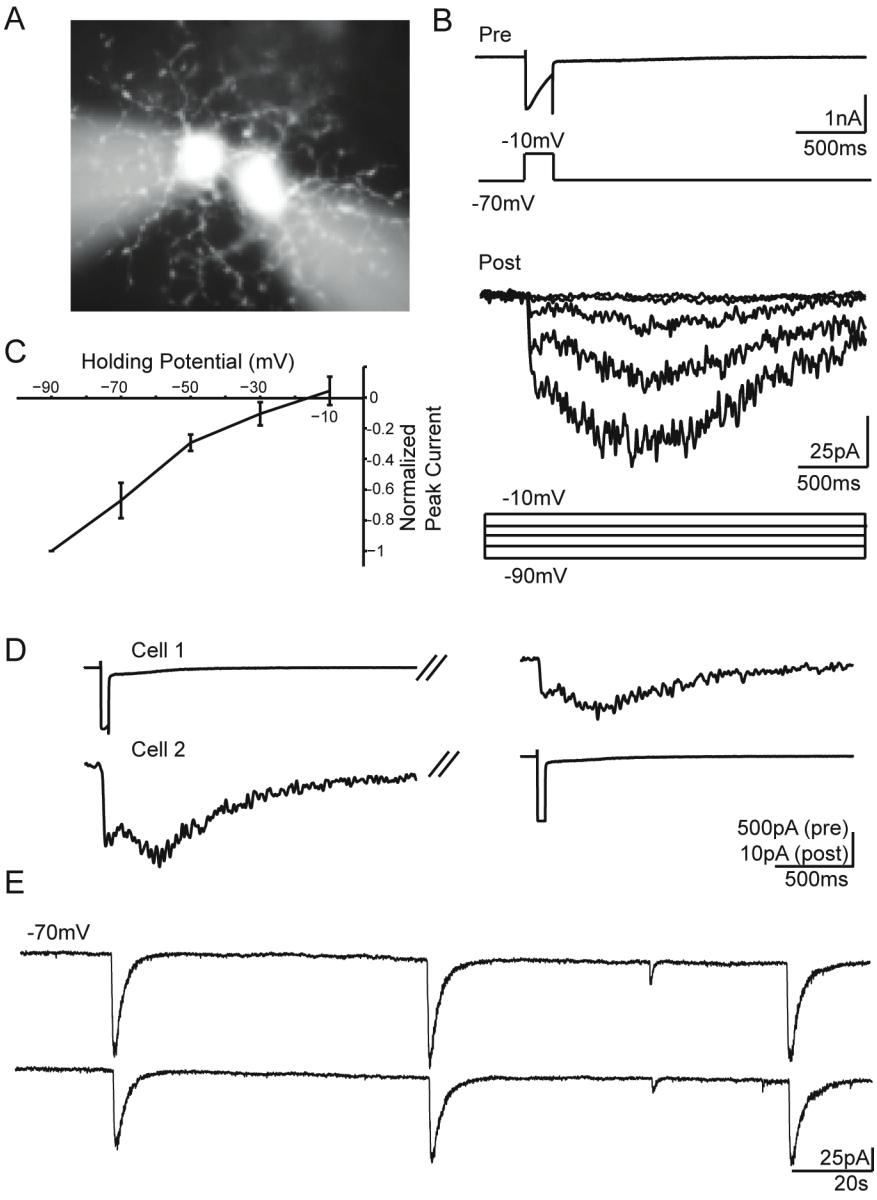
A
B
Pre
1nA
500ms
-10mV
-70mV
Post
25pA
500ms
-10mV
-90mV
C
Holding Potential (mV)
−90
−70
−50
−30
−10
0
-0.2
-0.4
-0.6
-0.8
-1
Normalized Peak Current
D
Cell 1
Cell 2
500pA (pre)
10pA (post)
500ms
E
-70mV
25pA
20s

Figure II-4: Acetylcholine is released diffusely by SACs
(A) Inset: Schematic of experimental design. DIC image of whole mount retina with fluorescent overlay of M1 and mCherry CNiFERs resting on top of the ILM of a P4 retina. Boxes indicate the region of interest around M1 (green) and mCherry (blue) CNiFERs for traces below.
(B) YFP and CFP channel fluorescence (M1 only) and YFP/CFP ratio of CNiFERs in control (left) and 8μM DHβE (right). Voltage clamp recording (VC=-70mV) from a nearby RGC (see DIC image) are shown below.
(C) Wave triggered average YFP/CFP ratio. FRET ratios for M1 (green) and mCherry (blue) CNiFERs are aligned to the peak inward current during waves as measured from simultaneous voltage clamp recordings from nearby RGCs. N=108 waves from 10 retinas (M1) and 46 waves from 5 retinas (mCherry). Shaded region represents mean±SD.
(D) Average peak ΔR of CNiFERs FRET transients in control ACSF and during application of 8μM DHβE. Data from retinas aged P0 to P6.
(E) Distribution of inter-peak intervals of FRET transients in control (white) and 8μM DhβE (red). Data from retinas aged P0 to P6.

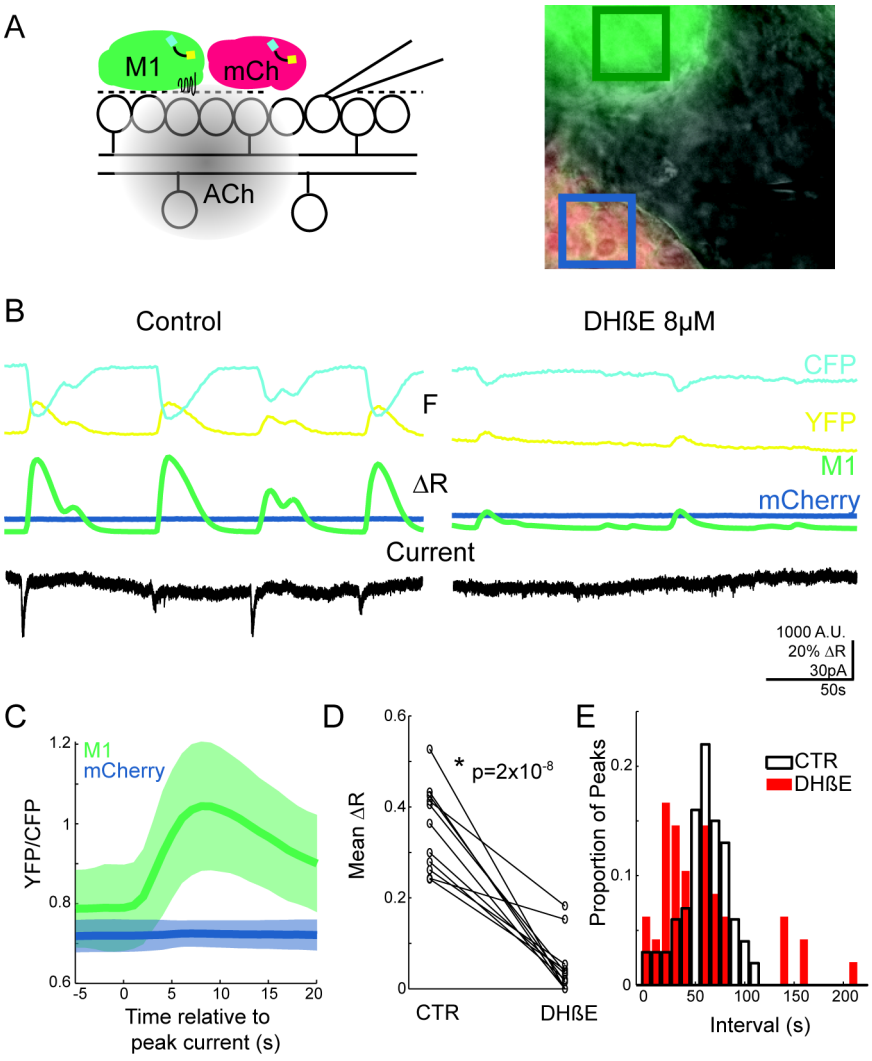
A
M1
mCh
ACh
B
Control
DHßE 8µM
CFP
YFP
F
M1
mCherry
ΔR
Current
1000 A.U.
20% ΔR
30pA
50s
C
M1
mCherry
YFP/CFP
Time relative to
peak current (s)
D
* p=2x10-8
Mean ΔR
CTR
DHßE
E
CTR
DHßE
Proportion of Peaks
Interval (s)

Figure II-5. SACs exhibit a slow afterhyperpolarization (sAHP).
(A) Left: Live fluorescence image of an mGluR2-GFP retina. Right: Same retina with SAC targeted for whole cell recording and filled with Alexa 568. Scale bar: 10μm.
(B) Current clamp perforated patch recording from a SAC exhibiting wave-induced depolarizations followed by sAHPs. Inset: Magnified view of calcium spikes during wave-induced depolarization.
(C) Left: Current clamp perforated patch recording showing sAHP following current injection (100 pA for 500 msec). Inset: Calcium spikes during current injection. Vertical scale bar: 10mV; Horizontal scale bar: 1s.
(D) Voltage clamp perforated patch recording from SAC. Average current (black line) ± SD (gray region) measured following depolarization from -64mV to -14mV.

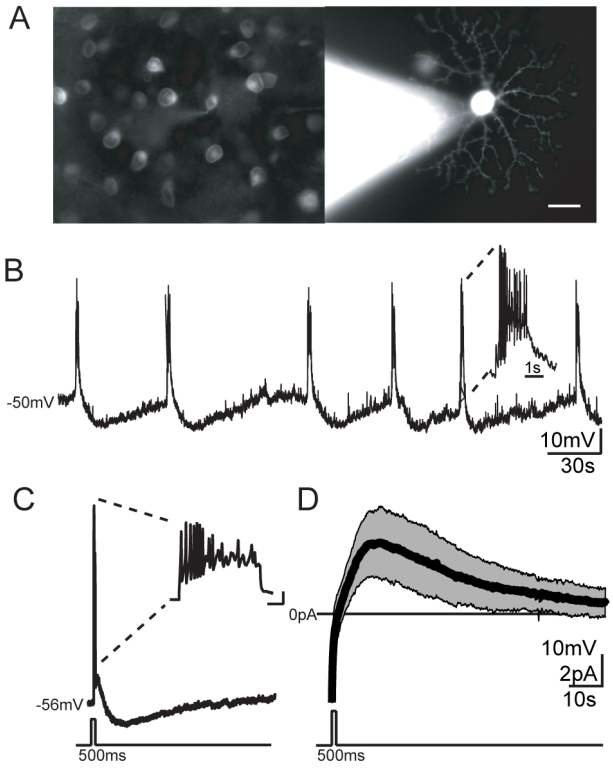
A
B
-50mV
1s
10mV
30s
C
-56mV
500ms
D
0pA
10mV
2pA
10s
500ms

Figure II-6. Two-photon imaging in SACs reveals variable participation in waves
(A) Fluorescence images of mGluR2-GFP mice labeled with calcium indicator OGB-1AM. Single two-photon optical section through ganglion cell layer using 790nm to excite OGB (top) or 920nm to excite GFP (bottom). Regions of interest are shown around non-SACs (white) and SACs (blue).
(B) ΔF/F traces from non-SACs (top, black) or SACs (bottom, blue). Dotted lines precede waves for clarity.
(C) Average of all peak ΔF/F of non-SACs and SACs with somas in the ganglion cell layer (mean±SD).
(D) Cumulative probability of within-cell variance of peak ΔF/F for non-SACs and SACs in the ganglion cell layer.
(E) Amplitude of peak ΔF/F as a function of the preceding peak ΔF/F in non-SACs (left) and SACs (right) in the ganglion cell layer. Peak amplitudes are normalized to the mean peak amplitude for each cell.

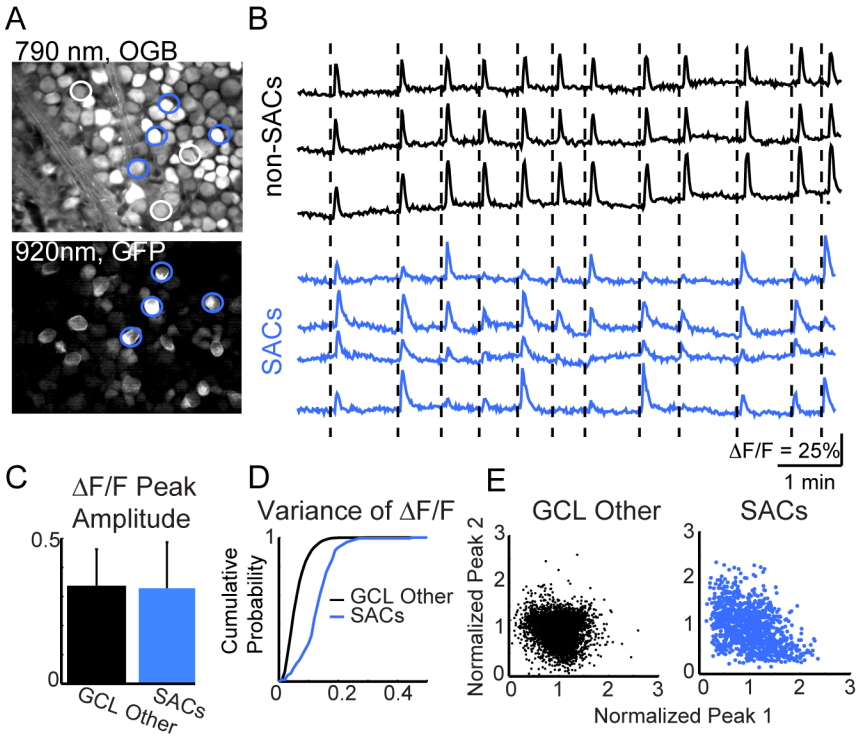
A
790 nm, OGB
920nm, GFP
B
non-SACs
SACs
ΔF/F = 25%
1 min
C
ΔF/F Peak Amplitude
0.5
0
GCL Other
SACs
D
Variance of ΔF/F
Cumulative Probability
1
0
0.2
0.4
GCL Other
SACs
E
GCL Other
SACs
Normalized Peak 2
Normalized Peak 1
0
1
2
3

Figure II-7. A computational model based on infrequent SAC spontaneous depolarizations recapitulates spatial and temporal properties of retinal waves.
(A) Schematic of excitatory connections between SACs in the model. Colored circles represent the scale factor that defines the strength of the synaptic connections between neighboring cell and the center cell. Depolarization due to synaptic input is the product of synaptic scale factor, $G_{synaptic}$, and the amount of presynaptic depolarization.
(B) Membrane potential of modeled SACs in response to current injection (arrowhead). The responses for two values for the slow AHP parameter (β) are shown. For this example, the noise rate constant (K_0) was set to 1050Hz. Asterisk indicates a spontaneous depolarization generated by membrane noise.
(C) Top: Spatial extent of three experimentally recorded waves. Bottom: Three simulated waves using simulation parameter values: K_0 1050Hz; β 200; $G_{synaptic}$ 650; τ_{sAHP} 50±25s. Gray scale encodes 750 msec intervals between images with lighter shades indicating earlier activity. Black regions were not active.
(D) Distributions of interwave interval, wave speed, and wave size from calcium imaging (white) and simulated using the Hennig model with parameter values as in (C, blue).

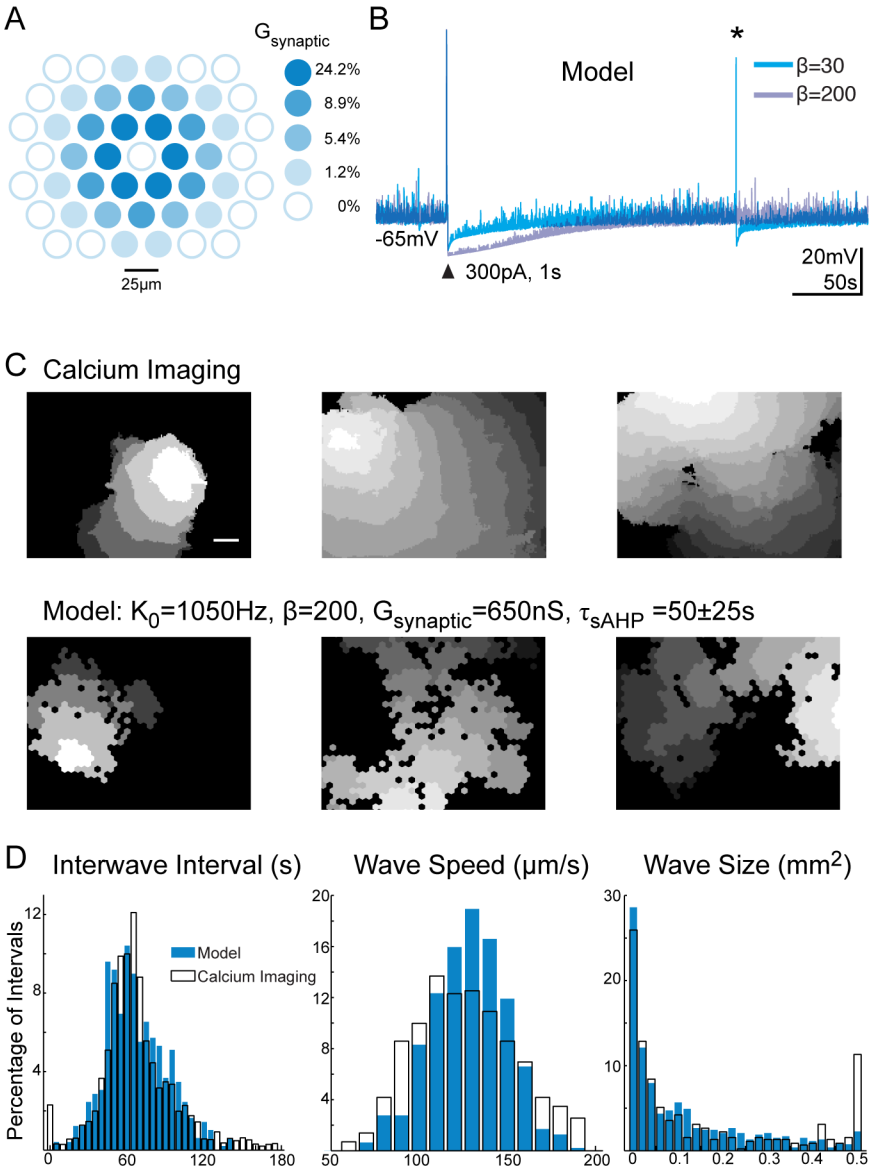
A
$G_{synaptic}$
24.2%
8.9%
5.4%
1.2%
0%
25μm
B
Model
β=30
β=200
*
-65mV
300pA, 1s
20mV
50s
C Calcium Imaging
Model: K_0=1050Hz, β=200, $G_{synaptic}$=650nS, τ_{sAHP} =50±25s
D
Interwave Interval (s)
Wave Speed (μm/s)
Wave Size (mm^2)
Percentage of Intervals
Model
Calcium Imaging
0
60
120
180
50
100
150
200
0
0.1
0.2
0.3
0.4
0.5

Figure II-8. Variability in the slow afterhyperpolarization is necessary to produce physiological waves

Distribution of mean interwave interval (left), wave speed (middle), and wave size (right) as a function of $G_{synaptic}$ and β parameters in the Hennig model. For each set of $G_{synaptic}$ and β parameters tested, the average interwave interval, wave speed, and wave size was computed. The color axis is centered such that green corresponds to the mean value measured from calcium imaging (see Figure II-7D) and the range of color intensities covers 1 SD on either side of the mean for interwave interval, wave speed and size. Saturated blue and red colors indicate values outside of the mean ± 1SD.
(A) K_0 was set to 1050Hz and each cell in the simulation had a decay constant for the slow AHP drawn from a random Gaussian distribution with a mean of 50s and SD of 25s. Values for β and $G_{synaptic}$ used in Figure II-7C-D are shown by red circle (β=200, $G_{synaptic}$=650). 8 values each of β and $G_{synaptic}$ were tested.
(B) K_0 was set to 1050Hz and all cells in the simulation had a decay constant for the slow AHP of 50s. 8 values of β and 6 values for $G_{synaptic}$ were tested.
(C) Membrane potentials from 3 neighboring cells showing variable participation during simulated waves using parameter values indicated by the red circle in A. The corresponding τ_{sAHP} values are indicated above each trace.
(D) Summary of variability in local participation during simulated waves for simulation with (Top, parameters as indicated by red circle in A) or without (Bottom, parameters as indicated by black triangle in B) variability in τ_{sAHP}. Number of cells in a neighborhood of 7 cells that were co-active within a 750ms window (Left) and peak membrane potential of three neighboring cells during a 750ms window when at least 2 cells within the 7 cell neighborhood are active (Right). Data from six 20min simulations.
(E) Histogram distribution of the intervals between simulated current injection (300pA, 1s) and the time of the previous wave using parameters indicated by the red circle in (B). Black bars are the distribution of all intervals between current injections and the preceding wave. Red bars indicate the subset of current injections that evoked a wave.

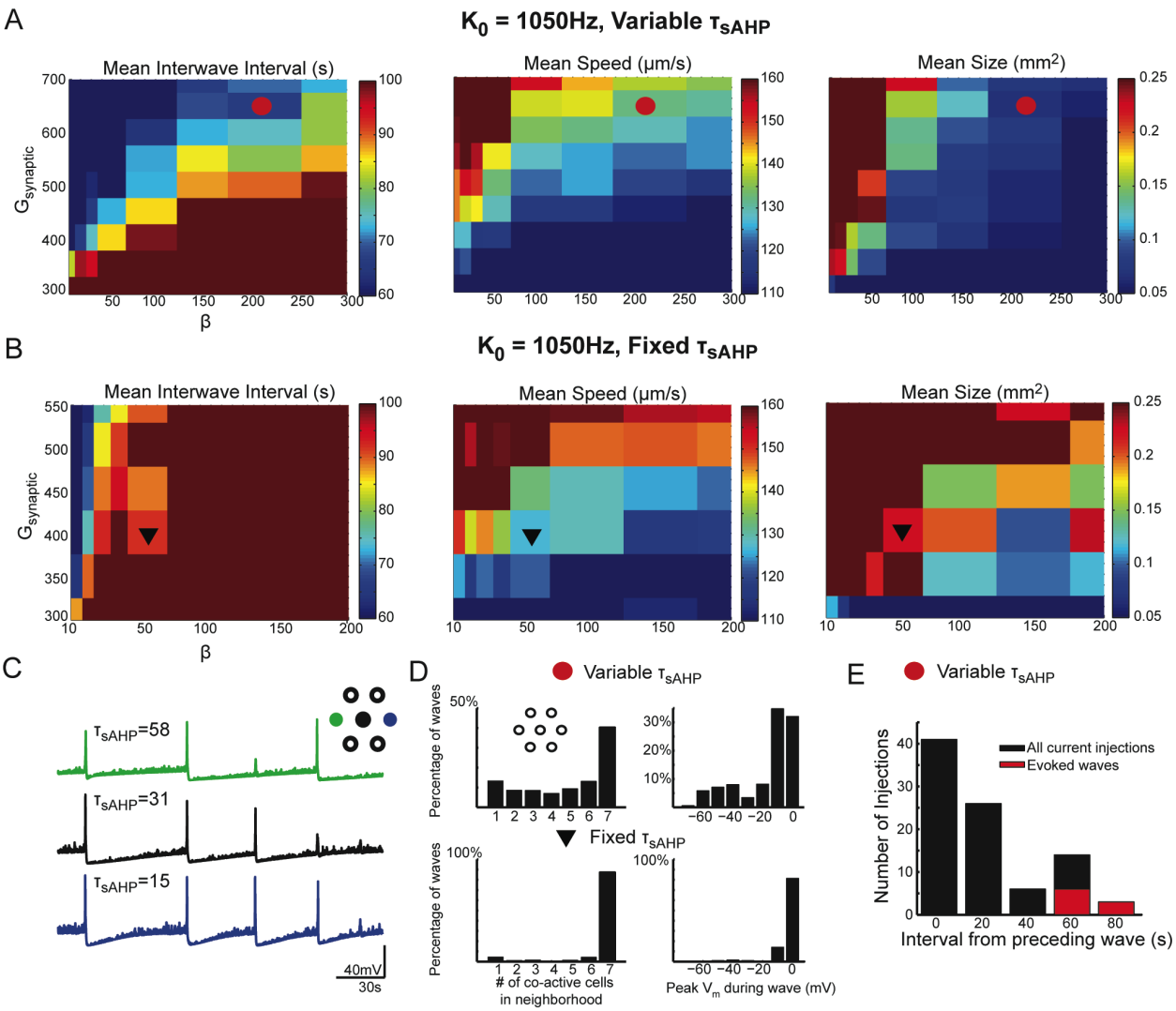
A
K0 = 1050Hz, Variable τsAHP
Mean Interwave Interval (s)
Mean Speed (μm/s)
Mean Size (mm2)
Gsynaptic
β
B
K0 = 1050Hz, Fixed τsAHP
Mean Interwave Interval (s)
Mean Speed (μm/s)
Mean Size (mm2)
Gsynaptic
β
C
τsAHP=58
τsAHP=31
τsAHP=15
40mV
30s
D
Variable τsAHP
Percentage of waves
Fixed τsAHP
# of co-active cells in neighborhood
Peak Vm during wave (mV)
E
Variable τsAHP
All current injections
Evoked waves
Number of Injections
Interval from preceding wave (s)

III. Molecular mechanisms underlying a slow afterhyperpolarization in developing starburst amacrine cells

Abstract

Calcium activated potassium channels are thought to underlie slow afterhyperpolarizations in myriad neuronal types. However, the molecular identity of these channels and the mechanism linking calcium entry to channel activation are still unknown. Here we describe a slow afterhyperpolarization in developing starburst amacrine cells that sets the frequency of spontaneous retinal waves. The conductance underlying the slow afterhyperpolarization is mediated by a potassium channel that is resistant to several potassium channel antagonists but is blocked by barium, implicating a role for two-pore potassium channels. In addition, activating adenylyl cyclase and inhibiting calcium-activated phosphodisterase inhibits the slow afterhyperpolarization. Imaging of cAMP and PKA levels indicate that depolarization of starburst cells decreases levels of cAMP. We propose a model in which depolarization induced decreases in cAMP lead to lower levels of PKA activation and disinhibition of channels and that the kinetics of this biochemical pathway dictates the slow activation and deactivation of the conductance. This represents a novel pathway for activation of a physiologically important conductance.

Introduction

Several types of neurons throughout the central and peripheral nervous system exhibit prolonged hyperpolarizations following bursts of action potentials (Hirst *et al.*, 1985; Lancaster & Nicoll, 1987; Schwindt *et al.*, 1988). These slow afterhyperpolarizations (sAHPs) underlie oscillatory burst firing in cholinergic striatal neurons and gonadotropin releasing hormone neurons (Goldberg *et al.*, 2009; Lee *et al.*, 2010) and give rise to spike frequency adaptation in principal cells of the cortex, hippocampus, and amygdala (Lancaster & Adams, 1986; Lorenzon & Foehring, 1992; Faber & Sah, 2002). The kinetics of sAHPs can alter network function. For example, enhancement of sAHPs in hippocampal CA1 neurons is correlated with cognitive decline during aging (Matthews *et al.*, 2009).

Despite the prevalence and functional importance of the sAHP, the channel that gives rise to it is unknown. It is generally accepted that the sAHP is mediated by a potassium channel that is activated upon calcium influx through a variety of voltage gated calcium channels (Sah & Louise Faber, 2002). No specific antagonists of the sAHP have been found, but several intracellular signaling pathways modulate the sAHP including signaling through PKA and PKC pathways (Lancaster & Nicoll, 1987; Sah & Isaacson, 1995; Vogalis *et al.*, 2002; Lancaster *et al.*, 2006). The slow kinetics of the sAHP have led to the speculation that calcium entry does not directly activate sAHP channels, but rather a signaling cascade, possibly involving phosphorylation of the channel, opens channels (Abel *et al.*, 2004). The calcium activated phosphatase calcineurin (Vogalis *et al.*, 2004) and calcium sensors hippocalcin (Tzingounis *et al.*, 2007) and neurocalcin (Villalobos & Andrade, 2010) have been implicated in activation

of sAHP, however the pathway leading from calcium entry to channel activation is still unknown.

Two-pore potassium (K2P) channels share similar properties with the channels underlying the sAHP. K2P channels, which give rise to the hyperpolarized resting membrane potential in most neurons (Enyedi & Czirjak, 2010), are insensitive to most potassium channel antagonists but are modulated by second messenger cascades (Mathie, 2007). The K2P channel family has several members that can be distinguished based upon current rectification, modulation by protein kinases, as well as activation by heat, stretch, and lipids (Lesage & Lazdunski, 2000; Enyedi & Czirjak, 2010). While no member of K2P family has been shown to be directly activated by calcium, activation of calcium dependent signaling cascades can gate channel opening (Czirjak *et al.*, 2004).

Recently, a sAHP has been described in developing retinal interneurons called starburst amacrine cells (Zheng *et al.*, 2006)(Chapter II). This sAHP plays a functional role within the developing retina by setting the frequency of spontaneous retinal waves (Zheng *et al.*, 2006; Godfrey & Swindale, 2007; Hennig *et al.*, 2009)(Chapter II). Here we describe the cellular pathways involved in activation of the conductance that gives rise to the sAHP.

Results

Starburst amacrine cells (SACs) in developing mouse retina exhibit a slow afterhyperpolarization (sAHP) following depolarization during waves (Chapter II, Figure III-1). To determine the current underlying this sAHP, we performed perforated patch voltage clamp experiments from SACs. To isolate cell-intrinsic conductances, synaptic input was blocked using cholinergic and GABAergic antagonists (DHBE + Gabazine). Depolarizing steps (from -60mV to 0mV; 500 msec duration) evoked a slow outward current at -60mV (Figure III-1B), as previously described (Chapter II). The current measured has a similar slow rise time and decay to sAHPs measured in current clamp (Figure III-B), hence, we refer to this current as I_{sAHP}.

Several lines of evidence indicate that I_{sAHP} is mediated by a potassium channel. First, activation of the channel was associated with an increase in conductance (Figure III-1D, n=3), implying the opening of a channel rather than activation of a transporter, a potential alternative source of the slow outward current. Second, I_{sAHP} reversed at the reversal potential for potassium (Figure III-1C). The current exhibited outward rectification at physiological external potassium concentration (4.5mM), consistent with activation of a leak conductance. Third, the reversal potential for I_{sAHP} shifted with increasing external potassium consistent with the Nernst equation prediction for a potassium conductance. In addition, I_{sAHP} was reversibly inhibited upon removal of calcium from the bath solution (Figure III-1E). These data indicate that I_{sAHP} is mediated by a potassium conductance that relies upon calcium entry for activation.

Next we conducted several pharmacology experiments to further identify the channel underlying I_{sAHP}. Calcium activated potassium channels include the BK and SK families (Sah, 1996). BK channels mediate rapid repolarization during action potentials. SK channels underlie a medium length afterhyperpolarization following individual action potentials. The amplitude of I_{sAHP} was unaffected by 1mM tetraethylammonium chloride

(TEA) (Figure III-1F, n=5), which blocks BK channels as well as other voltage gated channels. Note, TEA induced a prolonged inward tail current following the depolarizing step, indicating that increased calcium entry during depolarization in TEA activates a depolarizing conductance but does not affect I_{sAHP}. In addition, the amplitude of I_{sAHP} was unaffected by apamin, a specific antagonist for SK channels (Figure III-1F, n=5). Hence, neither BK nor SK channels contribute to the generation of I_{sAHP}.

We also tested the hypothesis that I_{sAHP} was mediated by an ATP-dependent potassium channels (Katp), which is activated by depolarization and contributes to a slow afterhyperpolarization in hippocampal pyramidal cells (Tanner *et al.*, 2011). Katp is thought to be activated by a decrease in ATP levels in cells. In support of SACs expressing a Katp channel, following gaining whole cell access to SACs we observed a rapidly developing conductance that led to a dramatic drop in input resistance (Figure III-2A). This conductance reversed at E_K (data not shown), indicating opening of potassium channels. Subsequent depolarizing steps result in activation of a transient outward tail current (Figure III-2A-B), similar to I_{sAHP} measured in perforated patch configuration. However, both the whole cell activated conductance and transient tail current following depolarization were blocked by tolbutamide (100μM, n= 5 Figure III-2B), an antagonist of Katp channels, in contrast to I_{sAHP} recorded in perforated patch configuration (Figure II-2C). These data indicate that Katp channels are activated by a reduction of intracellular ATP due to intracellular dialysis during whole cell recordings. Hence, we conclude that although SACs express Katp channels, these channels do not contribute to the sAHP.

Finally, we next tested the hypothesis that I_{sAHP} was mediated by a two-pore potassium (K2P) channel. K2P channels -- a broad family of channels that includes TWIK, TASK, TREK, TALK, THIK, and TRESK subfamilies -- are insensitive to several potassium channel antagonists including TEA, 4-aminopyridine, and cesium (Lesage, 2003). Consistent with this, the I_{sAHP} recorded in SACs was not blocked by a combination of 1mM TEA, 1mM 4-AP, and 2mM cesium (data not shown, see Methods). However, I_{sAHP} was blocked by barium (2 mM, n=2, Figure III-1F), consistent with I_{sAHP} being mediated by one of several subtypes of K2P channels, including TREK, TASK, TWIK and TRESK (Deng *et al.*, 2009). Last, the outward rectification of I_{sAHP} (Figure III-1C) is consistent with currents through a variety of K2P channels, including TREK, TASK, and TRESK channels. In future experiments, we will investigate whether I_{sAHP} is blocked by a recently characterized inhibitor of TREK-1 channels, spadin (Mazella *et al.*, 2010).

To confirm that SACs express K2P channels, we searched through the results of a microarray analysis of mRNA isolated from SACs (Kay *et al.*, 2011a; Kay *et al.*, 2011b). These arrays indicate that *kcnk2*, which encodes the K2P channel TREK-1, is selectively expressed in SACs during the first postnatal week (Jeremy Kay and Joshua Sanes, personal communication). Together with pharmacology and rectification properties of channel indicate that TREK-1 channels are likely to mediate the slow potassium conductance underlying the sAHP.

A hallmark of both TREK channels and channels underlying the sAHP in other neurons is their regulation by intracellular signaling cascades. PKA phosphorylation inhibits TREK channels (Honore *et al.*, 2002) and has also been shown to inhibit channels underlying the sAHP in other neurons (Lancaster & Nicoll, 1987; Sah &

Isaacson, 1995; Lancaster *et al.*, 2006). To test whether I_{sAHP} in SACs is sensitive to intracellular cAMP, we measured the current during application of forskolin (1μM) to activate adenylyl cylcase. Forskolin inhibited I_{sAHP} measured in voltage clamp perforated patch recordings (Figure III-3A, n=6), indicating that I_{sAHP} is sensitive to levels of cAMP.

I_{sAHP} requires calcium influx for activation, yet TREK channels are not activated by changes in intracellular calcium (Fink *et al.*, 1996). How might these channels be activated to generate the sAHP in SACs? The activation of I_{sAHP} occurs over several seconds, which suggests that a signaling cascade, rather than direct activation of calcium, may lead to opening of channels following depolarization. Calcium influx can regulate levels of cAMP by activation of adenylyl cyclases (ACs) and phosphodiesterases (PDEs) (Cooper *et al.*, 1995; Landa *et al.*, 2005). Activation of TREK channels via a decrease in cAMP has been shown to occur with activation of metabotropic GABA (Deng *et al.*, 2009) and glutamate receptors (Lesage *et al.*, 2000; Chemin *et al.*, 2003). Therefore, we investigated whether calcium influx causes a decrease in cAMP levels, which in turn would activate TREK-1, giving rise to I_{sAHP}.

First, we imaged cAMP/PKA levels using genetically encoded FRET based indicators (DiPilato *et al.*, 2004; Zhang *et al.*, 2006) to determine how levels of cAMP and PKA are regulated by calcium influx. Retinal neurons were transfected with AKAR3 or ICUE2 to monitor intracellular PKA activity and cAMP levels, respectively. Transfected cells were imaged to in response to brief application of high potassium solution to evoke depolarizations. In retinal ganglion cells, slow, transient increases in cAMP occur following calcium influx (Dunn *et al.*, 2006). However, a subset of transfected neurons exhibited depolarization induced decreases in PKA/cAMP signaling (Figure III-4B, n=2 AKAR3, n=3 ICUE2). Subsequent staining for choline acetyltransferease, a marker for cholinergic SACs, revealed that cells with depolarization induced decreases were SACs. Depolarization induced decreases were only observed in the presence of 1μM forskolin in the bathing solution, which may indicate that normal changes in cAMP/PKA are below the dynamic range of the indicators and are only visible when baseline levels are increased. Hence, in contrast to retinal ganglion cells, SACs exhibit depolarization induced decreases in cAMP/PKA. Future experiments will determine the mechanisms that give rise to these decreases in cAMP/PKA following depolarization.

Next, we determined whether calcium-dependent decreases in cAMP activate I_{sAHP}. Calcium influx can decrease levels of cAMP by activating calcium-activated PDEs. SACs have been shown to express the calcium-activated phosphodiesterase PDE-1C (Santone, 2006). To test whether PDE-1C activation during depolarization may lead to activation of I_{sAHP} by decreasing levels of cAMP, we inhibited calcium-activated PDEs using 8-Methoxymethyl-3-isobutyl-1-methyl xanthine (MMPX, 100μM). Similar to forskolin, MMPX inhibited I_{sAHP} (Figure III-3A, n=6), indicating calcium activated PDEs play a role in the activation of I_{sAHP}. Together, these experiments indicate that I_{sAHP} may be generated via activation of TREK-1 channels by a calcium-dependent decrease in cAMP.

To determine how sAHPs alter network function in the developing retina, we tested how altering the sAHP altered retinal waves using calcium imaging (Chapter II). In the developing retina, the sAHP in SACs is thought to regulate the frequency of

spontaneous retinal waves by generating a refractory period following depolarization during a wave. Elevating levels of cAMP by activating ACs with forskolin, inhibiting all PDEs with IMBX, or with a cell-permeable non-hydorlyzable cAMP analogue (CPT-cAMP) all decreased the interwave interval (Figure III-4A). Specific inhibition of calcium activated PDEs with MMPX also decreased interwave interval. These results indicate that disrupting the cAMP regulation of the sAHP in SACs alters properties of retinal waves. To further test the role of the sAHP in setting wave frequency, we tested the effects of potassium channel antagonists. 4-AP, cesium, tolbutamide, and XE-991, an antagonist of KCNQ channels that partially mediate a sAHP in hippocampus (Tzingounis *et al.*, 2010), had no effect or increased interwave intervals (Figure III-4A), however, apamin, which has no effect on the sAHP (Figure III-1F), slightly reduced the interwave interval. In contrast, 2mM barium dramatically increased baseline fluorescence and induced epileptic activity (Figure III-4B, n=2). These data show that manipulations of the sAHP in SACs alter the frequency of retinal waves, indicating that the sAHP plays an important role in the control circuit behavior.

Discussion and future directions

We have demonstrated that developing starburst amacrine cells exhibit a slow hyperpolarization that is mediated by a potassium channel with pharmacology and rectification properties consistent with a K2P channel. The channel underlying the sAHP is inhibited tonic elevation of cAMP and is blocked by preventing the calcium dependent degradation of cAMP by PDEs. Indeed, cAMP levels are decreased in SACs following depolarization, which would disinhibit I_{sAHP} channels and give rise to the slow kinetics of activation. Finally, we show that the sAHP serves a functional role in the developing retina by setting the frequency of retinal waves. Below we discuss the role of the two-pore channel TREK-1 in generation of I_{sAHP} and propose a model for activation by regulation of cAMP levels.

TREK-1 as a candidate I_{sAHP} channel

A role for K2P channels in generating slow currents has become increasingly evident. Metabotropic GABAB receptors generate second long hyperpolarizations by cAMP dependent disinhibition of TREK-2 channels (Deng *et al.*, 2009). Serotonin activates TWIK-1 (Deng *et al.*, 2007) or TASK-1 (Talley *et al.*, 2000) channels through a similar mechanism resulting in a decrease in neuronal excitability. Conversely, metabotropic glutamate receptor activation of phospholipase C inhibits TREK and TASK channels generates slow depolarizations in neurons (Chemin *et al.*, 2003). These findings suggest that slow modulation of second messengers, including cAMP and IP3, are read out by K2P channels to alter neuronal excitability.

Our results are consistent with a role for the K2P channel TREK-1 in generation of I_{sAHP} in starburst cells. Several lines of evidence support this claim. First, I_{sAHP} is not inhibited by TEA (1mM), 4-AP (1mM), cesium (2mM), apamin (1 μM), or tolbutamide (100μM) which rule out voltage gated, A-type, SK, BK, and ATP-dependent potassium channels. K2P channels, however, are resistant to channel block by these antagonists. Second, 2mM barium blocked I_{sAHP}, which is consistent with block of TASK, TREK, TWIK, and TRESK channels. K2P channels lack specific antagonists, however, some

channels are activated by manipulations of pressure, pH, and lipids (Lesage & Lazdunski, 2000; Enyedi & Czirjak, 2010). Further experiments are needed to test the effect of these manipulations on I_{sAHP} in SACs. Third, the outward rectification of I_{sAHP} is consistent with outward rectification of TREK, TASK, and TRESK channels, but not TWIK. Furthermore, outward rectification excludes the possibility that other inward rectified channels that are sensitive to barium, such as Katp, underlie I_{sAHP}. Fourth, I_{sAHP} is inhibited by elevating intracellular cAMP, consistent with the known inhibition of TREK channels by PKA phosphorylation. Finally, genetic evidence supports the specific expression of *kcnk2* transcripts in SACs during development (Jeremy Kay and Josh Sanes, personal communication). Genetic manipulations to knock down TREK-1 in SACs will confirm a role for these channels in I_{sAHP}.

A cAMP model for activation of I_{sAHP}

How is IsAHP activated? We propose a model (Figure III-5) for activation of IsAHP that links calcium entry to regulation of cAMP levels that control activation of the potassium channel underlying the sAHP. During depolarization, calcium influx through voltage gated calcium channels leads to a decrease in cAMP (Figure III-3B). Calcium-dependent PDE1C is likely to contribute to the observed decrease, although further experiments are needed to determine the effects of inhibiting calcium-dependent PDEs on the depolarization induced decrease in cAMP. Other pathways may also contribute to the decrease in cAMP. Some ACs, including AC5, AC6 and AC9, are inhibited by intracellular calcium signaling (Halls & Cooper, 2011). AC5 and AC9 are expressed early in development within the retina (Nicol *et al.*, 2006), though their specific localization is unknown.

Another way in which calcium entry may decrease cAMP levels is by depletion of ATP following calcium extrusion. Calcium is extruded from neurons in an ATP dependent manner by plasma membrane calcium pumps (Renteria *et al.*, 2005). As calcium is extruded, ATP levels would be depleted, thus depleting the substrate for cAMP production by ACs. Depletion of ATP following depolarization has been shown to cause activation of Katp channels that contribute to a sAHP in hippocampus (Tanner *et al.*, 2011). Indeed, in whole cell recordings, we find that Katp channels are activated by depolarization (Figure III-2) to generate an I_{sAHP}-like current. This current has faster activation kinetics than the I_{sAHP} measured during perforated patch recordings and may reflect a more rapid depletion of ATP followed by the slower depletion of cAMP.

A decrease in cAMP leads to activation of the channel underlying the sAHP. The corresponding decrease in PKA activity would result in a decrease in phosphorylation that disinhibits the channel. TREK-1 channels in neurons are associated with PKA anchoring proteins (AKAPs) that allow for rapid regulation by PKA (Sandoz *et al.*, 2006). Furthermore, I_{sAHP} in hippocampal CA1 neurons is modulated by both PKA and phosphatases (Pedarzani *et al.*, 1998) suggesting that a balance of kinase and phosphatase activity actively regulates the channel phosphorylation state.

Calcium may also play a role in activation of channels by acting via the calcium dependent phosphatase calcineurin. We find that long application of the calcineurin inhibitor cyclosporine-A results in a decrease in interwave interval (Figure III-4A), suggesting that it may play a role in generating the sAHP. Calcineurin might act to directly dephosphorylate the channel, or may play a more indirect role in inhibiting

adenylyl cyclase (Antoni *et al.*, 1998). Calcineurin activation has been implicated in activating a sAHP found in myenteric neurons (Vogalis *et al.*, 2004). Interestingly, NCS-1, a calcium binding protein of the same family as hippocalcin and neurocalcin, can substitute for calmodulin in activating calcineurin and PDEs (Schaad *et al.*, 1996). Whether calcium sensing proteins involved in generating the sAHP play a similar role is an intriguing question.

Experimental procedures

Animals. All experiments were performed on acutely isolated mouse retinas. Male and female C57Bl/6 mice obtained from Harlan were used for all WT recordings. mGluR2-GFP mice contain a transgene insertion of interleukin-2 receptor fused GFP under control of the mGluR2 promoter (Watanabe *et al.*, 1998). ChAT-Cre/TdTom mice were generated by crossing a mouse in which an IRES-Cre recombinase is knocked in downstream of the endogenous choline acetyl transferase gene (Ivanova *et al.*, 2010) with a separate tdTomato driver line (B6.129S6-ChAT$^{tm1(cre)Iowl}$/J x B6.129S6-Gt(ROSA)26Sor$^{tm9(CAG-tdTomato)Hze}$/J, Jackson Labs). All animal procedures were approved by the University of California, Berkeley and conformed to the National Institutes of Health *Guide for the Care and Use of Laboratory Animals*, the Public Health Service Policy, and the Society for Neuroscience Policy on the Use of Animals in Neuroscience Research.

Whole-Mount Retinal Preparation. P4-P7 mice were anesthetized with isoflurane and decapitated. Retinas were isolated in cold artificial cerebrospinal fluid (ACSF) (in mM: 119 NaCl, 26.2 $NaHCO_3$, 11 glucose, 2.5 KCl, 1 K_2HPO_4, 2.5 $CaCl_2$, 1.3 $MgCl_2$) and mounted RGC side-up on filter paper. Retinas were incubated at room temperature in oxygenated ACSF until transfer to the recording chamber, where they were continually superfused with oxygenated ACSF at 30-34C.

Electrophysiology. Perforated patch and whole cell recordings were made from whole-mount retinas from mice aged P4-P7. The inner limiting membrane was removed using a glass recording pipette and SACs were identified using fluorescence and targeted using a Sutter micromanipulator. Voltage clamp recordings were sampled at 2.5kHz and filtered at 1kHz. Current clamp recordings were sampled at 5kHz and filtered at 2kHz. Analysis was performed using custom MATLAB (Mathworks) scripts. All reported voltages are corrected for liquid junction potential.

Perforated patch voltage and current clamp recordings were performed in the presence of DHβE (4μM) and gabazine (5μM), which block nAChR and GABA-A receptor mediated synaptic conductances, and tolbutamide (100μM), to block an ATP sensitive potassium conductance that develops during prolonged recordings (Figure III-2). During recordings of conductance (Figure III-1D) and current-voltage relationship (Figure III-1C), TTX (200nM), 4-AP (1mM), TEA (1mM), cesium chloride (2mM) were included in the bath solution to block voltage activated conductances. A gluconate-based perforated patch internal (in mM: 122 KGluconate, 20 HEPES, 0.5 EGTA, 2 NaCl, pH 7.2, liquid junction potential: 14mV) was front filled into electrodes and then back-filled with internal solution containing 750μg/ml Amphotericin B made fresh hourly.

Seals were formed and then access resistance was monitored continuously. Recordings were performed when access resistance was stable and less than 5% of the input resistance of the cell (typically, R_a 30-80 MOhm, R_{in} 1-2GOhm). Maximum amplitude and kinetics of the slow AHP were not correlated with access resistance.

Whole cell recordings from SACs were made using potassium phosphate based internal (in mM: 110 KH_2PO_4, 6 $MgCl_2$, 1 EGTA, 4 adenosine 5′-triphosphate magnesium salt, 0.3 guanosine 5′-triphosphate trisodium salt, 10 HEPES and 10 phosphocreatine disodium salt, pH 7.2, liquid junction potential: 14mV).

Calcium Imaging. Retinas from mice aged P2- P6 were bulk loaded with the calcium indicator Oregon Green Bapta-1 AM (OGB-1 AM) using the multicell bolous loading technique (Stosiek *et al.*, 2003; Blankenship *et al.*, 2009). Epifluorscence imaging and analysis as described earlier (Blankenship *et al.*, 2009).

cAMP/PKA imaging. Retinal explants were isolated and mounted on filter paper with the RGCs facing up. Then, 0.2 mg/mL plasmid (CMV-AKAR3 or CMV-ICUE2, (Dunn *et al.*, 2006)) was electroporated (30 V, 4 mm, 2 pulses at 1 second interval, BTX ECM 830 electroporator). Retinal explants were then cultured in serum free culture medium (Neurobasal-A medium supplemented with B27 (Gibco), 0.6% glucose, 2 mM glutamine, 10 mM HEPES, 1 mM Na-Pyruvate, 50 mg/mL penicillin G, 50 units/mL streptomycin, 2.5 mg/mL Insulin, 6 µM forskolin, 10 ng/mL CNTF & 50 ng/mL BDNF) for 12–48 hours. Explants were removed to forskolin-free media overnight prior to imaging.

FRET images were acquired at 0.33Hz using a 60x objective. The excitation wavelength was 435nm. Individual FRET channel detection was accomplished by using a Dual-View image splitter (Optical Insights) with appropriate yellow and cyan channel filters. Images were digitized as during calcium imaging experiments above. Background fluorescence was subtracted from both channels. FRET ratios were computed as background corrected YFP/CFP fluorescence averaged over a region of interest around cell bodies and corrected for bleed through ($F_{YFP} = F_{FRET} - 0.51 \times F_{CFP}$).

References

Abel, H.J., Lee, J.C., Callaway, J.C. & Foehring, R.C. (2004) Relationships between intracellular calcium and afterhyperpolarizations in neocortical pyramidal neurons. *J Neurophysiol*, **91**, 324-335.

Antoni, F.A., Palkovits, M., Simpson, J., Smith, S.M., Leitch, A.L., Rosie, R., Fink, G. & Paterson, J.M. (1998) Ca2+/calcineurin-inhibited adenylyl cyclase, highly abundant in forebrain regions, is important for learning and memory. *J Neurosci*, **18**, 9650-9661.

Blankenship, A.G., Ford, K.J., Johnson, J., Seal, R.P., Edwards, R.H., Copenhagen, D.R. & Feller, M.B. (2009) Synaptic and Extrasynaptic Factors Governing Glutamatergic Retinal Waves. *Neuron*, **62**, 230.

Chemin, J., Girard, C., Duprat, F., Lesage, F., Romey, G. & Lazdunski, M. (2003) Mechanisms underlying excitatory effects of group I metabotropic glutamate receptors via inhibition of 2P domain K+ channels. *EMBO J*, **22**, 5403-5411.

Cooper, D.M.F., Mons, N. & Karpen, J.W. (1995) Adenylyl cyclases and the interaction between calcium and cAMP signalling. *Nature*, **374**, 421.

Czirjak, G., Toth, Z.E. & Enyedi, P. (2004) The two-pore domain K+ channel, TRESK, is activated by the cytoplasmic calcium signal through calcineurin. *J Biol Chem*, **279**, 18550-18558.

Deng, P.Y., Poudel, S.K., Rojanathammanee, L., Porter, J.E. & Lei, S. (2007) Serotonin inhibits neuronal excitability by activating two-pore domain k+ channels in the entorhinal cortex. *Mol Pharmacol*, **72**, 208-218.

Deng, P.Y., Xiao, Z., Yang, C., Rojanathammanee, L., Grisanti, L., Watt, J., Geiger, J.D., Liu, R., Porter, J.E. & Lei, S. (2009) GABA(B) receptor activation inhibits neuronal excitability and spatial learning in the entorhinal cortex by activating TREK-2 K+ channels. *Neuron*, **63**, 230-243.

DiPilato, L.M., Cheng, X. & Zhang, J. (2004) Fluorescent indicators of cAMP and Epac activation reveal differential dynamics of cAMP signaling within discrete subcellular compartments. *Proc Natl Acad Sci U S A*, **101**, 16513-16518.

Dunn, T.A., Wang, C.T., Colicos, M.A., Zaccolo, M., DiPilato, L.M., Zhang, J., Tsien, R.Y. & Feller, M.B. (2006) Imaging of cAMP Levels and Protein Kinase A Activity Reveals That Retinal Waves Drive Oscillations in Second-Messenger Cascades. *J. Neurosci.*, **26**, 12807.

Enyedi, P. & Czirjak, G. (2010) Molecular background of leak K+ currents: two-pore domain potassium channels. *Physiol Rev*, **90**, 559-605.

Faber, E.S. & Sah, P. (2002) Physiological role of calcium-activated potassium currents in the rat lateral amygdala. *J Neurosci*, **22**, 1618-1628.

Fink, M., Duprat, F., Lesage, F., Reyes, R., Romey, G., Heurteaux, C. & Lazdunski, M. (1996) Cloning, functional expression and brain localization of a novel unconventional outward rectifier K+ channel. *EMBO J*, **15**, 6854-6862.

Godfrey, K.B. & Swindale, N.V. (2007) Retinal Wave Behavior through Activity-Dependent Refractory Periods. *PLoS Computational Biology*, **3**, e245.

Goldberg, J.A., Teagarden, M.A., Foehring, R.C. & Wilson, C.J. (2009) Nonequilibrium calcium dynamics regulate the autonomous firing pattern of rat striatal cholinergic interneurons. *J Neurosci*, **29**, 8396-8407.

Halls, M.L. & Cooper, D.M. (2011) Regulation by Ca2+-signaling pathways of adenylyl cyclases. *Cold Spring Harb Perspect Biol*, **3**, a004143.

Hennig, M.H., Adams, C., Willshaw, D. & Sernagor, E. (2009) Early-Stage Waves in the Retinal Network Emerge Close to a Critical State Transition between Local and Global Functional Connectivity. *J. Neurosci.*, **29**, 1077.

Hirst, G.D., Johnson, S.M. & van Helden, D.F. (1985) The slow calcium-dependent potassium current in a myenteric neurone of the guinea-pig ileum. *J Physiol*, **361**, 315-337.

Honore, E., Maingret, F., Lazdunski, M. & Patel, A.J. (2002) An intracellular proton sensor commands lipid- and mechano-gating of the K(+) channel TREK-1. *EMBO J*, **21**, 2968-2976.

Ivanova, E., Hwang, G.S. & Pan, Z.H. (2010) Characterization of transgenic mouse lines expressing Cre recombinase in the retina. *Neuroscience*, **165**, 233-243.

Kay, J.N., De la Huerta, I., Kim, I.J., Zhang, Y., Yamagata, M., Chu, M.W., Meister, M. & Sanes, J.R. (2011a) Retinal ganglion cells with distinct directional preferences differ in molecular identity, structure, and central projections. *J Neurosci*, **31**, 7753-7762.

Kay, J.N., Voinescu, P.E., Chu, M.W. & Sanes, J.R. (2011b) Neurod6 expression defines new retinal amacrine cell subtypes and regulates their fate. *Nat Neurosci*, **14**, 965-972.

Lancaster, B. & Adams, P.R. (1986) Calcium-dependent current generating the afterhyperpolarization of hippocampal neurons. *J Neurophysiol*, **55**, 1268.

Lancaster, B., Hu, H., Gibb, B. & Storm, J.F. (2006) Kinetics of ion channel modulation by cAMP in rat hippocampal neurones. *J Physiol*, **576**, 403.

Lancaster, B. & Nicoll, R.A. (1987) Properties of two calcium-activated hyperpolarizations in rat hippocampal neurones. *J Physiol*, **389**, 187-203.

Landa, L.R., Harbeck, M., Kaihara, K., Chepurny, O., Kitiphongspattana, K., Graf, O., Nikolaev, V.O., Lohse, M.J., Holz, G.G. & Roe, M.W. (2005) Interplay of Ca2+ and cAMP Signaling in the Insulin-secreting MIN6 {beta}-Cell Line. *J. Biol. Chem.*, **280**, 31294.

Lee, K., Duan, W., Sneyd, J. & Herbison, A.E. (2010) Two slow calcium-activated afterhyperpolarization currents control burst firing dynamics in gonadotropin-releasing hormone neurons. *J Neurosci*, **30**, 6214-6224.

Lesage, F. (2003) Pharmacology of neuronal background potassium channels. *Neuropharmacology*, **44**, 1-7.

Lesage, F. & Lazdunski, M. (2000) Molecular and functional properties of two-pore-domain potassium channels. *Am J Physiol Renal Physiol*, **279**, F793-801.

Lesage, F., Terrenoire, C., Romey, G. & Lazdunski, M. (2000) Human TREK2, a 2P domain mechano-sensitive K+ channel with multiple regulations by polyunsaturated fatty acids, lysophospholipids, and Gs, Gi, and Gq protein-coupled receptors. *J Biol Chem*, **275**, 28398-28405.

Lorenzon, N.M. & Foehring, R.C. (1992) Relationship between repetitive firing and afterhyperpolarizations in human neocortical neurons. *J Neurophysiol*, **67**, 350-363.

Mathie, A. (2007) Neuronal two-pore-domain potassium channels and their regulation by G protein-coupled receptors. *J Physiol*, **578**, 377-385.

Matthews, E.A., Linardakis, J.M. & Disterhoft, J.F. (2009) The fast and slow afterhyperpolarizations are differentially modulated in hippocampal neurons by aging and learning. *J Neurosci*, **29**, 4750-4755.

Mazella, J., Petrault, O., Lucas, G., Deval, E., Beraud-Dufour, S., Gandin, C., El-Yacoubi, M., Widmann, C., Guyon, A., Chevet, E., Taouji, S., Conductier, G., Corinus, A., Coppola, T., Gobbi, G., Nahon, J.L., Heurteaux, C. & Borsotto, M. (2010) Spadin, a sortilin-derived peptide, targeting rodent TREK-1 channels: a new concept in the antidepressant drug design. *PLoS Biol*, **8**, e1000355.

Nicol, X., Bennis, M., Ishikawa, Y., Chan, G.C., Reperant, J., Storm, D.R. & Gaspar, P. (2006) Role of the calcium modulated cyclases in the development of the retinal projections. *Eur J Neurosci*, **24**, 3401-3414.

Pedarzani, P., Krause, M., Haug, T., Storm, J.F. & Stuhmer, W. (1998) Modulation of the Ca2+-Activated K+ Current sIAHP by aPhosphatase-Kinase Balance Under Basal Conditions inRat CA1 Pyramidal Neurons. *J Neurophysiol*, **79**, 3252.

Renteria, R.C., Strehler, E.E., Copenhagen, D.R. & Krizaj, D. (2005) Ontogeny of plasma membrane Ca2+ ATPase isoforms in the neural retina of the postnatal rat. *Vis Neurosci*, **22**, 263-274.

Sah, P. (1996) Ca2+-activated K+ currents in neurones: types, physiological roles and modulation. *Trends in Neurosciences*, **19**, 150.

Sah, P. & Isaacson, J.S. (1995) Channels underlying the slow afterhyperpolarization in hippocampal pyramidal neurons: neurotransmitters modulate the open probability. *Neuron*, **15**, 435.

Sah, P. & Louise Faber, E.S. (2002) Channels underlying neuronal calcium-activated potassium currents. *Progress in Neurobiology*, **66**, 345.

Sandoz, G., Thummler, S., Duprat, F., Feliciangeli, S., Vinh, J., Escoubas, P., Guy, N., Lazdunski, M. & Lesage, F. (2006) AKAP150, a switch to convert mechano-, pH- and arachidonic acid-sensitive TREK K(+) channels into open leak channels. *EMBO J*, **25**, 5864-5872.

Santone, R. (2006) Gene expression and protein localization of calmodulin-dependent phosphodiesterase in adult rat retina. *Journal of Neuroscience Research*, **84**, 1020.

Schaad, N.C., De Castro, E., Nef, S., Hegi, S., Hinrichsen, R., Martone, M.E., Ellisman, M.H., Sikkink, R., Rusnak, F., Sygush, J. & Nef, P. (1996) Direct modulation of calmodulin targets by the neuronal calcium sensor NCS-1. *Proc Natl Acad Sci U S A*, **93**, 9253-9258.

Schwindt, P.C., Spain, W.J., Foehring, R.C., Chubb, M.C. & Crill, W.E. (1988) Slow conductances in neurons from cat sensorimotor cortex in vitro and their role in slow excitability changes. *J Neurophysiol*, **59**, 450-467.

Sipila, S.T., Huttu, K., Voipio, J. & Kaila, K. (2006) Intrinsic bursting of immature CA3 pyramidal neurons and consequent giant depolarizing potentials are driven by a persistent Na+ current and terminated by a slow Ca2+ -activated K+ current. *Eur J Neurosci*, **23**, 2330-2338.

Stosiek, C., Garaschuk, O., Holthoff, K. & Konnerth, A. (2003) In vivo two-photon calcium imaging of neuronal networks. *Proceedings of the National Academy of Sciences of the United States of America*, **100**, 7319-7324.

Talley, E.M., Lei, Q., Sirois, J.E. & Bayliss, D.A. (2000) TASK-1, a two-pore domain K+ channel, is modulated by multiple neurotransmitters in motoneurons. *Neuron*, **25**, 399-410.

Tanner, G.R., Lutas, A., Martinez-Francois, J.R. & Yellen, G. (2011) Single KATP channel opening in response to action potential firing in mouse dentate granule neurons. *J Neurosci*, **31**, 8689-8696.

Tzingounis, A.V., Heidenreich, M., Kharkovets, T., Spitzmaul, G., Jensen, H.S., Nicoll, R.A. & Jentsch, T.J. (2010) The KCNQ5 potassium channel mediates a component of the afterhyperpolarization current in mouse hippocampus. *Proceedings of the National Academy of Sciences*, **107**, 10232.

Tzingounis, A.V., Kobayashi, M., Takamatsu, K. & Nicoll, R.A. (2007) Hippocalcin Gates the Calcium Activation of the Slow Afterhyperpolarization in Hippocampal Pyramidal Cells. *Neuron*, **53**, 487.

Villalobos, C. & Andrade, R. (2010) Visinin-like neuronal calcium sensor proteins regulate the slow calcium-activated afterhyperpolarizing current in the rat cerebral cortex. *J Neurosci*, **30**, 14361-14365.

Vogalis, F., Harvey, J.R. & Furness, J.B. (2004) Suppression of a slow post-spike afterhyperpolarization by calcineurin inhibitors. *Eur J Neurosci*, **19**, 2650-2658.

Vogalis, F., Harvey, J.R., Neylon, C.B. & Furness, J.B. (2002) Regulation of K+ channels underlying the slow afterhyperpolarization in enteric afterhyperpolarization-generating myenteric neurons: Role of calcium and phosphorylation. *Clinical and Experimental Pharmacology and Physiology*, **29**, 935.

Watanabe, D., Inokawa, H., Hashimoto, K., Suzuki, N., Kano, M., Shigemoto, R., Hirano, T., Toyama, K., Kaneko, S., Yokoi, M., Moriyoshi, K., Suzuki, M., Kobayashi, K., Nagatsu, T., Kreitman, R.J., Pastan, I. & Nakanishi, S. (1998) Ablation of Cerebellar Golgi Cells Disrupts Synaptic Integration Involving GABA Inhibition and NMDA Receptor Activation in Motor Coordination. *Cell*, **95**, 17.

Zhang, L.L., Pathak, H.R., Coulter, D.A., Freed, M.A. & Vardi, N. (2006) Shift of intracellular chloride concentration in ganglion and amacrine cells of developing mouse retina. *J Neurophysiol*, **95**, 2404.

Zheng, J., Lee, S. & Zhou, Z.J. (2006) A transient network of intrinsically bursting starburst cells underlies the generation of retinal waves. *Nat Neurosci*, **9**, 363.

Figure III-1. Slow afterhyperpolarization (sAHP) in starburst amacrine cells (SACs) is mediated by a two-pore potassium channel

A. Two-photon fluorescence image of SAC from mGluR2-GFP retina filled with fluorescent indicator.

B. Left: Current clamp perforated patch recording of sAHP evoked by 500ms 100pA current injection. Right. Voltage clamp perforated patch recording of IsAHP evoked by 500ms voltage step to -14mV from holding potential of -64mV. Average from n=32 cells, gray is +-SD.

C. Left: Voltage command protocol used to determine current voltage relationship of I_{sAHP}. Average I_{sAHP} shown above for reference. Scale: 2pA, 10s. Middle: Current voltage relationship at peak of I_{sAHP}. N=4, Mean+-SD. Right: Change in reversal potential as a function of external potassium concentration. Dots represent individual cells, boxes are mean. Line is fit to prediction from Nearnst equation for a potassium conductance.

D. Example conductance (top) and current (bottom) measurements taken from a baseline of -64mV following 500ms voltage step to -14mV. Inset: Voltage command protocol used to determine conductance.

E. Average current evoked by 500ms voltage step to -14mV, as in B-D, in the presence (black) and absence (gray) of external calcium (n=4). Right: Peak amplitude of evoked current in control, 0 calcium, and rinse.

F. Average current as in E in control (black) or during bath application (gray) of apamin (1μM, left, n=5), TEA (1mM, middle, n=5), or barium (2mM, right, n=2).

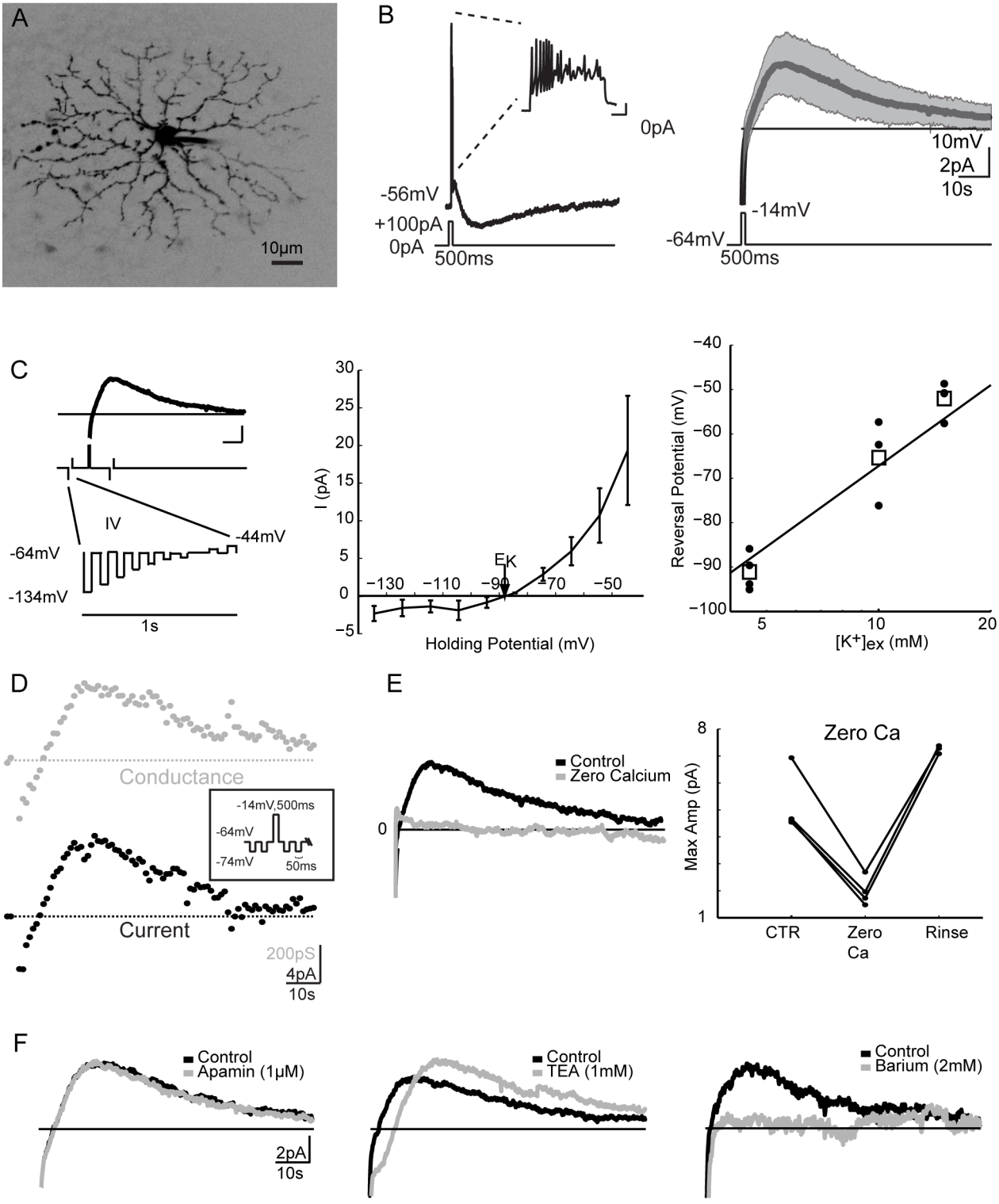
A
10μm
B
-56mV
+100pA
0pA
500ms
0pA
10mV
2pA
10s
-14mV
-64mV
500ms
C
IV
-64mV
-44mV
-134mV
1s
I (pA)
Holding Potential (mV)
EK
Reversal Potential (mV)
[K+]ex (mM)
D
Conductance
Current
-14mV,500ms
-64mV
-74mV
50ms
200pS
4pA
10s
E
Control
Zero Calcium
Zero Ca
Max Amp (pA)
CTR
Zero Ca
Rinse
F
Control
Apamin (1μM)
2pA
10s
Control
TEA (1mM)
Control
Barium (2mM)

Figure III-2. Whole cell recordings from SACs reveal a Katp conductance
A. Whole cell voltage clamp recording from SAC. VC=-60mV. Arrows indicate 500ms voltage step to 0mV followed by return to -60mV. Dotted lines indicate changes in holding current at -60mV in control, tolbutamide (100μM), and rinse.
B. Peak amplitude of transient outward current following 500ms depolarization voltage step in whole cell configuration before, during, and after tolbutamide application.
C. Left: Example perforated patch current clamp recording of sAHP evoked by 500ms, 100pA current injection before and during tolbutamide bath application. Right: Example voltage clamp perforated patch recording of I_{sAHP} evoked by 500ms step to -14mV from -64mV before and during tolbutamide batch application.

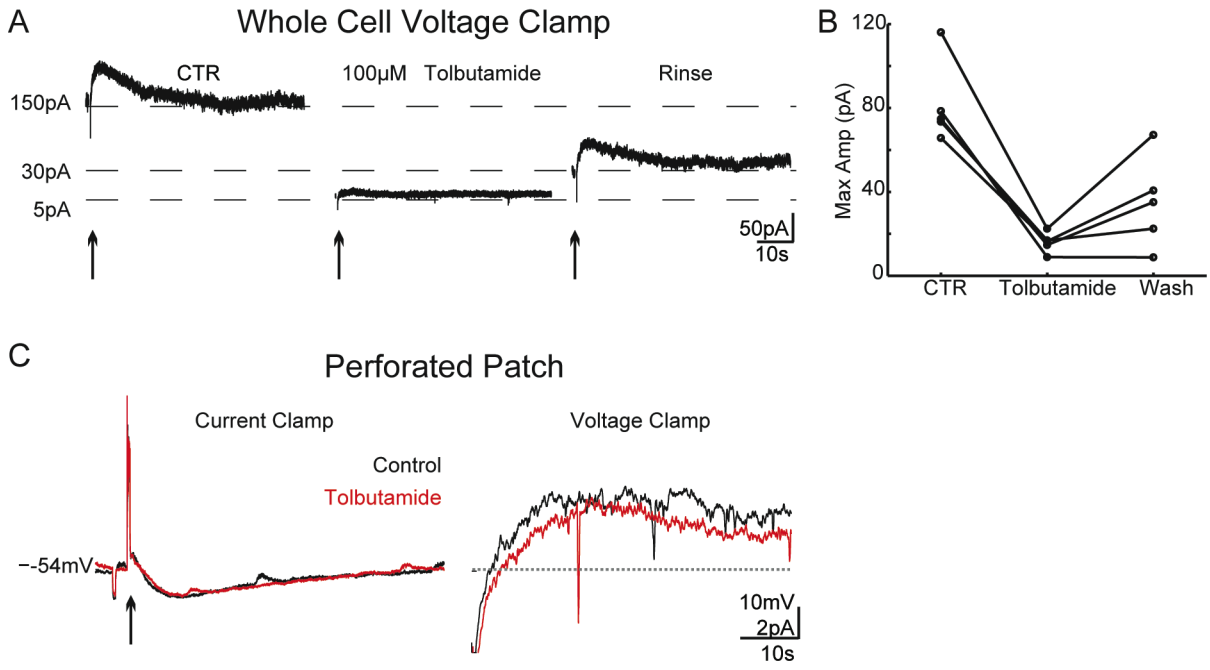
A
Whole Cell Voltage Clamp
CTR
100μM Tolbutamide
Rinse
150pA
30pA
5pA
50pA
10s
B
120
80
40
0
Max Amp (pA)
CTR
Tolbutamide
Wash
C
Perforated Patch
Current Clamp
Voltage Clamp
Control
Tolbutamide
−-54mV
10mV
2pA
10s

Figure III-3. Regulation of cAMP/PKA controls activation of sAHP channels
A. Left: Average current evoked by 500ms voltage step to -14mV from -64mV, in the control (black) and during application of forskolin (1μM, gray, top) or MMPX (100μM, gray, bottom). Right: Peak amplitude of evoked currents before, during, and after rinse of forskolin or MMPX.
B. Schematic of genetically encoded PKA (top, AKAR3) and cAMP (bottom, ICUE2) indicators. AKAR3 undergoes an increase in FRET efficiency following phosphorylation by PKA. ICUE2 undergoes a decrease in FRET efficiency following binding by cAMP.
C. PKA and cAMP responses to 3s application of 100mM potassium solution measured from cultured SACs expressing AKAR3 (n=2) or ICUE2 (n=3). Traces represent the normalized ratio of YFP/CFP (AKAR3) or CFP/YFP (ICUE2) fluorescence average over cell somas. Note: Measurements of cAMP and PKA were performed in the presence of 1μM forskolin in the bathing solution.

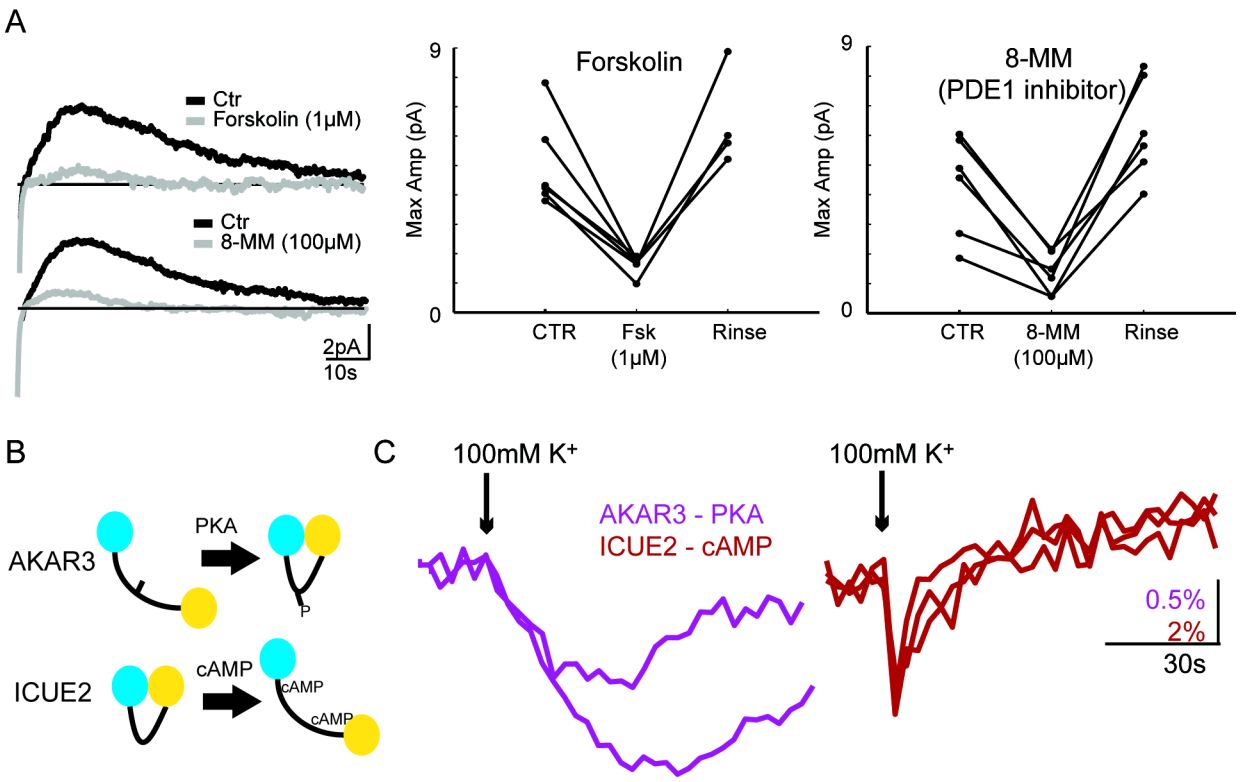
A
Ctr
Forskolin (1μM)
Ctr
8-MM (100μM)
2pA
10s
Forskolin
Max Amp (pA)
9
0
CTR
Fsk
(1μM)
Rinse
8-MM
(PDE1 inhibitor)
Max Amp (pA)
9
0
CTR
8-MM
(100μM)
Rinse
B
AKAR3
PKA
P
ICUE2
cAMP
cAMP
cAMP
C
100mM K+
AKAR3 - PKA
ICUE2 - cAMP
100mM K+
0.5%
2%
30s

Figure III-4. Modulation of sAHP alters frequency of spontaneous retinal waves
A. Fold change in mean interwave interval measured by calcium imaging in the presence of manipulations to sAHP. Manipulations are: Fsk, forskolin (1μM); IBMX (100μM); CPT-cAMP (500μM); MMPX (100μM); CsA, cyclosporine-A (10uM); apamin (500nM); tolb, tolbutamide (100μM); Cs+, cesium (2mM); 4-AP (0.5mM); XE991 (10μM). Number of retinas per manipulation shown on each bar. Mean+-SD.
B. Example fluorescence trace from calcium imaging during application of 2mM barium.

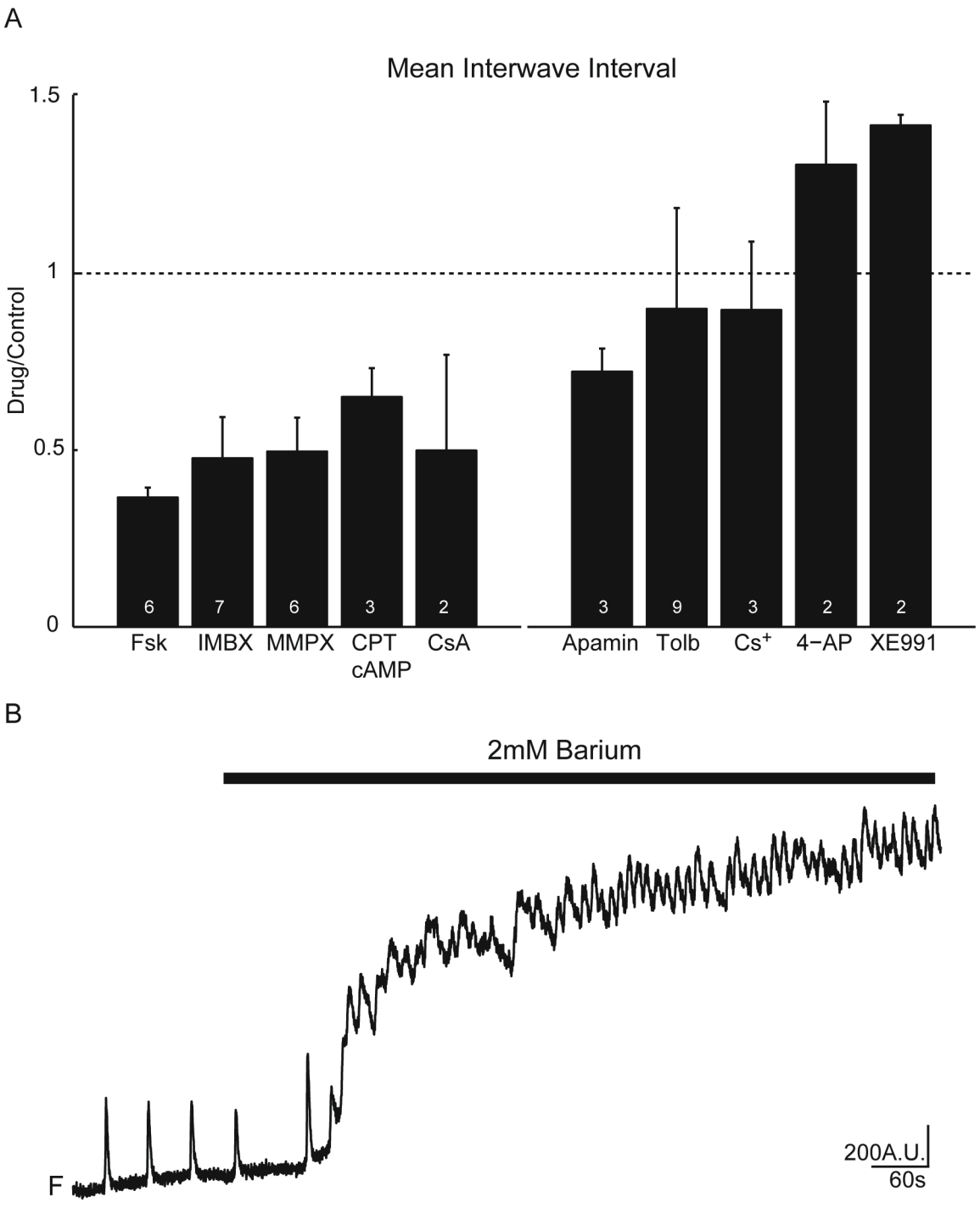
A
Mean Interwave Interval
1.5
1
0.5
0
Drug/Control
6
7
6
3
2
3
9
3
2
2
Fsk
IMBX
MMPX
CPT cAMP
CsA
Apamin
Tolb
Cs+
4−AP
XE991
B
2mM Barium
F
200A.U.
60s

Figure III-5. Model for cAMP dependent activation of sAHP
Calcium influx through voltage gated calcium channels activates calcium dependent PDE, which decreases levels of cAMP. Extrusion of calcium by PMCAs depletes levels of ATP, which results in a reduction in cAMP synthesis by ACs and also activates Katp channels. K2P channels are disinhibited by the decrease in PKA phosphorylation resulting from the decrease in cAMP levels. Direct activation by calcium or indirect activation via dephosphorylation by calcineurin may also activate K2P channels. Abbreviations: Cav, voltage gated calcium channel; PMCA, plasma membrane calcium ATPase; Katp, ATP sensitive potassium channel; PDE, phosphodiesterase; AC, adenylyl cyclase; PKA, protein Kinase A; K2P, two-pore potassium channel.

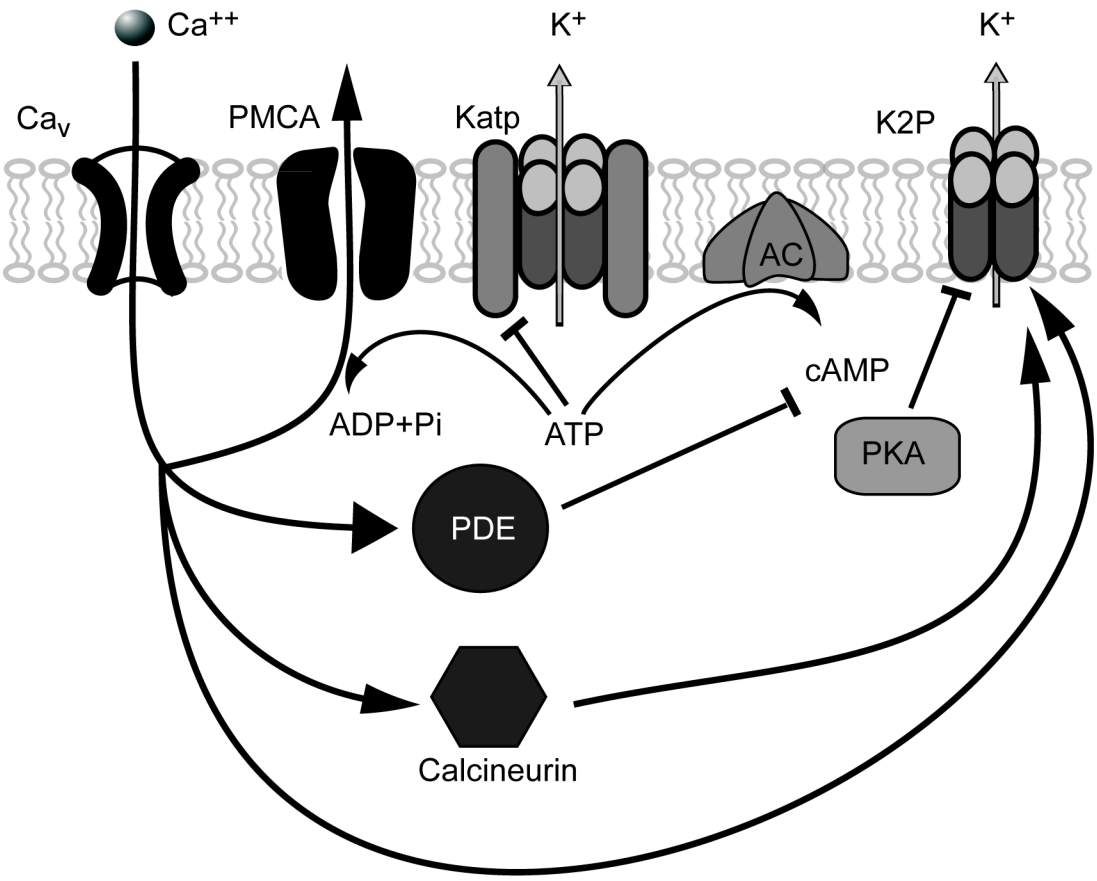
Ca++
K+
K+
Cav
PMCA
Katp
K2P
AC
cAMP
ADP+Pi
ATP
PKA
PDE
Calcineurin